

A TOTAL SYNTHESIS OF (+)-RYANODOL

Thesis by

Kangway V. Chuang

In Partial Fulfillment of the Requirements

for the Degree of

Doctor of Philosophy

CALIFORNIA INSTITUTE OF TECHNOLOGY

Pasadena, California

2016

(Defended June 1, 2016)

© 2016

Kangway V. Chuang

All Rights Reserved

ABSTRACT

Highly oxygenated, architecturally complex terpenoids constitute a biologically important class of natural products, yet their development into medicinally relevant analogs and effective biological probes are obstructed by their synthetic accessibility. Ryanodine is a unique diterpenoid that exhibits high affinity to a class of intracellular calcium ion channels bearing its name: ryanodine receptors. Structure-activity relationship studies have demonstrated how peripheral structural modifications affect binding affinity and selectivity among receptor isoforms, but to date have been limited to analogs prepared via chemical derivatization of natural material due to the intractability of total chemical synthesis.

This thesis details synthetic efforts culminating in a total synthesis of ryanodol that proceeds in only 15-steps from commercially available (–)-pulegone. Early stage oxygen atom incorporation is strategically implemented to facilitate key, stereoselective carbon-carbon bond formation. In particular, a rhodium-catalyzed, intramolecular Pauson–Khand reaction is utilized to rapidly assemble the tetracyclic ABCD-ring system that constitutes the anhydroryanodol core. A novel, selenium-dioxide mediated oxidation to install three oxidation states and three oxygen atoms was discovered, enabling the rapid oxidative functionalization of the ryanodol A-ring. The modular route described herein allows for the preparation of synthetic structural analogs not readily accessible via chemical degradation, and is anticipated to enable rapid construction and evaluation of biologically active ryanodine analogs.

TABLE OF CONTENTS

CHAPTER 1 **1**

An Introduction to *Ryania* Natural Products

1.1 INTRODUCTION.....	1
1.2 ISOLATION AND STRUCTURE.....	2
1.3 BIOLOGICAL ACTIVITY AND RYANODINE RECEPTORS.....	5
1.4 PRIOR TOTAL SYNTHESSES OF (+)-RYANODOL.....	6
1.4.1 Deslongchamps's Total Synthesis of (+)-Ryanodol	7
1.4.2 Inoue's Total Synthesis of (+)-Ryanodol and (+)-Ryanodine.....	9
1.5 PRIOR EFFORTS TOWARDS (+)-RYANODOL	11
1.5.1 Wiesner's Approach to Anhydroryanodol	12
1.5.2 Sieburth's C2-Symmetric Approach to Ryanodol.....	12
1.5.3 Wood's Phenolic Oxidation Approach to Ryanodol.....	14
1.5 CONCLUDING REMARKS	15
1.6 NOTES AND REFERENCES.....	16

CHAPTER 2 **22**

Total Synthesis of (+)-Ryanodol

2.1 INTRODUCTION.....	22
2.1.1 Structure and Synthetic Challenges	30

2.1.2 Retrosynthetic Analysis	32
2.2 FORWARD SYNTHETIC EFFORTS	30
2.2.1 Oxidation Studies of (S)-Pulegone.....	30
2.2.2 Synthesis of the D-Ring Lactone.....	32
2.2.3 Synthesis of the ABCD-Ring System.....	32
2.2.4 Selenium Dioxide Mediated A-Ring Functionalization.....	32
2.2.5 Total Synthesis of (+)-Anhydroryanodol	32
2.2.6 Conversion of (+)-Anhydroryanodol to (+)-Ryanodol	32
2.3 CONCLUDING REMARKS	33
2.4 EXPERIMENTAL SECTION.....	40
2.4.1 Materials and Methods	40
2.4.2 Experimental Procedures	42
2.5 NOTES AND REFERENCES.....	80
 APPENDIX 1	 84
Spectra Relevant to Chapter 2	
 APPENDIX 2	 126
X-Ray Crystallography Reports Relevant to Chapter 2	

LIST OF ABBREVIATIONS

$[\alpha]_D$	angle of optical rotation of plane-polarized light
Å	angstrom(s)
Ac	acetyl
APCI	atmospheric pressure chemical ionization
app	apparent
aq	aqueous
Ar	aryl group
atm	atmosphere(s)
BHT	2,6-di- <i>tert</i> -butyl-4-methylphenol (“ <u>b</u> utylated <u>h</u> ydroxy <u>t</u> oluene”)
Bn	benzyl
Boc	<i>tert</i> -butoxycarbonyl
BOM	benzyloxymethyl
bp	boiling point
br	broad
Bu	butyl
<i>i</i> -Bu	<i>iso</i> -butyl
<i>n</i> -Bu	butyl or <i>norm</i> -butyl
<i>t</i> -Bu	<i>tert</i> -butyl
Bz	benzoyl
<i>c</i>	concentration of sample for measurement of optical rotation
^{13}C	carbon-13 isotope

/C	supported on activated carbon charcoal
°C	degrees Celsius
calc'd	calculated
CAN	ceric ammonium nitrate
Cbz	benzyloxycarbonyl
CCDC	Cambridge Crystallographic Data Centre
CDI	1,1'-carbonyldiimidazole
cf.	consult or compare to (Latin: <i>confer</i>)
cm ⁻¹	wavenumber(s)
cod	1,5-cyclooctadiene
comp	complex
conc.	concentrated
Cy	cyclohexyl
CSA	camphorsulfonic acid
d	doublet
<i>d</i>	dextrorotatory
D	deuterium
dba	dibenzylideneacetone
DBU	1,8-diazabicyclo[5.4.0]undec-7-ene
DCC	<i>N,N</i> -dicyclohexylcarbodiimide
DCE	1,2-dichloroethane
<i>de</i>	diastereomeric excess
DIAD	diisopropyl azodicarboxylate

DMAD	dimethyl acetylenedicarboxylate
DMAP	4-dimethylaminopyridine
DME	1,2-dimethoxyethane
DMF	<i>N,N</i> -dimethylformamide
DMSO	dimethylsulfoxide
DNA	deoxyribonucleic acid
DPPA	diphenylphosphorylazide
dppp	1,3-bis(diphenylphosphino)propane
dr	diastereomeric ratio
DTT	dithiothreitol
<i>ee</i>	enantiomeric excess
E	methyl carboxylate (CO ₂ CH ₃)
E ⁺	electrophile
<i>E</i>	trans (entgegen) olefin geometry
EC ₅₀	median effective concentration (50%)
e.g.	for example (Latin: <i>exempli gratia</i>)
EI	electron impact
eq	equation
ESI	electrospray ionization
Et	ethyl
<i>et al.</i>	and others (Latin: <i>et alii</i>)
FAB	fast atom bombardment
Fmoc	fluorenylmethyloxycarbonyl

g	gram(s)
G	guanine
h	hour(s)
^1H	proton
^2H	deuterium
^3H	tritium
[H]	reduction
HATU	2-(7-aza-1 <i>H</i> -benzotriazol-1-yl)-1,1,3,3-tetramethyluronium hexafluorophosphate
HMDS	hexamethyldisilamide or hexamethyldisilazide
HMPA	hexamethylphosphoramide
<i>hν</i>	light
HPLC	high performance liquid chromatography
HRMS	high resolution mass spectrometry
Hz	hertz
IC ₅₀	half maximal inhibitory concentration (50%)
i.e.	that is (Latin: <i>id est</i>)
IR	infrared spectroscopy
<i>J</i>	coupling constant
<i>k</i>	rate constant
kcal	kilocalorie(s)
kg	kilogram(s)
L	liter or neutral ligand
<i>l</i>	levorotatory

LA	Lewis acid
LD ₅₀	median lethal dose (50%)
LDA	lithium diisopropylamide
LTMP	lithium 2,2,6,6-tetramethylpiperidide
m	multiplet or meter(s)
M	molar or molecular ion
<i>m</i>	meta
μ	micro
<i>m</i> -CPBA	<i>meta</i> -chloroperbenzoic acid
Me	methyl
mg	milligram(s)
MHz	megahertz
MIC	minimum inhibitory concentration
min	minute(s)
mL	milliliter(s)
MM	mixed method
mol	mole(s)
MOM	methoxymethyl
mp	melting point
Ms	methanesulfonyl (mesyl)
MS	molecular sieves
<i>m/z</i>	mass-to-charge ratio
N	normal or molar

NBS	<i>N</i> -bromosuccinimide
nm	nanometer(s)
NMR	nuclear magnetic resonance
NOE	nuclear Overhauser effect
NOESY	nuclear Overhauser enhancement spectroscopy
Nu	nucleophile
<i>o</i>	ortho
[O]	oxidation
<i>t</i> -Oct	<i>tert</i> -octyl (1,1,3,3-tetramethylbutyl)
<i>p</i>	para
PCC	pyridinium chlorochromate
PDC	pyridinium dichromate
Ph	phenyl
pH	hydrogen ion concentration in aqueous solution
pK_a	acid dissociation constant
PMB	<i>para</i> -methoxybenzyl
ppm	parts per million
PPTS	pyridinium <i>para</i> -toluenesulfonate
Pr	propyl
<i>i</i> -Pr	isopropyl
<i>n</i> -Pr	propyl or <i>norm</i> -propyl
psi	pounds per square inch
py	pyridine

q	quartet
R	alkyl group
<i>R</i>	rectus
RED-Al	sodium bis(2-methoxyethoxy)aluminum hydride
ref	reference
<i>R_f</i>	retention factor
s	singlet or seconds
<i>S</i>	sinister
sat.	saturated
SEM	2-(trimethylsilyl)ethoxymethyl
Su	succinimide
t	triplet
T	thymine
TBAF	tetra- <i>n</i> -butylammonium fluoride
TBAT	tetra- <i>n</i> -butylammonium difluorotriphenylsilicate
TBDPS	<i>tert</i> -butyldiphenylsilyl
TBS	<i>tert</i> -butyldimethylsilyl
TCA	trichloroacetic acid
temp	temperature
TES	triethylsilyl
Tf	trifluoromethanesulfonyl
TFA	trifluoroacetic acid
TFE	2,2,2-trifluoroethanol

THF	tetrahydrofuran
THIQ	tetrahydroisoquinoline
TIPS	triisopropylsilyl
TLC	thin layer chromatography
TMEDA	<i>N,N,N',N'</i> -tetramethylethylenediamine
TMS	trimethylsilyl
TOF	time-of-flight
tol	tolyl
Ts	<i>para</i> -toluenesulfonyl (tosyl)
UV	ultraviolet
w/v	weight per volume
v/v	volume per volume
X	anionic ligand or halide
Z	cis (zusammen) olefin geometry

Chapter 1

An Introduction to Ryania Natural Products

1.1 INTRODUCTION

In the nearly 70 years since its isolation, the natural product (+)-ryanodine (**1**, **Figure 1**) has inspired significant efforts towards understanding its structure, biological activity, and synthesis. Nearly three decades were required before the full details of its complex and highly caged structure were fully elucidated, whereas synthetic efforts have now spanned over half a century. The following chapter aims to summarize key aspects of its isolation, structure, biological activity, and to highlight efforts toward the synthesis of this synthetically intriguing diterpene.

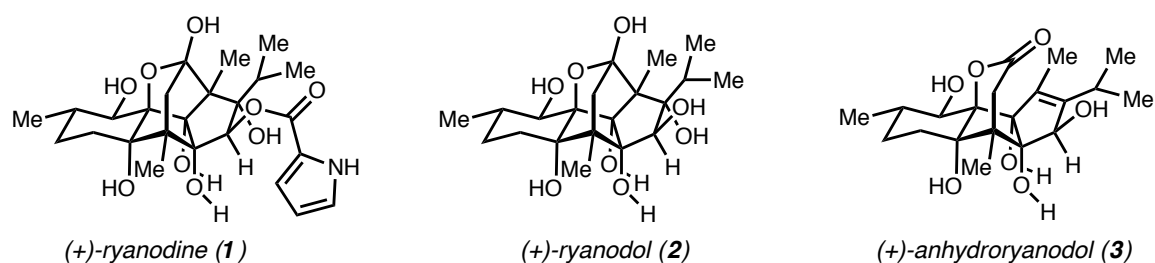


Figure 1. The diterpenoid structures of (+)-ryanodine, ryanodol, and anhydroryanodol

1.2 ISOLATION AND STRUCTURE

In 1948, Folkers and coworkers isolated a unique diterpenoid from the wet wood of the South American shrub *Ryania speciosa* Vahl. *Ryania* had long been of interest due to its biological activity in both insects and humans; extracts had historically been utilized as arrowhead poisons in Central and South America,¹ and interest in powdered *Ryania* as a potent insecticide had been determined years earlier. Continuous extraction with chloroform, followed by repeated recrystallizations from diethyl ether afforded pure (+)-ryanodine (**1**), a compound found to have an insecticidal potency 700 times greater than crude extracts alone.² Although a molecular formula in this original report was provided, a full structure of ryanodine could not be assigned with the physical data obtained at the time.

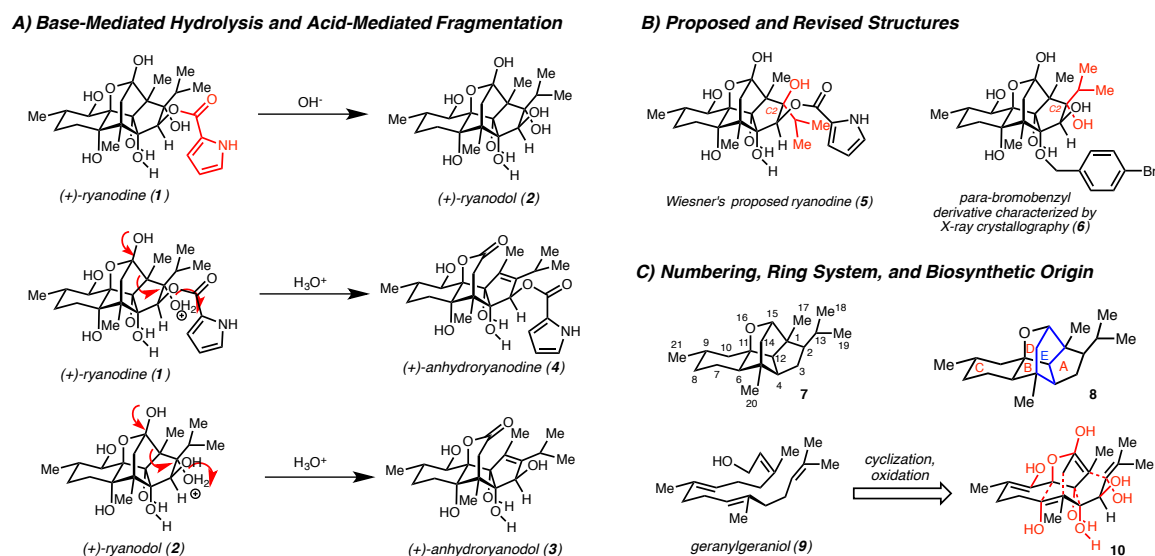


Figure 2. Key degradation studies and the structural elucidation of (+)-ryanodine and ryanodol

It was subsequent work spanning nearly three decades by Wiesner and coworkers that fully established the complex molecular structure of ryanodine in a classic example

of structure elucidation by chemical degradation.³⁻⁹ In particular, two key observations proved critical not only for structural determination, but for subsequent synthetic work (**Figure 2A**): 1) ryanodine undergoes basic hydrolysis to liberate one equivalent of pyrrole-2-carboxylic acid and ryanodol (**2**), its deacylated congener; 2) both ryanodine and ryanodol undergo efficient fragmentation under acidic conditions giving rise to tetracyclic products, termed anhydroryanodine (**4**) and anhydroryanodol (**3**). An exhaustive set of degradation studies enabled Wiesner to propose that ryanodine possesses the structure shown in **Figure 2B (5)** bearing an isopropyl group on the convex face of the molecule. A subsequent X-ray crystal structure of a *para*-bromobenzyl ether derivative of ryanodol (**6**) was obtained in 1968 by Srivastava and Przybylska that corroborated all major structural features of Wiesner's assignment with only the minor revision of the C2-stereocenter, instead placing the isopropyl group in the concave pocket of the molecule.^{10,11} This final confirmation of the structural identity of ryanodine led Wiesner to conclude that the biosynthetic origin was likely geranylgeraniol (**9**), which can be suggestively arranged to highlight that no significant rearrangements are necessary to generate the natural product (**10**).^{7,12} However, the specific order and nature of the bond forming events, as well as oxidations and oxygen-atom incorporations, remain unclear.

The ryanodane carbon numbering system (**7**), as well as the ring-lettering conventions (**8**), are illustrated in **Figure 2C**. Notably, of the five rings within its pentacyclic system, *only* the D-ring is oxygen bridged, with the remaining ABCE-rings all being carbocyclic in nature. From a structural standpoint, ryanodol bears an exceptionally caged and highly functionalized pentacyclic core, containing 11 contiguous

stereocenters and seven free hydroxyl moieties, one of which exists as part of an acidic hemiketal. Of these, the C3-oxygen bearing the pyrrole ester in ryanodine is sterically shielded within the concave AE ring system. The oxygenation of the molecule is largely distributed on one face of the 5-5-6, ABC-ring system, thus differentiating the two faces of the molecule as hydrophilic and hydrophobic. Indeed, ryanodol (**2**) itself is amphoteric in nature. It is soluble in both organic solvents and highly soluble in water; the extraction of ryanodol from an aqueous solution requires continuous extraction with refluxing chloroform over several days.^{2,9,13}

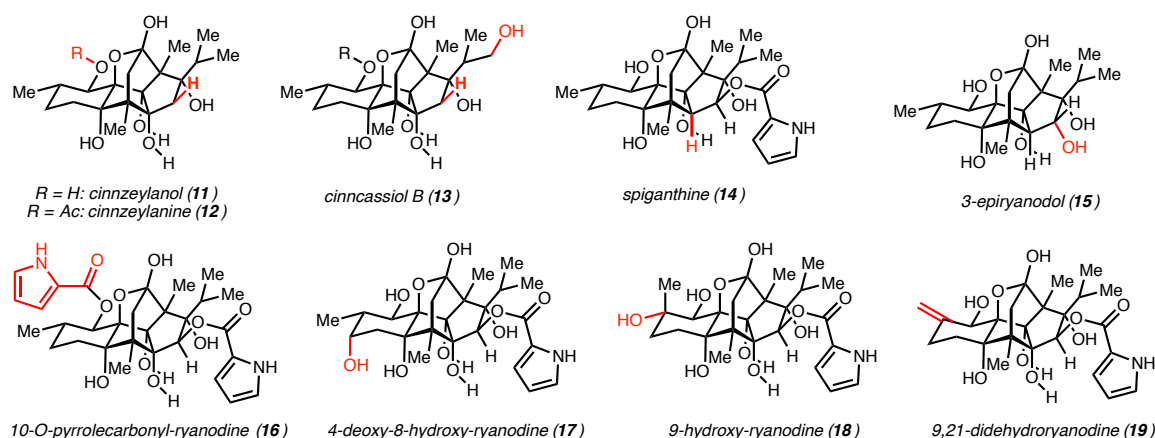


Figure 3. A survey of ryanodane natural products varying in functionality and oxidation state

Since the initial isolation of ryanodine, numerous ryanodane natural products have been identified, not only from the genus *Ryania*,¹⁴⁻¹⁸ but also from *Cinnamomum*,¹⁹⁻²⁴ *Spigelia*,^{25,26} and *Persea*.²⁷⁻²⁹ (**Figure 3**). The new natural products isolated vary substantially in both substitution and oxidation level along the molecular periphery, providing a diverse array of ryanodanes with varying biological activities. Furthermore, isolation from certain genera tend to lack the pyrrole-2-ester, necessary for bioactivity in

humans, such as the C3-deoxygenated natural products cinnzeylanol (**11**) and cinnzeylanine (**12**) from *Cinnamomum*,³⁰ and 3-epiryanodol (**15**) from *Persea*.^{27-29,31}

1.3 BIOLOGICAL ACTIVITY AND RYANODINE RECEPTORS

Although noted for its potent insecticidal activity,² (+)-ryanodine bears historical significance as [3H]-**1** was instrumental for the purification and characterization of ryanodine receptors (RyRs), a group of intracellular calcium ion channels present in skeletal muscle, cardiac muscle, as well as the brain.^{14,32,33} Ryanodine potently binds to RyRs with exceptionally high affinity, yet interestingly, exhibits concentration dependent effects: at nanomolar concentrations, **1** locks RyRs in an open, sub-conductance state,³⁴ whereas at higher concentrations, ryanodine causes closure of the channels.³⁵

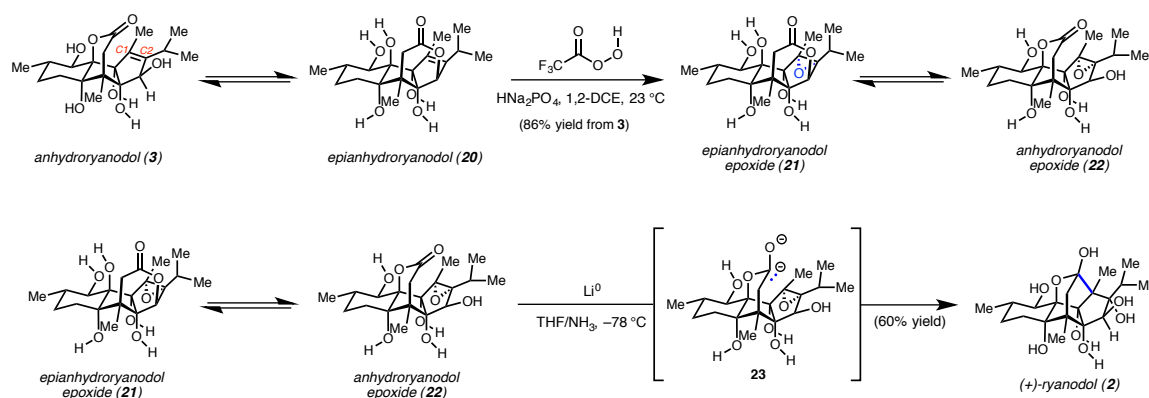
In mammalian cells, these proteins exist in three isoforms (RyR1, RyR2, RyR3) with varying distributions dependent on the tissue type, and play a critical role in signal transduction, thereby mediating our movement and cognitive function.^{36,37} Mutations of RyRs are associated with numerous genetic diseases such as central core disease,³⁸ malignant hyperthermia,³⁹ and catecholaminergic polymorphic ventricular tachycardia (CPVT).⁴⁰ Furthermore, leaky hippocampal RyR2 channels have been demonstrated to contribute to stress-induced cognitive dysfunction,⁴¹ and altered expression of RyR2 and RyR3 have been implicated in the pathogenesis of neurodegenerative disorders such as Alzheimer's disease.^{42,43} Given these implications, it has been suggested that these ion channels may serve as therapeutic targets for a range of diseases.⁴⁴⁻⁴⁷

From a structural standpoint, it has been established that the pyrrole-2-carboxylate ester moiety is critical for high binding affinity in humans, and is the major orienting factor in binding to RyRs.⁴⁸ A variety of structure activity relationship studies have been

conducted, exclusively through derivatization of material obtained from natural sources, and have demonstrated the ability to achieve binding selectivity amongst RyR isoforms via chemical modification of the molecular periphery.² Despite these studies, to date, the precise mode of binding and the mechanism of channel modulation have not yet been fully determined.

1.4 PRIOR TOTAL SYNTHESSES OF (+)-RYANODOL

1.4.1 Deslongchamps's Total Synthesis of (+)-Ryanodol



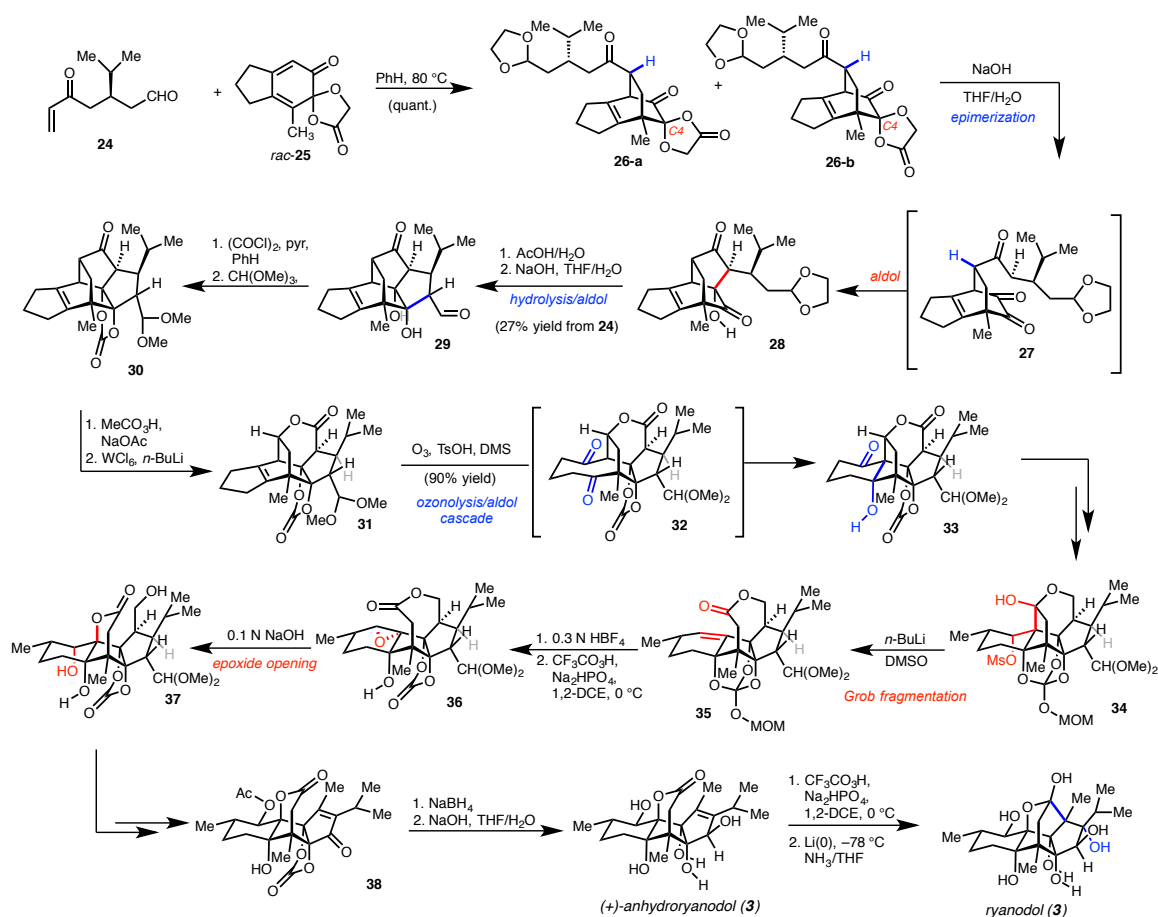
Scheme 1. Relay studies by Deslongchamps (1979) on the reconversion of (+)-anhydroryanodol to (+)-ryanodol.

In 1979, Deslongchamps and coworkers reported on the total synthesis of (+)-ryanodol in a classic demonstration of relay synthesis.^{13,49-52} Access to multigram quantities of natural (+)-ryanodine was instrumental to the rapid assessment of their synthetic endgame strategy; specifically, it was hypothesized that the primary acid degradation product, anhydroryanodol (3), could be potentially reconverted to ryanodol (1) via the appropriate oxidation/reduction sequence. To this end, initial studies on anhydroryanodol (3) obtained from natural sources established several key, late-stage equilibrium processes that proved critical to identifying suitable reaction conditions.

Although anhydroryanodol itself proved resistant toward C1-C2 olefin epoxidation, epianhydroryanodol (**20**), an isomer resulting from intramolecular translactonization, is readily epoxidized. Noting this difference in reactivity between lactone isomers, it was established that by employing trifluoroperacetic acid under phosphate buffered conditions, equilibration to **20** could precede oxidation, enabling the direct synthesis of epianhydroryanodol epoxide (**21**) in excellent yield. Similarly, epoxide **21** readily equilibrates to anhydroryanodol epoxide (**22**) under basic conditions. Subjection of either epoxide to Li(0)-metal in NH₃ at –78 °C results in an intramolecular, reductive cyclization to provide ryanodol with a reported yield of 60%. It is believed that in this final transformation, anhydroryanodol epoxide (**22**) is the on-path substrate, leading to productive cyclization, whereas premature reduction of epianhydroryanodol epoxide (**21**) results in the generation of carbonyl-reduction side products.¹³

Simultaneous with studies assessing the viability of the conversion of **3** to **2** were synthetic efforts aimed at accessing anhydroryanodol (**Scheme 2**). To this end, a key Diel–Alder cycloaddition between enone **24**, derived from (*S*)-carvone, and *rac*-spirolactone **25** proceeded in quantitative yield to provide a mixture of diastereomeric Diels–Alder adducts. It was recognized that cleavage of the spirolactone under basic conditions results in ablation of the C4-stereocenter, resulting in convergence of isomers **26a** and **26n** to the same 1,2-diketone intermediate (**27**). Thus, treatment of the isomeric mixture obtained from the Diels–Alder reaction with aqueous hydroxide resulted a diastereoconvergent, epimerization/aldol cascade, providing ketone **28**. Further hydrolysis of the dioxolane moiety followed by basification effected an additional intramolecular aldol reaction, affording pentacyclic aldehyde **29** in 27% yield overall

from **24**. Protection of the 1,2-diol and aldehyde moieties generated carbonate **30**, which was elaborated via Baeyer-Villiger oxidation and tungsten-mediated de-epoxidation to olefin **31**. Subjection under ozonolytic conditions with an acidic workup effected an intramolecular aldol cascade to forge the necessary 5-5-6 tricyclic ABC-ring system of ryanodol (**33**).



Scheme 2. The first total synthesis of (+)-ryanodol by Deslongchamps (1979)

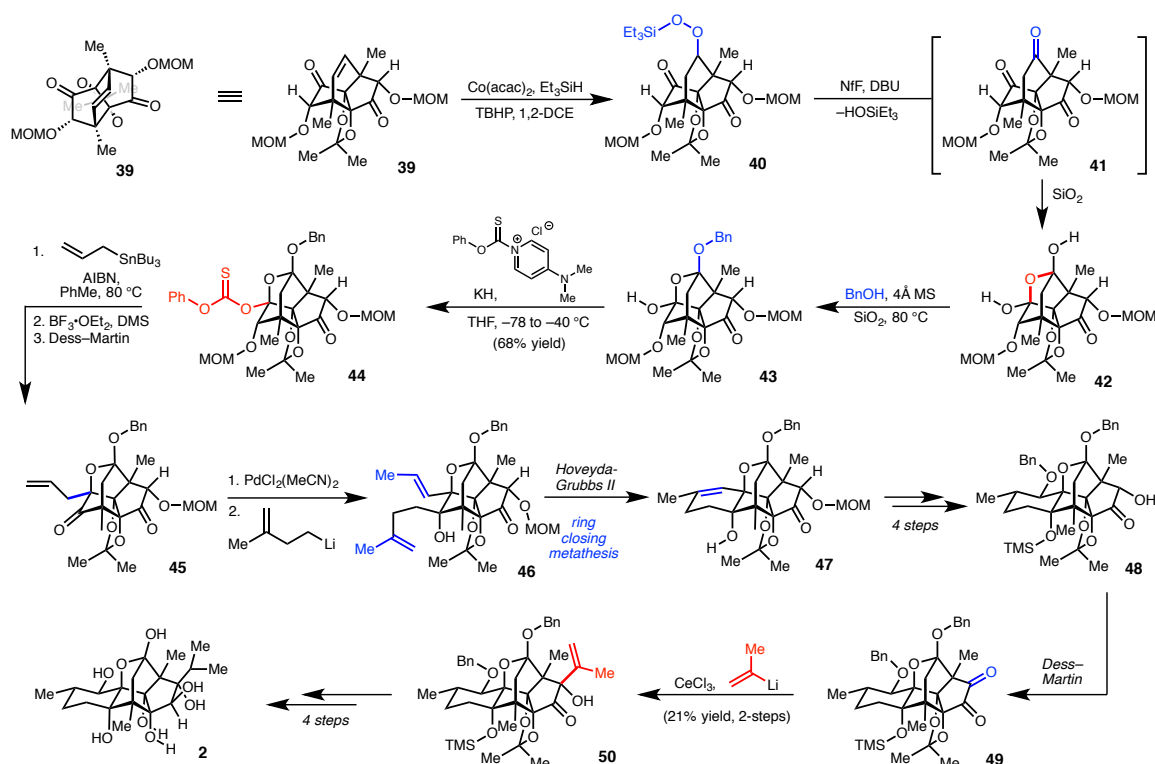
At this juncture, functional group manipulations provided mesylate **34**, which cleanly underwent Grob fragmentation by use of dimsyllithium in DMSO. Gentle hydrolysis of the *ortho*-carbonate protecting group with aqueous tetrafluoroboric acid, followed by treatment with trifluoroacetic acid under buffered conditions provided epoxide **36**. Saponification of the seven membered lactone resulted in epoxide opening,

thereby forming the key anhydroryanodol framework and establishing the ABCD tetracyclic framework (**37**). Subsequent functional group adjustments and removal of the protecting groups provided (+)-anhydroryanodol in a total of 35 steps (longest linear sequence). Finally, conversion to (+)-ryanodol (**2**) was achieved by epoxidation and reductive cyclization as established in their relay protocol.

1.4.2 Inoue's Total Synthesis of (+)-Ryanodol and (+)-Ryanodine

In 2014, Inoue and coworkers completed the second total synthesis of (+)-ryanodol, capitalizing on latent C_2 -symmetry embedded within ryanodol's congested pentacyclic core, a strategy first described by Sieburth and coworkers in 1994 (*vide infra*, **Scheme 6**) and others.^{59,60} The C_2 -symmetric building block **39**, already constituting a functionalized ABE-ryanodol ring system, was prepared in 14-steps from commercially available starting materials, previously reported in an earlier publication.⁵³⁻⁵⁵ Treatment of **39** with $\text{Co}(\text{acac})_2$, Et_3SiH , and catalytic TBHP resulted in desymmetrization by olefin hydroperoxidation. A Kornblum DeLaMare rearrangement was then effected by treatment with NfF and DBU to provide triketone **41**, that spontaneously hydrates on silica to generate hemiketal **42**. Protection of the hemiketal as its benzyl ketal (**43**), followed by generation of the thiocarbonate moiety, results in a handle for generation of a stabilized, carbon-based radical. Construction of the ryanodol C-ring was subsequently effected in six steps via installation of two tethered alkenes and a ring-closing metathesis reaction utilizing the 2nd generation Hoveyda-Grubbs catalyst, in the process completing the preparation of the full pentacyclic ABCDE-ring system (**47**). A series of functional group manipulations then provided 1,2-diketone **49**, which underwent a sluggish but

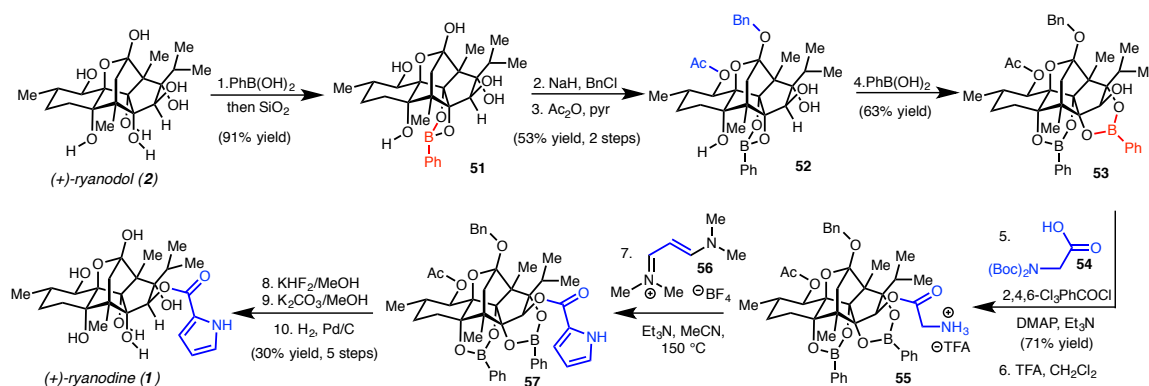
selective 1,2-addition reaction with 2-propenyllithium to install the final three-carbon unit in 21% yield over two steps. Finally, an additional four synthetic steps enabled the removal of the necessary protecting groups to provide (+)-ryanodol in a total of 35-steps (longest linear sequence).



Scheme 3. An approach to (+)-ryanodol based on latent C2-symmetry by Inoue (2014)

With a total synthesis of (+)-ryanodol completed, the Inoue group subsequently focused on its conversion to (+)-ryanodine (**1**). Attempts by Deslongchamps and coworkers had previously demonstrated that the steric hindrance of the C3-alcohol prohibited selective acylation, instead favoring reactivity at the more sterically accessible C10-alcohol.¹³ In 2016, Inoue successfully demonstrated the conversion of (+)-ryanodol to (+)-ryanodine by employing an elaborate protecting group strategy.⁵⁶ All reactive alcohol functionalities were first protected, in total employing two phenylboronic acid

protecting groups, one benzyl protecting group, and one acetyl protecting group, to afford protected ryanodol **53** and leaving only the C3-alcohol accessible. Acylation was subsequently achieved with Yamaguchi's reagent in conjunction with protected glycine **54** and transformed to the carboxypyrrole derivative via cyclocondensation with tetrafluoroborate salt **56**. Finally, removal of the protecting groups was effected in three steps to provide (+)-ryanodine. The implementation of this study subsequently informed the choice of protecting groups necessary to intercept previously described synthetic intermediates in their prior total synthesis of (+)-ryanodol, thus enabling the first total synthesis of (+)-ryanodine, proceeding in 42 total steps.⁵⁷



Scheme 4. A ten step conversion of (+)-ryanodol to (+)-ryanodine by Inoue (2016)

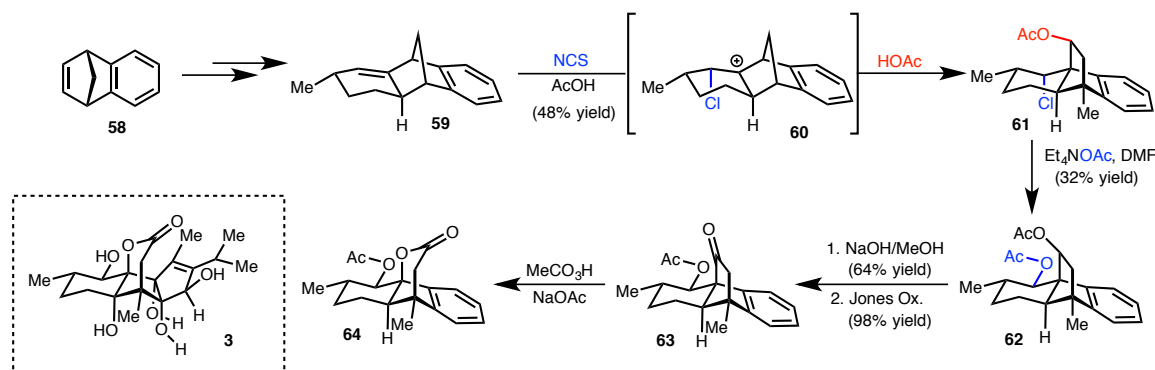
1.5 PRIOR EFFORTS TOWARDS (+)-RYANODOL

Although the Deslongchamps⁴⁹ (1979) and Inoue⁵⁸ (2014) approaches outlined in the previous section above constitute the only two completed total syntheses reported to date, the pursuit of ryanodol has been the focus of a number of publications and Ph. D. dissertations⁵⁹⁻⁶¹ since its initial structural elucidation. These reports have established the viability of new synthetic strategies to establish model fragments mapping onto the

congested pentacyclic framework of ryanodol and educated the design of synthetic work in this area.

1.5.1 Wiesner's Approach to Anhydroryanodol

An early report of a model system toward the anhydroryanodol framework was published by Wiesner in 1972 (**Scheme 5**), utilizing a key, oxidation-triggered rearrangement to build the BCD-ring system.⁶² Starting from benzonorbornadiene (**58**), tetracyclic olefin **59** was treated with *N*-chlorosuccinimide in acetic acid, resulting in a 1,2-aryl shift to generate chloroacetate **61**. Selective displacement of the chloride moiety with Et₄NOAc in DMF afforded bisacetate **62**, which could be selectively saponified and subsequently oxidized using Jones reagent to afford tetracyclic ketone **63**. Late stage Baeyer-Villiger oxidation then affords the corresponding lactone **64**, generating a structure that maps well onto the anhydroryanodol BCD-ring system.

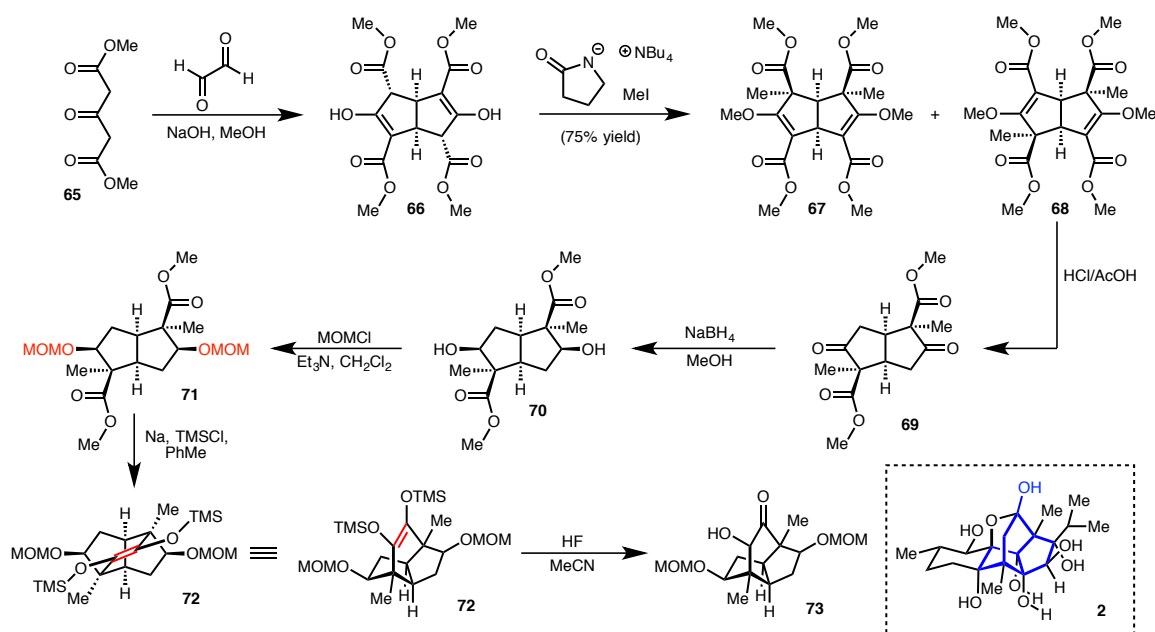


Scheme 5. Wiesner's rearrangement approach to the anhydroryanodol BCD-ring system.

1.5.2 Sieburth's C₂-Symmetric Approach to Ryanodol

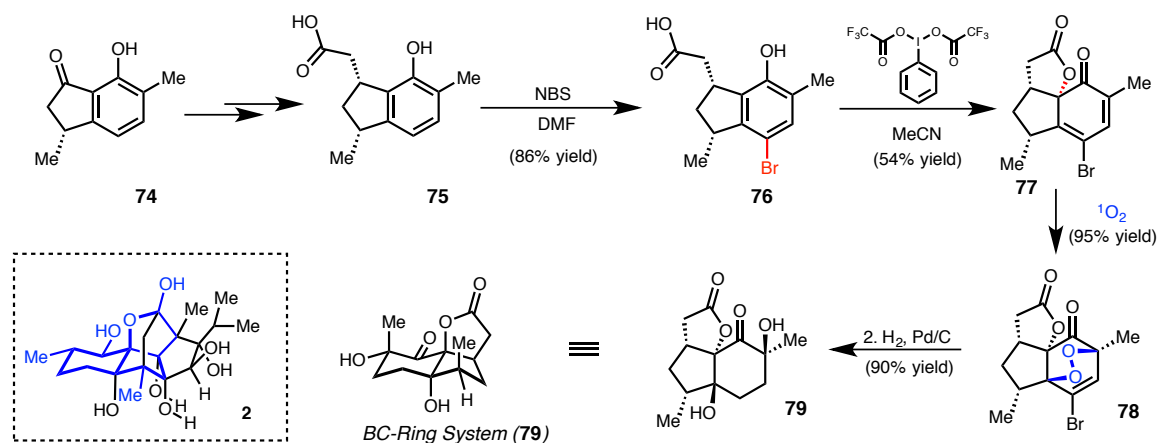
In 1994, Sieburth and Santos reported a concise method to access the central tricyclo[3.3.2^{1,4}.0]decane ring system present in the ryanodol core, recognizing the latent

C_2 -symmetry present within the diterpenoid framework (**Scheme 6**).⁶³ Notably, identification of this hidden symmetry element was the central strategy within Inoue's subsequent total synthesis published in 2014 (see **Scheme 3**),^{53-55,58} and similarly pursued by other laboratories.^{59,60} Condensation of dimethylacetonedicarboxylate (**65**) with glyoxal resulted in the C_2 -symmetric, tetraester **66**, which could be methylated under mild conditions to afford a 1:1 mixture of *meso*- to *rac*- substrates **67** and **68**. Krapcho-type decarboxylation under acidic conditions, followed by 1,2-carbonyl reduction and protection of the resulting secondary alcohols as their MOM-ethers provided diester **71**. A key acyloin condensation employing Na(0)-metal in the presence of TMSCl resulted in bis(trimethylsiloxy)alkene **72**, establishing a deoxygenated ABE-ring system within ryanodol.



Scheme 6. A C_2 -symmetric approach to ryanodol's ABE-ring system by Sieburth (1994)

1.5.3 Wood's Phenolic Oxidation Approach to Ryanodol



Scheme 7. A phenolic oxidation approach to the BC-ring system by Wood (2003)

A phenolic oxidation strategy to access the BC-ring system of the ryanodol core was employed by Wood and coworkers in 2003, in which the tetrahydrofuran ring was envisioned to be prepared via intramolecular cyclization of a pendant nucleophile onto the *ortho*-position of an appropriately functionalized phenol.^{61,64} To this end, phenol **76**, bearing a *para*-bromide as a blocking group, was readily prepared from hydroxyindanone **74**. Oxidative dearomatization using iodobenzene(bistrifluoroacetate) in acetonitrile afforded lactone **77** in 80% yield. Notably, attempts to effect this transformation without a *para*-bromide resulted in decomposition products as a result of trapping with the nucleophilic solvent. The product was then elaborated via a [4 + 2] cycloaddition with singlet oxygen to provide endoperoxide **78**, that was then reduced via Pd-catalyzed hydrogenation to afford the hydroxylated BC-ring system (**79**) in 90% yield.

1.6 CONCLUDING REMARKS

Ryanodine, ryanodol, and related natural products have inspired numerous studies in the nearly 70 years since ryanodine's isolation, ranging from chemical structure elucidation to protein purification of the RyR calcium ion channels. By understanding the structure, activity, and synthesis of this challenging diterpenoid natural product, considerable insights have been gained in a number of interdisciplinary fields. Within the context of chemical synthesis, the novel molecular architecture has not only uncovered important aspects of the reactivity of these molecules, but also motivated the design of new synthetic methods and approaches to complex molecule synthesis. It is clear from these studies that continued interest in and attention to this remarkable class of polyoxygenated molecules will inspire the development of new synthetic methods. Ultimately, it is anticipated that a truly practical and efficient preparation of (+)-ryanodine and related analogs will be accessible via *de novo* chemical synthesis.

REFERENCES AND NOTES

- (1) Crosby, D. G. *Naturally Occurring Insecticides*; Marcel Dekker, 1971.
- (2) Rogers, E. F.; Koniuszy, F. R.; Shavel, J., Jr.; Folkers, K. *J. Am. Chem. Soc.* **1948**, *70* (9), 3086.
- (3) Kelly, R. B.; Whittingham, D. J.; Wiesner, K. *Can. J. Chem.* **1951**, *29*, 905.
- (4) Babin, D. R.; Findlay, J. A.; Forrest, T. P.; Fried, F.; Götz, M.; Valenta, Z.; Wiesner, K. *Tetrahedron Lett.* **1960**, *1* (36), 31.
- (5) Valenta, Z.; Wiesner, K.; Babin, D. R.; Bögli, T.; Forrest, T. P.; Fried, F.; Reinshagen, H. *Experientia* **1962**, *18* (3), 111.
- (6) Babin, D. R.; Forrest, T. P.; Valenta, Z.; Wiesner, K. *Experientia* **1962**, *18* (12), 549.
- (7) Wiesner, K. *Collect. Czech. Chem. Commun.* **1968**, *33* (8), 2656.
- (8) Wiesner, K.; Valenta, Z.; Findlay, J. A. *Tetrahedron Lett.* **1967**, *8* (3), 221.
- (9) Babin, D. R. "The Structures of Delphinine and Neoline; Ryanodine." Ph. D. Thesis. University of New Brunswick, **1962**.
- (10) Srivastava, S. N.; Przybylska, M. *Can. J. Chem.* **1968**, *46* (5), 795.
- (11) Srivastava, S. N.; Przybylska, M. *Acta Crystallogr., Sect. B: Struct. Sci* **1970**, *26* (6), 707.
- (12) Wiesner, K. *Adv. Org. Chem.* **1972**, *8*, 295.
- (13) Deslongchamps, P.; Bélanger, A.; Berney, D. J. F.; Borschberg, H.-J.; Brousseau, R.; Doutheau, A.; Durand, R.; Katayama, H.; Lapalme, R.; Leturc, D. M.; Liao, C.-C.; MacLachlan, F. N.; Maffrand, J.-P.; Marazza, F.; Martino, R.; Moreau, C.; Ruest, L.; Saint-Laurent, L.; Saintonge, R.; Soucy, P. *Can. J. Chem.* **1990**, *68* (1),

- 186.
- (14) Waterhouse, A. L.; Holden, I.; Casida, J. E. *J. Chem. Soc., Chem. Commun.* **1984**, 0 (19), 1265.
- (15) Jefferies, P. R.; Toia, R. F.; Casida, J. E. *J. Nat. Prod.* **1991**, 54 (4), 1147.
- (16) Ruest, L.; Berthelette, C.; Dodier, M.; Dubé, L.; St-Martin, D. *Can. J. Chem.* **1999**, 77 (1), 12.
- (17) Ruest, L.; Dodier, M.; De Sève, H.; Lessard, C.; Mongrain, P. *Can. J. Chem.* **2011**, 80 (5), 483.
- (18) Jefferies, P. R.; Toia, R. F.; Brannigan, B.; Pessah, I.; Casida, J. E. *J. Agric. Food Chem.* **1992**, 40, 142.
- (19) Yagi, A.; Tokubuchi, N.; Nohara, T.; Nonaka, G.; Nishioka, I.; Koda, A. *Chem. Pharm. Bull.* **1980**, 28 (5), 1432.
- (20) Nohara, T.; Tokubuchi, N.; Kuroiwa, M.; Nishioka, I. *Chem. Pharm. Bull.* **1980**, 28 (9), 2682.
- (21) Nohara, T.; Kashiwada, Y.; Tomimatsu, T.; Nishioka, I. *Phytochemistry* **1982**, 21 (8), 2130.
- (22) Nohara, T.; Nishioka, I.; Tokubuchi, N.; Miyahara, K.; Kawasaki, T. *Chem. Pharm. Bull.* **1980**, 28 (6), 1969.
- (23) Kashiwada, Y.; Nohara, T.; Tomimatsu, T.; Nishioka, I. *Chem. Pharm. Bull.* **1981**, 29 (9), 2686.
- (24) Nohara, T.; Kashiwada, Y.; Nishioka, I. *Phytochemistry* **1985**, 24 (8), 1849.
- (25) Achenbach, H.; Hübner, H.; Vierling, W.; Brandt, W.; Reiter, M. *J. Nat. Prod.* **1995**, 58 (7), 1092.

- (26) Hübner, H.; Vierling, W.; Brandt, W.; Reiter, M.; Achenbach, H. *Phytochemistry* **2001**, 57 (2), 285.
- (27) González-Coloma, A.; Hernandez, M. G.; Perales, A.; Fraga, B. M. *J. Chem. Ecol.* **1990**, 16 (9), 2723.
- (28) Fraga, B. M.; Terrero, D.; Gutiérrez, C.; González-Coloma, A. *Phytochemistry* **2001**, 56 (4), 315.
- (29) González-Coloma, A.; Terrero, D.; Perales, A.; Escoubas, P.; Fraga, B. M. *J. Agric. Food Chem.* **1996**, 44 (1), 296.
- (30) Isogai, A.; Murakoshi, S.; Suzuki, A.; Tamura, S. *Agric. Biol. Chem.* **2014**, 41 (9), 1779.
- (31) Koshimizu, M.; Nagatomo, M.; Inoue, M. *Angew. Chem. Int. Ed.* **2016**, 55 (7), 2493.
- (32) Sutko, J. L.; Thompson, L. J.; Schlatterer, R. G.; Lattanzio, F. A.; Fairhurst, A. S.; Campbell, C.; Martin, S. F.; Deslongehamps, P.; Ruest, L.; Taylor, D. R. *J. Labelled Comp. Radiopharm.* **2006**, 23 (2), 215.
- (33) Sutko, J. L.; Airey, J. A.; Welch, W.; Ruest, L. *Pharmacol. Rev.* **1997**, 49 (1), 53.
- (34) Rousseau, E.; Smith, J. S.; Meissner, G. *Am. J. Physiol., Cell Physiol.* **1987**, 253 (3), C364.
- (35) Meissner, G. *Annu. Rev. Physiol.* **1994**, 56 (1), 485.
- (36) Kimlicka, L.; Van Petegem, F. *Sci. China Life Sci.* **2011**, 54 (8), 712.
- (37) Lanner, J. T.; Georgiou, D. K.; Joshi, A. D.; Hamilton, S. L. *Cold Spring Harb. Perspect. Biol.* **2010**, 2 (11), a003996.
- (38) Wu, S.; Ibarra, M. C. A.; Malicdan, M. C. V.; Murayama, K.; Ichihara, Y.;

- Kikuchi, H.; Nonaka, I.; Noguchi, S.; Hayashi, Y. K.; Nishino, I. *Brain* **2006**, *129* (Pt 6), 1470.
- (39) Rosenberg, H.; Davis, M.; James, D.; Pollock, N.; Stowell, K. *Orphanet J. Rare Dis.* **2007**, *2* (1), 21.
- (40) Wehrens, X. H. T.; Marks, A. R. *Mayo Clin. Proc.* **2004**, *79* (11), 1367.
- (41) Liu, X.; Betzenhauser, M. J.; Reiken, S.; Meli, A. C.; Xie, W.; Chen, B.-X.; Arancio, O.; Marks, A. R. *Cell* **2012**, *150* (5), 1055.
- (42) Wu, B.; Yamaguchi, H.; Lai, F. A.; Shen, J. *Proc. Natl. Acad. Sci. U.S.A.* **2013**, *110* (37), 15091.
- (43) D’Adamio, L.; Castillo, P. E. *Proc. Natl. Acad. Sci. U.S.A.* **2013**, *110* (37), 14825.
- (44) Belevych, A. E.; Terentyev, D.; Gyorke, S. *Novel Therapeutic Targets For Antiarrhythmic Drugs*; Billman, G. E., Ed.; John Wiley & Sons, Inc.: Hoboken, NJ, USA, 2010; pp 299–312.
- (45) Dulhunty, A. F.; Casarotto, M. G.; Beard, N. A. *Curr. Drug Targets* **2011**, *12* (5), 709.
- (46) Turan, B.; Vassort, G. *Antioxid. Redox Signal.* **2011**, *15* (7), 1847.
- (47) Fauconnier, J.; Roberge, S.; Saint, N.; Lacampagne, A. *Pharmacol. Ther.* **2013**, *138* (3), 323.
- (48) Welch, W.; Sutko, J. L.; Mitchell, K. E.; Airey, J.; Ruest, L. *Biochemistry* **1996**, *35* (22), 7165.
- (49) Bélanger, A.; Berney, D.; Borschberg, H.-J.; Brousseau, R.; Doutheau, A.; Durand, R.; Katayama, H.; Lapalme, R.; Leturc, D. M.; Liao, C.-C.;

- MacLachlan, F. N.; Maffrand, J.-P.; Marazza, F.; Martino, R.; Moreau, C.; Saint-Laurent, L.; Saintonge, R.; Soucy, P.; Ruest, L.; Deslongchamps, P. *Can. J. Chem.* **1979**, *57*, 3348.
- (50) Deslongchamps, P.; Bélanger, A.; Berney, D. J. F.; Borschberg, H.-J.; Brousseau, R.; Doutheau, A.; Durand, R.; Katayama, H.; Lapalme, R.; Leturc, D. M.; Liao, C.-C.; MacLachlan, F. N.; Maffrand, J.-P.; Marazza, F.; Martino, R.; Moreau, C.; Ruest, L.; Saint-Laurent, L.; Saintonge, R.; Soucy, P. *Can. J. Chem.* **1990**, *68* (1), 115.
- (51) Deslongchamps, P.; Bélanger, A.; Berney, D. J. F.; Borschberg, H.-J.; Brousseau, R.; Doutheau, A.; Durand, R.; Katayama, H.; Lapalme, R.; Leturc, D. M.; Liao, C.-C.; MacLachlan, F. N.; Maffrand, J.-P.; Marazza, F.; Martino, R.; Moreau, C.; Ruest, L.; Saint-Laurent, L.; Saintonge, R.; Soucy, P. *Can. J. Chem.* **1990**, *69*, 127.
- (52) Deslongchamps, P.; Bélanger, A.; Berney, D. J. F.; Borschberg, H.-J.; Brousseau, R.; Doutheau, A.; Durand, R.; Katayama, H.; Lapalme, R.; Leturc, D. M.; Liao, C.-C.; MacLachlan, F. N.; Maffrand, J.-P.; Marazza, F.; Martino, R.; Moreau, C.; Ruest, L.; Saint-Laurent, L.; Saintonge, R.; Soucy, P. *Can. J. Chem.* **1990**, *68*, 153.
- (53) Hagiwara, K.; Himuro, M.; Hirama, M.; Inoue, M. *Tetrahedron Lett.* **2009**, *50* (9), 1035.
- (54) Tabuchi, T.; Urabe, D.; Inoue, M. *Beilstein J. Org. Chem.* **2013**, *9* (1), 655.
- (55) Urabe, D.; Nagatomo, M.; Hagiwara, K.; Masuda, K.; Inoue, M. *Chem. Sci.* **2013**, *4* (4), 1615.

- (56) Masuda, K.; Nagatomo, M.; Inoue, M. *Chem. Pharm. Bull. In Press.* **2016**.
- (57) Masuda, K.; Koshimizu, M.; Nagatomo, M.; Inoue, M. *Chem. Eur. J.* **2016**, 22 (1), 230.
- (58) Nagatomo, M.; Koshimizu, M.; Masuda, K.; Tabuchi, T.; Urabe, D.; Inoue, M. *J. Am. Chem. Soc.* **2014**, 136, 5916.
- (59) Wang, B. "Photochemistry of 6- Alkenyl- 2- Cyclohexenones. Synthetic Studies towards Precursors of Ryanodol." Ph. D. Thesis. Oregon State University, **1998**.
- (60) Morales, C. A. "Biomimetic Synthesis of (–)-Longithorone A and Synthesis of the Ryanodine Core." Ph. D. Thesis. Harvard University, **2004**.
- (61) Graeber, J. K. "Studies Toward the Total Synthesis of Ryanodine." Ph. D. Thesis. Yale University, **2003**.
- (62) Brownlee, B. G.; Ho, P.-T.; Wiesner, K. *Can. J. Chem.* **2011**, 50, 4013.
- (63) Sieburth, S. M.; Santos, E. D. *Tetrahedron Lett.* **1994**, 35 (44), 8127.
- (64) Wood, J. L.; Graeber, J. K.; Njardarson, J. T. *Tetrahedron* **2003**, 59 (45), 8855.

Chapter 2

Total Synthesis of (+)-Ryanodol

2.1 INTRODUCTION

The potent biological activity and unique structure of (+)-ryanodine (**1**) prompted our laboratory in 2011 to begin synthetic investigations toward this diterpenoid natural product, with the goal of executing a practical and enantioselective synthesis. Numerous synthetic approaches were attempted in order to construct the sterically congested and richly decorated ryanodane framework, which, along with model studies, are schematically summarized in **Appendix 3**. This chapter describes a successful and optimized total synthesis of (+)-ryanodol from the commercially available monoterpene (*S*)-pulegone, proceeding in only 15-steps. It is anticipated that the strategic blueprint detailed within this chapter will enable the future preparation of numerous *Ryania* natural products including (+)-ryanodine, and serve as the basis for detailed structure-activity relationship studies for the identification of potent synthetic ryanoids.

2.1.1 Structure and Synthetic Challenges

From a structural standpoint, ryanodol possesses numerous synthetic challenges. Embedded within its highly caged, pentacyclic core are 11-contiguous stereocenters, two

of which are all-carbon quaternary centers, and possesses seven free hydroxyl moieties. In the absence of these hydroxyl groups, the carbocyclic core itself presents a formidable challenge; the 5-5-6, ABC-ring system is spanned by a two-carbon bridge constituting the E-ring, and an oxygen bridge forming the D-ring. The C2-isopropyl group is buried within the concave face of the AE-pocket, creating a highly congested environment for the C3-alcohol. Further analysis reveals that the high level of oxidation and specific oxygen atom placement is nontrivial. Perhaps best stated by Deslongchamps after a similar structural analysis, “It can be concluded from this analysis that ryanodol is indeed a very complex diterpene in which only three carbons of the skeleton are left unfunctionalized as methylene groups.”¹

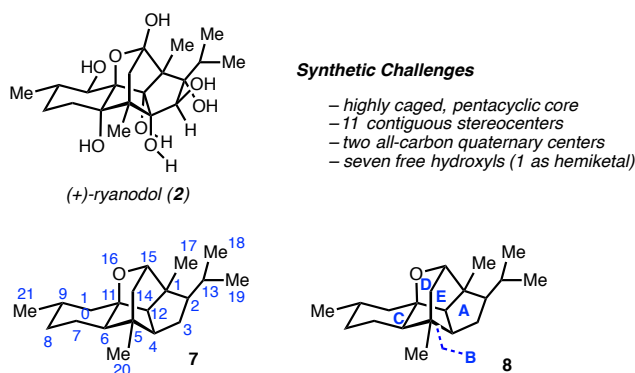
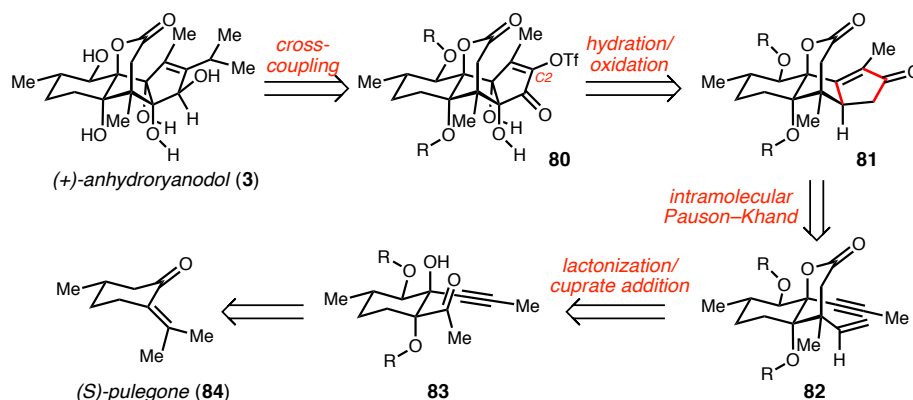


Figure 1. The structure and synthetic challenges of (+)-ryanodol

2.1.2 Retrosynthetic Analysis

Considerable revisions to our initial retrosynthetic analysis were performed in an effort to continuously improve and evaluate multiple synthetic strategies. Extensive route scouting and optimization were necessary to arrive at the approach described within this chapter, with the pursuit of numerous unsuccessful avenues necessary for educating the specific design herein.

Guided by the landmark studies of Deslongchamps and coworkers,¹⁻⁵ our final retrosynthetic analysis posited that the C1-C14 bond of ryanodol (**2**) was, in fact, the most simplifying and strategic retrosynthetic disconnection, in turn revealing tetracyclic anhydroryanodol as an initial synthetic target (**Scheme 1**). Envisioning that late-stage introduction of the isopropyl group could occur through a transition metal-catalyzed cross-coupling reaction of vinyl triflate **80**, we anticipated that the requisite A-ring oxidation pattern could be accessed via chemo- and stereoselective functionalization of cyclopentenone **81**, whereby the enone would provide a functional group handle to install the critical C3, C4, and C12 alcohols of **2**. Enone **81** was expected to be accessible via an intramolecular Pauson–Khand reaction, a transformation that we expected to be facilitated by the conformational rigidity of bicyclic lactone **82**. In turn, it was thought that the lactone moiety would be prepared from an appropriately functionalized cyclohexane building block (**83**), accessible from a simple monoterpene unit such as the commercially available (*S*)-pulegone (**84**). By this analysis, the oxygen atoms at C6, C10, and C11 would be incorporated early in the synthesis, while the oxygen atoms at C3, C4, and C12 would be introduced at a late stage. With the implementation of appropriate protecting groups, we anticipated that this strategy would minimize unnecessary synthetic redox manipulations, resulting in a concise step count.

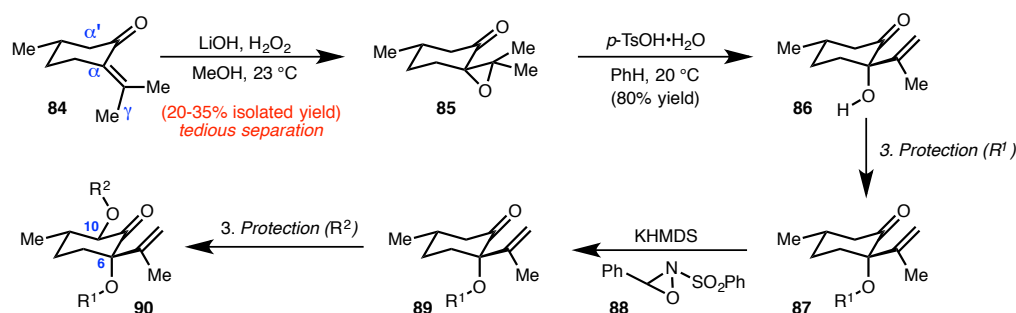


Scheme 1. Retrosynthetic analysis of (+)-anhydroryanodol

2.2 FORWARD SYNTHETIC EFFORTS

2.2.1 Oxidation Studies of (S)-Pulegone

Our studies commenced with the appropriate functionalization of (S)-pulegone, a commercially available monoterpene unit conveniently prepared on decagram scale by the procedure of Corey and Suggs.⁶ Given our retrosynthetic analysis, it was envisioned that early stage C6- and C10-hydroxyl incorporation should be performed at the earliest stage possible in the synthesis. In light of this assessment, it was determined that pulegone could be stereoselectively functionalized in five steps to afford oxygenated ketone **90**, possessing a range of potential protecting groups. In this sequence, pulegone is first epoxidized under nucleophilic conditions to provide epoxyketone **85**. Tedious and repetitive chromatographic separation of the diastereomeric epoxides enables isolation of pure **85**,⁷ typically in 20-35% isolated yield after additional recrystallization. Acid-mediated isomerization and protection provides ketone **87**,⁸ which can be subsequently oxidized through treatment with KHMDS and Davis oxaziridine **88**.⁹ A final protection provides **90** in five chemical steps, in total requiring several chromatographically challenging separations and offering limited material throughput.

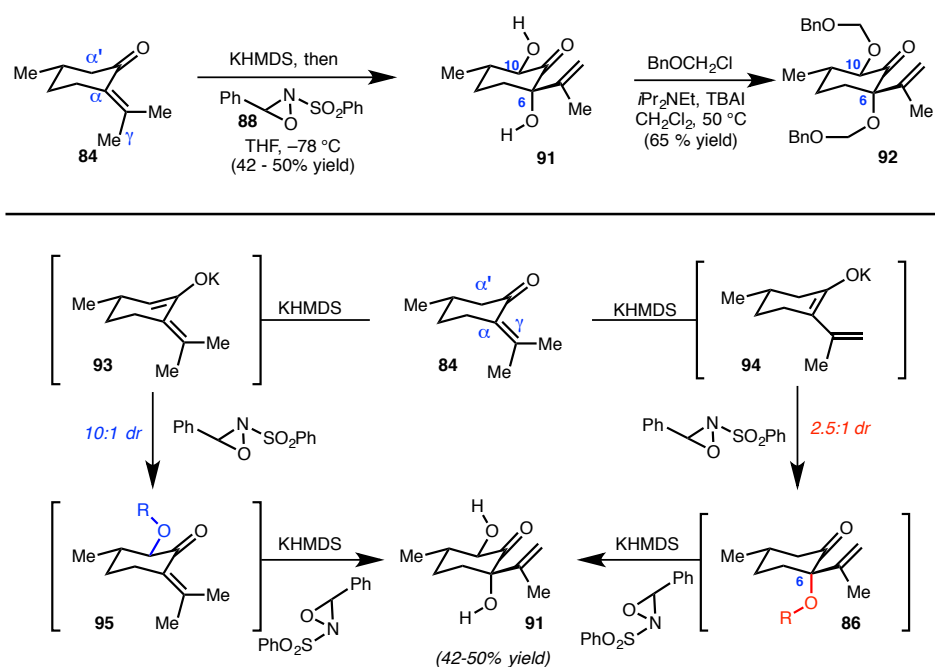


Scheme 2. Initial route for the preparation of protected ketone building block **90**.

Positing that a more efficient approach should be feasible, we hypothesized that the C6-oxidation state might also be directly installed via enolate oxidation (**Scheme 3**). Treatment of (*S*)-pulegone at $-78\text{ }^{\circ}\text{C}$ with 0.95 equiv KHMDS followed by warming to $0\text{ }^{\circ}\text{C}$ for 1h enabled efficient equilibration to the thermodynamic, potassium enolate (**94**), which could be oxidatively trapped at C6, providing a 2.5 : 1 mixture of diastereomeric alcohols. Next, noting the apparent compatibility of Davis oxaziridine **88** with excess KHMDS, we hypothesized that a one-pot protocol to simultaneously install both the C6- and C10-alcohols in a single step might be possible. Indeed, treatment of **84** with 2.5 equiv of KHMDS at $-78\text{ }^{\circ}\text{C}$ followed by dropwise addition of 2.4 equiv of **88** provided α,α' -diol **91**, which could be isolated as a single diastereomer in 42% yield on 120 mmol scale. Although the yield is modest, we note that in a single transformation, a simple terpene is converted to a valuable building block possessing the requisite ryanodol C-ring oxidation pattern. Further investigations revealed that the efficiency of this transformation could be improved to 50% yield by initial equilibration to the thermodynamic enolate (**94**) and use of toluene as a cosolvent. However, given the operational simplicity of the former procedure on larger scales, this protocol was preferentially employed for increased material throughput. A screen of oxaziridines

varying in substitution and parent structure did not reveal improved yields;¹⁰⁻¹² in particular, oxaziridines bearing acidic α -protons were not compatible with this one pot protocol.¹²

Notably, the difference in reactivity of the secondary and tertiary alcohols of **91** are pronounced; selective monoprotection of the C10-alcohol is readily achieved under mild conditions, whereas more forcing conditions enable protection of the C6-tertiary alcohol. Seeking a mild protecting group for elaboration in our studies, diol **91** was readily bisprotected by treatment with excess benzyl chloromethyl ether in the presence of di-*iso*-propylethylamine and tetrabutylammonium iodide to provide ketone **92** in 65% yield.



Scheme 3. A direct, bishydroxylation of pulegone via double enolate oxidation

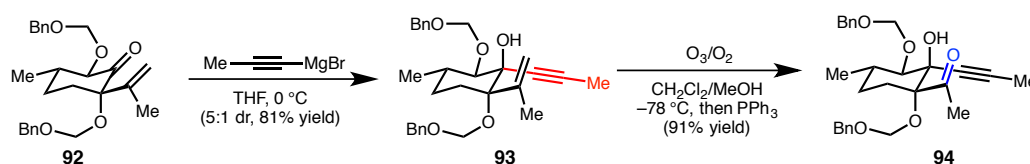
2.2.2 Synthesis of the D-Ring Lactone

At this stage, preparation of the D-ring lactone became the focus of our studies. To this end, addition of propynylmagnesium bromide to **92** at 0 °C proceeded in 5:1 dr, providing the equatorially-disposed alkyne in 81% isolated yield. It is notable that the C10-secondary ether results in significant improvements in the diastereoselectivity of this addition. Model substrates lacking the C10-oxidation state result in a nearly non-selective process, giving rise to an equal mixture of axial and equatorial alkyne adducts. Ozonolytic cleavage of the 1,1-disubstituted olefin proceeded in excellent yield to afford methyl ketone **94**; the use of methanol cosolvent in this transformation was found to be critical to avoid deleterious C5-C6 bond fragmentation¹³ that precluded high yields. With the β -hydroxyketone established, it was initially envisioned that lactone synthesis could be achieved via application of an *N, N'*-dicyclohexylcarbodiimide-mediated phosphonoacylation/intramolecular Horner–Wadsworth–Emmons lactone synthesis.^{14,15} This approach, known to be particularly effective for hindered tertiary alcohols, had proven serviceable in model studies lacking C10-oxidation. Unfortunately, **94** proved resistant to acylation under a number of conditions. Presumably, the increased steric encumbrance and inductively withdrawing C10-ether dramatically decreases the nucleophilicity of the tertiary alkynol. Instead, an alternative protocol was established, in which ketone **94** was first converted to diyne **97** via addition of ethoxyethynylmagnesium bromide, and subsequently converted to the α,β -unsaturated lactone via a AgOTf-mediated cyclization/elimination cascade.¹⁶

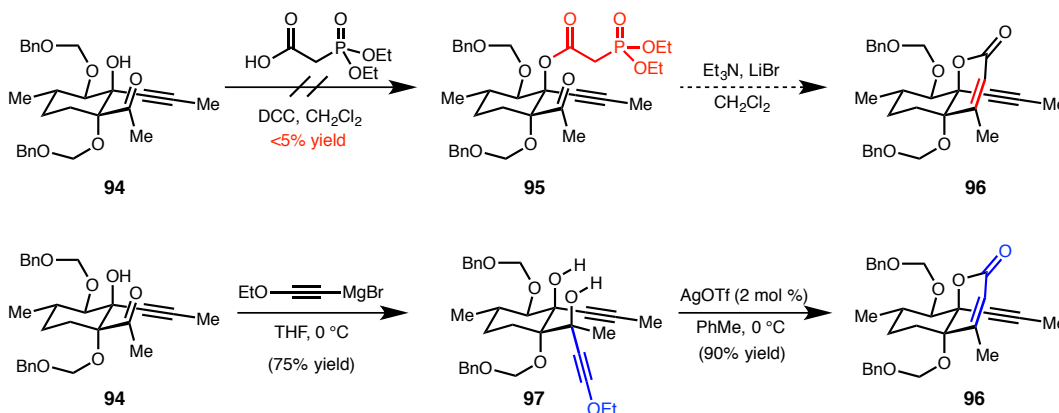
It was envisioned that the newly formed α,β -unsaturated lactone moiety could serve as an excellent electrophile for a carbon based nucleophile, and that construction of

one of the all-carbon quaternary centers might be achieved via the reliable addition of an appropriate cuprate. Indeed, treatment of **96** with vinylmagnesium bromide (6.0 equiv) in the presence of CuI (3.0) at cryogenic temperatures (-78 to -30 °C) effected a smooth 1,4-conjugate vinylation, providing a single diastereomer of **98** in 84% yield. Importantly, the establishment of this critical all-carbon C5-quaternary center provides a uniquely rigid bicyclic framework that enforces the proximity of the olefin and alkyne in a 1,3-diaxial fashion. By design, it was expected that the geometrical constraints imparted by the rigid framework should enable both an efficient and stereoselective intramolecular Pauson–Khand reaction.

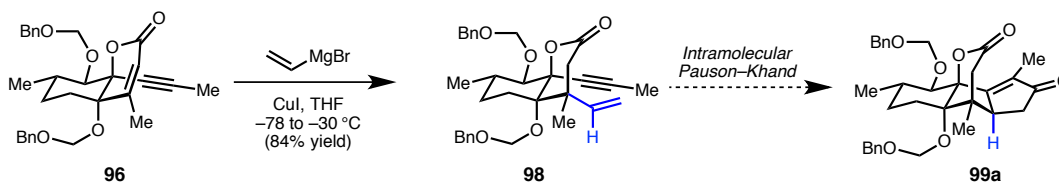
A) Alkynylation and Synthesis of β -Hydroxy Ketone **94**



B) D-Ring Lactone Synthesis



C) Conjugate Addition

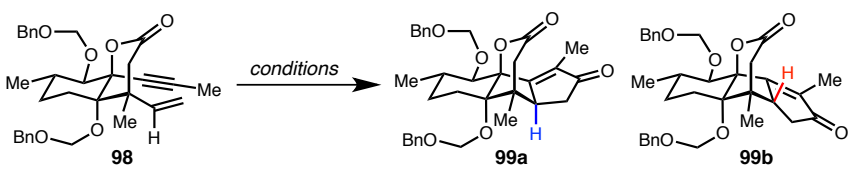


Scheme 4. Preparation of the CD-bicyclic ring system

2.2.3 Synthesis of the ABCD-Ring System

The preparation of the critical enyne **98** subsequently allowed for the evaluation of a key, intramolecular Pauson–Khand reaction, which was envisioned to deliver the ABCD-ring system of anhydroryanodol while providing a useful cyclopentenone moiety for further functionalization of the A-ring. A number of Pauson–Khand procedures were screened for high yield and diastereoselectivity (**Table 1**). Although standard conditions utilizing stoichiometric amounts of $\text{Co}_2(\text{CO})_8$ ^{17,18} produced the desired product, separation of diastereomeric enones **99a** and **99b** proved challenging and indicated that a more selective protocol was necessary. Monometallic mediators were found to improve the dr, with $\text{Mo}(\text{CO})_3(\text{DMF})_3$ ¹⁸ providing **99a** as a single diastereomer in 67% yield. Despite the serviceable yield and scalability of this transformation, we sought a more efficient protocol that could obviate the need for stoichiometric metals and their resulting byproducts. With this in mind, we were pleased to find that treatment of **98** with 1 mol% $[\text{RhCl}(\text{CO})_2]_2$ ¹⁹ under an atmosphere of carbon monoxide provided the desired product in 85% yield, again as a single diastereomer. Excitingly, the realization of this key Pauson–Khand reaction enables the efficient preparation of the ABCD-tetracycle in *only eight steps* from commercially available materials, providing multi-gram quantities of this key intermediate. Structural and stereochemical confirmation was provided both by rigorous NMR spectroscopic techniques, but furthermore, was unambiguously assigned via single crystal X-ray diffraction analysis of **99a**.

Table 1. Evaluation of reaction parameters for an intramolecular Pauson–Khand reaction



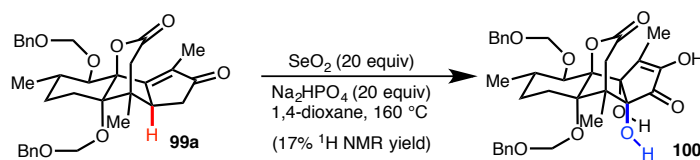
entry	conditions	dr ^b	yield (%) ^c
1	Co ₂ (CO) ₈ (1.2 equiv), THF, 12 h; then DMSO, 65 °C	2.2 : 1	46
2	Co ₂ (CO) ₈ (1.2 equiv), CH ₂ Cl ₂ , 9 h; then NMO, 23 °C	4.5 : 1	78
3	Mo(CO) ₆ (1.2 equiv), DMSO, PhMe, 110 °C	--	trace
4	Mo(CO) ₃ (DMF) ₃ (1.1 equiv), CH ₂ Cl ₂ , 23 °C	> 20 : 1	67
5	[RhCl(CO) ₂] ₂ (1 mol %), CO (1 atm), <i>m</i> -xylene, 110 °C	>20 : 1	85

^a Reactions conducted on 0.2 mmol scale. ^b Determined by ¹H NMR of the mixture of diastereomers.

^c Isolated yield after purification by silica gel chromatography.

2.2.4 Selenium Dioxide Mediated A-Ring Functionalization

The realization of our key Pauson–Khand cyclization led us to the next phase of our synthetic studies; specifically, chemo- and stereoselective functionalization of the A-ring through the introduction of the C3, C4, and C12-alcohols as well as the C2-isopropyl unit were anticipated to present formidable challenges. Indeed, initial forays into functionalization of the C4-H methine were immediately frustrated by undesired reactivity; established methods for allylic oxidation via generation of reactive radical species (e. g. Pd[OH]₂/TBHP,²⁰ Rh₂(cap)₄/TBHP²¹, Cr[V]-species²²) were unfruitful due to competitive functionalization of the C1-C12 olefin (e. g. epoxidation, 1,2-difunctionalization), while more forcing conditions typically led to nonselective oxidative fragmentation of the cyclopentenone. Although we entertained the possibility of advancing these unanticipated products further in the synthesis, it was unclear how transposition of the requisite oxidation pattern could be efficiently achieved.



Scheme 5. Initial discovery of a remarkable selenium dioxide mediated oxidation reaction

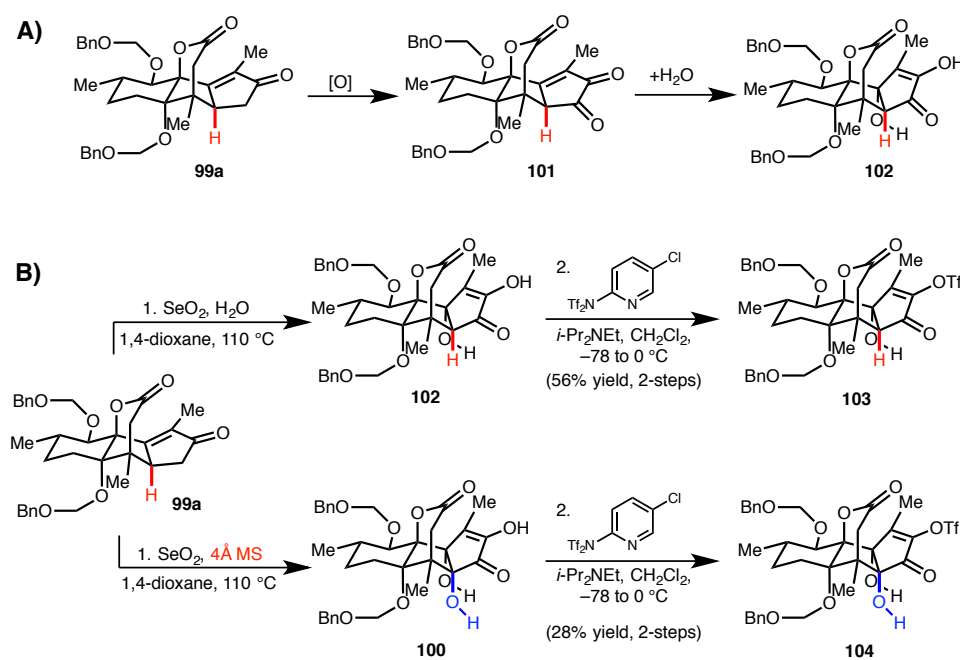
In continued attempts to directly functionalize the C4-position via non-radical based allylic oxidations, highly forcing conditions utilizing SeO_2 at significantly elevated temperatures were screened. Fortuitously, it was discovered that treatment with a large excess of SeO_2 in the presence of phosphate buffer at 160 °C for 15 minutes resulted in the isolation of a new, oxidized product (**Scheme 5**). Rigorous structural assignment of this compound revealed it to be the fully oxidized diosphenol **100**, a compound possessing the C4, C12 *syn*-vicinal diol of **2**. This astonishing single-step transformation installs the necessary oxygen atoms at C3, C4, and C12 while simultaneously providing a functional handle for incorporation of the C2-isopropyl group. In contrast, at lower temperatures in the presence of SeO_2 , diosphenol **102** is the predominant product, lacking the C4-oxidation state, but still effecting a formal Riley oxidation²³ and hydration of the C1-C12 olefin.

Since C4-deoxy analogs of ryanodine are themselves natural products and of potential interest for future biological studies,^{24,25} we optimized procedures to prepare both **100** and **102** (**Scheme 6**). Due to concerns that contamination by ^1H NMR silent, red selenium byproducts resulted in artificially inflated isolated yields, our optimization efforts were guided by ^1H NMR yields determined by integration versus an external standard, and isolated yields were determined after conversion to corresponding vinyl triflates **103** and **104**, which could be obtained as analytically pure compounds. Thus, subjection of tetracycle **99a** to 10 equiv of SeO_2 in wet 1,4-dioxane at 110 °C for 1 h

provided **102** in 67-69% ^1H NMR yield, and the corresponding vinyl triflate **103** in 56% isolated yield over two steps. Alternatively, treatment of **99a** with 10 equiv of SeO_2 in anhydrous 1,4-dioxane in the presence of freshly activated 4Å MS at 110 °C for 9 h provided **100** in 33-35% ^1H NMR yield, and vinyl triflate **104** in 28% isolated yield over two steps. Despite the modest yield, this reaction accomplishes the stereospecific incorporation of three oxygen atoms, proceeds with an average efficiency of approximately 70% yield per transformation, and fares well in comparison to conceivable multistep protocols to achieve the same reactivity.

The complexity of this transformation warrants a few additional comments. Formally, **100** can be thought to arise by oxidation to the α -diketone, hydration of the enone, and C–H oxidation of the C4 methine (**Scheme 6A**). Although the precise mechanism remains unclear at this time, a few observations are relevant: 1) reactions conducted under rigorously anhydrous conditions still result in formation of **102**, suggesting that the C12-alcohol may be incorporated directly from SeO_2 , rather than water; 2) reactions run under rigorously deoxygenated conditions inside a nitrogen-filled glovebox provide **100** in comparable yield, an observation that is inconsistent with the C4-alcohol arising from aerobic oxidation; 3) reactions run to low conversion result in isolation of diosphenol **102** with very little detection of **100**, suggesting that C4-hydroxylation occurs in a downstream event; 4) Resubjection of diosphenol **102** to the reaction conditions results in sluggish conversion to **100**, suggesting that the final C4 oxidation might proceed through non-isolated intermediate. Further mechanistic investigations of this reaction are ongoing and should aid the development of a more efficient protocol.

Furthermore, the rapid elaboration of the ryanodane A-ring to provide vinyl triflates **103** and **104** offers a potentially important diversification point for the study of ryanodane derivatives. The presence of a valuable functional group handle in the vinyl triflate enables not only additional functionalization to access the natural product, but enables diversification by cross-coupling, and could serve as a versatile precursor to assess the biological activity of ryanodine analogs varying in substitution at this position.



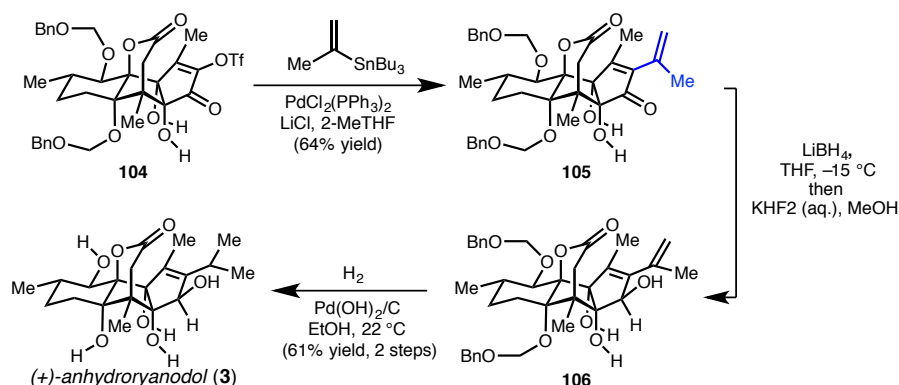
Scheme 6. The effect of water on the selenium-dioxide mediated oxidation of the enone **99a**

2.2.5 Synthesis of (+)-Anhydroryanodol

With an established protocol for the preparation of the highly functionalized vinyl triflate **104**, advancement to (+)-anhydroryanodol only necessitated installation of the C2-isopropyl unit, 1,2-enone reduction, and removal of the benzyloxymethyl protecting groups. Although we briefly evaluated direct methods to install the C2-isopropyl group via Negishi-coupling with isopropylzinc reagents,²⁶ or Stille-coupling with the more

reactive, 2-propylazastannatrane,²⁷ we ultimately opted for coupling of a 2-propenyl group with the expectation that hydrogenolysis of the two benzyloxymethyl-protecting groups could concurrently effect selective olefin hydrogenation. Thus, palladium-catalyzed cross-coupling between **104** and tributyl(2-propenyl)stannane installed the final three carbons, delivering **105** in 64% yield.

Efforts to elaborate **105** via stereoselective 1,2-reduction were initially met with poor reactivity. Treatment with NaBH₄ in MeOH, with or without added CeCl₃•7H₂O resulted in sluggish carbonyl reduction, instead rapidly reacting with the 1,2-diol moiety to generate the corresponding boronic ester. Turning to more reactive conditions, it was found that LiBH₄ cleanly effected 1,2-reduction, delivering the C3 alcohol with only partial borate formation that was readily removed through rapid treatment with KHF₂ during workup. Without additional purification, alcohol **106** was subsequently treated with H₂ in the presence of Pd(OH)₂/C in ethanol to cleanly promote removal of the benzyloxymethyl groups as well as effect alkene hydrogenation, delivering anhydroryanodol (**3**) in 61% yield over 2 steps. As Deslongchamps and coworkers have demonstrated the ability to synthesis (+)-ryanodol from (+)-anhydroryanodol,⁵ completion of this synthetic sequence constitutes a formal total synthesis of **2**. Notably, **3** is prepared from commercially available starting materials in only 13 steps with excellent material throughput.



Scheme 7. Palladium catalyzed cross-coupling and advancement to (+)-anhydroryanodol

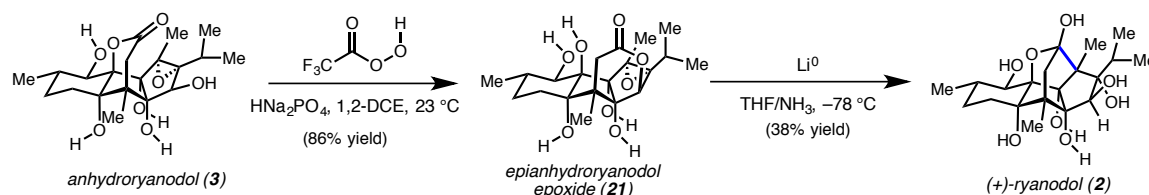
2.2.6 Conversion of (+)-Anhydroryanodol to (+)-Ryanodol

The successful development of a route to access (+)-anhydroryanodol left only two transformations to complete the total synthesis of **2**, namely, epoxidation of the C1-C2 olefin and reductive cyclization under dissolving metal conditions. Although reproduction of the protocol described by Deslongchamps and coworkers appeared straightforward at first, considerable efforts were required to reproduce and reoptimize the final step of this two-step protocol.⁵

Slight modifications of the epoxidation conditions were first explored in an attempt to circumvent the use of hazardous 90% hydrogen peroxide, a reagent known to spontaneously detonate during distillation.²⁸ Instead, simple application of a known protocol employing urea hydrogen peroxide adduct enabled a convenient and safe alternative for the preparation of trifluoroperacetic acid solution.²⁹ Treatment of **3** with freshly prepared trifluoroperacetic acid (3 equiv) in the presence of HNa_2PO_4 (6 equiv) for 3 hours enabled the clean conversion of **3** to translactonized epoxide **21**, in nearly identical yield to that reported by Deslongchamps.

Subjection of this material to Li(0) in NH₃, freshly distilled from sodium metal at –78 °C, resulted in reductive cyclization to produce (+)-**2** in 38% yield (lit. 60% yield) after isolation by continuous extraction and silica gel chromatography. In our hands, the reaction profile was highly dependent on the purity of the ammonia. Independent control reactions conducted with ammonia condensed directly from the gas cylinder, or utilizing redistilled ammonia with added H₂O (10 equiv), or exogenous Fe-salts revealed that these parameters all significantly affect the ratio of **2** to previously identified carbonyl-reduction products in addition to minor, unidentified degradation products. More specifically, the addition of exogenous H₂O resulted in nearly complete carbonyl reduction, whereas the addition of Fe-salts resulted in reduced reactivity and the formation of a new product. The significant effect of ferrous impurities from ammonia storage in iron based gas cylinders has been well documented in the context of Birch reductions.³⁰ In this context, iron-based impurities may rapidly catalyze lithium amide formation, thereby negatively affecting productive reductive cyclization and instead promoting a variety of non-productive, base-mediated decomposition pathways.

The modest 38% yield obtained in this report represents the highest reproducible yield in our hands, and is more consistent with initial, unoptimized yields obtained by Deslongchamps from an earlier report (lit. 30-35% yield).³¹ At this juncture, we believe that the inability to reproduce the reported 60% yield by Deslongchamps and coworkers may be attributed to additional unidentified reaction parameters or trace metal impurities that may potentially promote or inhibit the desired cyclization. Further investigations into the nature of these additional parameters will likely enable the identification of an improved protocol.

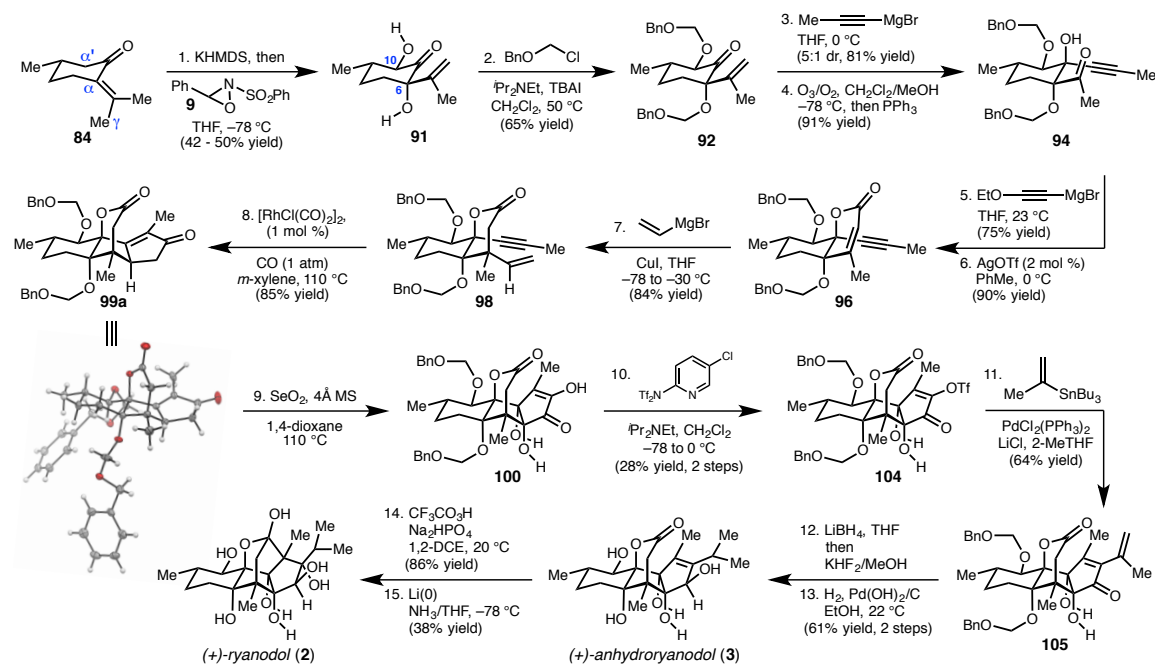


Scheme 8. Reductive cyclization of (+)-anhydroryanodol to (+)-ryanodol

2.3 CONCLUDING REMARKS

In summary, a concise and enantiospecific total synthesis of (+)-ryanodol has been accomplished, proceeding in 15 steps from commercially available starting materials. A schematic summary is presented in **Scheme 9**. The development of this final optimized route was enabled by extensive prior strategic investigations and considerations that illustrated the ability to rapidly assemble the ABCD-tetracycle by an intramolecular Pauson–Khand approach. Notable synthetic achievements of the route described above include, 1) the stereospecific oxidative functionalization of (*S*)-pulegone to directly arrive a versatile building block; 2) application of a Ag-catalyzed lactone synthesis for the preparation of the highly functionalized AD-ring system; 3) an efficient and diastereoselective, Rh-catalyzed, intramolecular Pauson–Khand to prepare the complex ABCD-ring system of anhydroryanodol; 4) discovery of a novel selenium-dioxide oxidative functionalization to install three oxidation states and three oxygen atoms and generate a fully functionalized A-ring. Furthermore, the synthesis described herein constitutes a significant advance when compared to the state-of-the-art in the preparation of these complex diterpenoids, requiring nearly 20 fewer steps than previous efforts.³²

The synthetic strategy employed in this total synthesis of (+)-ryanodol is anticipated to significantly enable the preparation of a diverse array of ryanodane natural products, as well as an array of structural ryanodane analogs. Indeed, multiple opportunities for structural diversification at a late stage, as well as early stage modifications, to systematically study the effect of specific oxygen-atoms, are entirely accommodated by the synthetic strategy described herein. Efforts in this vein are the current focus of ongoing studies within our laboratory.



Scheme 9. Complete synthetic sequence.

2.4 EXPERIMENTAL SECTION

2.4.1 Materials and Methods

Unless otherwise stated, reactions were performed under an inert atmosphere (dry N₂ or Ar) with freshly dried solvents utilizing standard Schlenk techniques. Glassware was oven-dried at 120 °C for a minimum of four hours, or flame-dried utilizing a Bunsen burner under high vacuum. Tetrahydrofuran (THF), methylene chloride (CH₂Cl₂), 1,4-dioxane, and toluene (PhMe) were dried by passing through activated alumina columns. 2-Methyltetrahydrofuran (anhydrous, >99%, inhibitor-free) and *m*-xylene (anhydrous, >99%) were purchased from Sigma-Aldrich and stored under argon. Absolute ethanol (200 Proof) was purchased from Koptec. Methanol (HPLC grade) was purchased from Fisher Scientific. 1,2-Dichloroethane was purified via distillation over calcium hydride immediately before use. Anhydrous ammonia (NH₃) was purchased from Matheson Tri-Gas and distilled over sodium metal prior to use. Triethylamine (Et₃N) and *N,N*-diisopropylethylamine (*i*-Pr₂NEt) were distilled over calcium hydride prior to use. All reactions were monitored by thin-layer chromatography using EMD/Merck silica gel 60 F254 pre-coated plates (0.25 mm) and were visualized by UV (254 nm), *p*-anisaldehyde, or KMnO₄ staining. Flash column chromatography was performed using silica gel (SiliaFlash® P60, particle size 40-63 microns [230 to 400 mesh]) purchased from Silicycle. ¹H and ¹³C NMR spectra were recorded on a Varian Inova 500 (at 500 MHz and 126 MHz, respectively) and are reported relative to internal CHCl₃ (¹H, δ = 7.26) or CD₂HOD (¹H, δ = 3.31), and CDCl₃ (¹³C, δ = 77.0), CD₃OD (¹³C, δ = 49.0). Data for ¹H NMR spectra are reported as follows: chemical shift (δ ppm) (multiplicity, coupling

constant (Hz), integration). Multiplicity and qualifier abbreviations are as follows: s = singlet, d = doublet, t = triplet, q = quartet, m = multiplet, br = broad, app = apparent. IR spectra were recorded on a Perkin Elmer Paragon 1000 spectrometer and are reported in frequency of absorption (cm^{-1}). HRMS were acquired using an Agilent 6200 Series TOF with an Agilent G1978A Multimode source in electrospray ionization (ESI), atmospheric pressure chemical ionization (APCI), or mixed (MM) ionization mode. Optical rotations were measured on a Jasco P-2000 polarimeter using a 100 mm path-length cell at 589 nm.

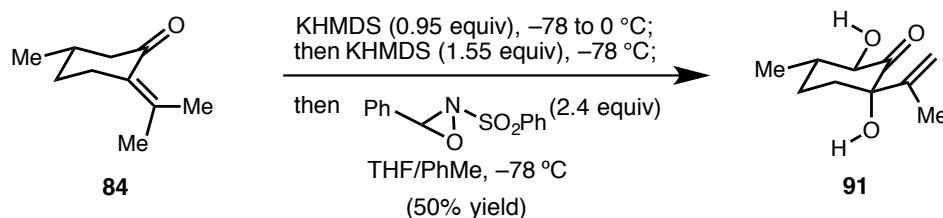
Reagents were purchased from commercial vendors or prepared as follows: Solid potassium hexamethyldisilazide (KHMDs, 95%) was purchased from Sigma-Aldrich and stored in a nitrogen-filled glovebox. Potassium hexamethyldisilazide solution (0.5 M in PhMe) was purchased from Sigma-Aldrich and stored under Argon. *Rac*-3-phenyl-2-(phenylsulfonyl)-1,2-oxaziridine (Davis Oxaziridine) was prepared according to literature procedures. Chloromethyl benzyl ether (BnOCH_2Cl) was prepared from paraformaldehyde, benzyl alcohol, and gaseous hydrogen chloride according literature procedures.³³ Propynylmagnesium bromide (0.5 M in THF) was purchased from Alfa Aesar or freshly prepared via direct deprotonation of propyne with ethylmagnesium bromide (1 M in THF). Ethoxyacetylene (50 wt % in hexanes) was purchased from GFS Chemicals and used as received. Silver triflate (AgOTf , 99%), selenium dioxide (SeO_2 , 99.8%), and chlorodicarbonyl rhodium (I) dimer ($[\text{RhCl}(\text{CO})_2]_2$) were purchased from Strem Chemicals and stored in a nitrogen-filled glovebox. *N*-(5-Chloro-2-pyridyl)bis(trifluoromethanesulfonimide) (Comins Reagent) was purchased from Oakwood Chemicals. Copper(I) iodide (CuI) and palladium hydroxide on Carbon

(Pearlman's Catalyst, 20 wt % on C) were purchased from Alfa Aesar. LiBH_4 (>95%) and lithium (wire stored in mineral oil, 99.9% trace metal basis) were purchased from Sigma-Aldrich.

2.4.2 Experimental Procedures

Notes on the preparation of Diol 91: Both the selectivity and yields obtained for the α,α' -bishydroxylation of pulegone were finely dependent on the quality of KHMDS utilized in the reaction, as well as precise temperature control. Improved selectivities and yields were more readily obtained on smaller scale (50% yield, 10 mmol scale) for the preparation of diol **91** via pre-equilibration of the potassium enolate at 0 °C to the thermodynamically-preferred, conjugated dienolate, as well as utilizing KHMDS (0.5 M) in PhMe solution. However, in order to improve material throughput on scale, a simplified protocol was established for larger scale (42% yield, 120 mmol scale) at the slight cost of reaction efficiency.

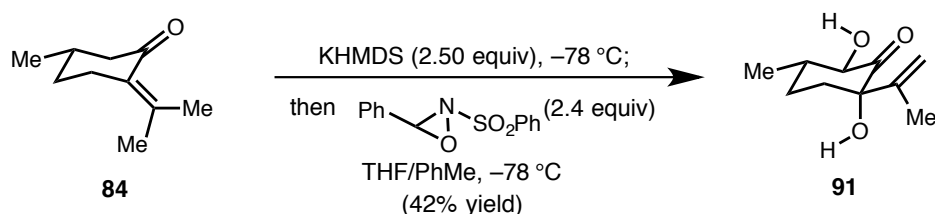
Additionally, separation of the diastereomeric products was improved via use of wet silica gel, prepared as follows: Silica gel (SiliaFlash® P60, particle size 40-63 microns [230 to 400 mesh], purchased from Silicycle, 950 g) was slowly mixed with deionized water (50 mL) in a 1-liter media bottle. The silica was then vigorously shaken for five minutes, and then allowed to equilibrate for 12 h before use as normal for silica gel purification. The product obtained by this method was typically 97% pure by ^1H NMR analysis, containing some minor oxaziridine-derived products.

Preparation of Diol 91 (10 mmol scale):

To a flame-dried, 250-mL, round-bottomed flask equipped with a magnetic stirbar was added (*S*)-pulegone (1.52 g, 10.0 mmol, 1.0 equiv) and THF (50 mL). The solution was cooled to $-78\text{ }^{\circ}\text{C}$ in a dry ice/acetone bath and KHMDS (19.0 mL, 0.5 M solution in PhMe, 9.50 mmol, 0.95 equiv) was added dropwise by cannula transfer over 10 minutes. After completion of the transfer, the dry ice/acetone bath was replaced with an ice/water bath, and the flask was stirred at $0\text{ }^{\circ}\text{C}$ for 1 h. The solution was then re-cooled to $-78\text{ }^{\circ}\text{C}$ in a dry ice/acetone bath, and additional KHMDS solution (31.0 mL, 0.5 M solution PhMe, 15.5 mmol, 1.55 equiv) was added rapidly via cannula transfer and the flask stirred for 15 minutes to ensure complete cooling of the solution. A solution of *rac*-3-phenyl-2-(phenylsulfonyl)-1,2-oxaziridine (6.31 g, 24.0 mmol, 2.4 equiv) in THF (400 mL) was then added dropwise by cannula transfer over the course of 1 h, producing a deep orange-red solution that was stirred for 15 minutes. It is critical that the enolate solution is efficiently stirred during the addition to maintain a consistent internal temperature. Sat. aq. NH_4Cl (90 mL) was then added and the flask allowed to warm to ambient temperature and stirred for 1 h, until TLC-analysis indicated complete hydrolysis of the imine byproduct (*N*-benzylidenebenzenesulfonamide). The resulting mixture was extracted with EtOAc (150 mL), washed with sat. aq. NH_4Cl (2 x 150 mL), and the combined aqueous layers extracted with EtOAc (200 mL). The combined organic layers were washed with brine (200 mL), dried over anhydrous MgSO_4 , filtered and

concentrated *in vacuo*. Purification by silica gel chromatography (20 to 30 to 40% EtOAc in hexanes) on wet silica gel (see above) affords diol **91** as a white solid (923 mg, 5.01 mmol, 50% yield).

Preparation of Diol 91 (120 mmol scale):



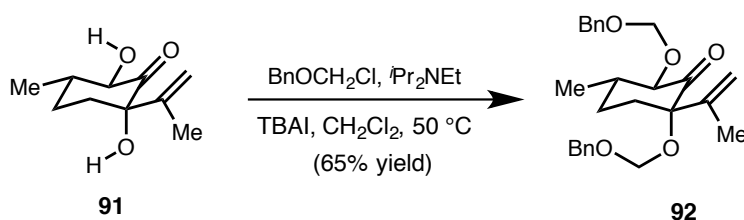
To a 1-liter, flame-dried flask equipped with a large magnetic stirbar was added solid KHMDS (95% KHMDS, 63.0 g, 300 mmol, 2.5 equiv) in a nitrogen-filled glovebox. The flask was capped with a rubber septum, removed from the glovebox, and anhydrous THF (300 mL) was charged to the flask and the resulting mixture stirred at $22\text{ }^{\circ}\text{C}$ for 10 minutes to ensure complete dissolution of the solid. The resulting solution was then cooled to $-78\text{ }^{\circ}\text{C}$ in a dry ice/acetone bath (Note: Adequate cooling of the reaction mixture is critical for this reaction. A large capacity Pope brand cryogenic dewar was utilized for this procedure). After stirring for 20 minutes at $-78\text{ }^{\circ}\text{C}$, a solution of (*S*)-pulegone (18.3 g, 120 mmol, 1.0 equiv) in THF (50 mL) was added dropwise by cannula transfer over 30 minutes, resulting in a homogenous yellow solution that was stirred for an additional 20 minutes. A solution of *rac*-3-phenyl-2-(phenylsulfonyl)-1,2-oxaziridine (72.1 g, 276 mmol, 2.3 equiv) in THF (400 mL) was then added dropwise by cannula transfer over the course of 1 h, producing a deep orange-red solution that was stirred for an additional 15 minutes. The reaction was then quenched by the addition of sat. aq. NH-

CH_2Cl_2 solution (250 mL) and the cold bath replaced with a water bath at ambient temperature. Once the temperature of the mixture had reached 23 °C, the biphasic mixture was then stirred rapidly for 1 h to allow for hydrolysis of the imine byproduct (*N*-benzylidenebenzenesulfonamide). The mixture was subsequently poured into a separatory funnel, diluted with EtOAc (500 mL), and washed with sat. aq. NH_4Cl (3 x 250 mL). The combined aqueous washings were then extracted with EtOAc (2 x 300 mL), and the combined organic layers washed with brine (500 mL), dried over anhydrous MgSO_4 , filtered, and concentrated *in vacuo*. The resulting thick slurry was then redissolved in EtOAc (100 mL) and treated with hexanes (400 mL), resulting in the precipitation of benzenesulfonamide, and the solids removed by filtration over Celite, rinsing with 4:1 hexanes/EtOAc (200 mL) to fully elute off the products. Concentration *in vacuo* affords an orange oil. Repeated purification by silica gel chromatography (500 g wet silica, 20 to 30 to 40% EtOAc in hexanes) affords a thick, slightly yellow oil that was determined to be 97% pure by ^1H NMR (9.19 g, 49.9 mmol, 42% yield).

Notes: Residual imine byproduct, *N*-benzylidenebenzenesulfonamide, has a slightly higher R_f than the product that can be challenging to remove by chromatography. In cases where the imine is not fully hydrolyzed, the product can be redissolved in EtOAc (200 mL) and stirred with sat. aq. NH_4Cl (200 mL) for 12 h. The resulting benzaldehyde and benzenesulfonamide products are then readily removed by silica gel chromatography. A sample was further purified by silica gel chromatography for characterization purposes.

TLC (40% EtOAc/Hexanes), R_f : 0.43 (*p*-anisaldehyde); **^1H NMR (CDCl_3 , 500 MHz):** δ 5.06 (m, 2H), 4.34 (dd, J = 10.9, 4.7 Hz, 1H), 3.37 (d, J = 4.7 Hz, 1H), 2.48 (s, 1H), 2.03 – 1.82 (m, 3H), 1.81 (app. s, 3H), 1.68 – 1.52 (m, 2H), 1.19 (d, J = 6.3 Hz, 3H); **^{13}C NMR (CDCl_3 , 126 MHz):** δ 209.7, 145.4, 112.5, 80.1, 77.8, 43.6, 37.1, 26.7, 19.7, 19.0; **FTIR (NaCl, thin film):** 3421, 2955, 2929, 1720, 1456, 1376 cm^{-1} ; **LRMS:** calc'd for $[\text{M}+\text{H}]^+$: 185.1, found: 185.1; **$[\alpha]_D^{25}$:** -38 (c = 1.0 CHCl_3).

Preparation of Ketone 92:

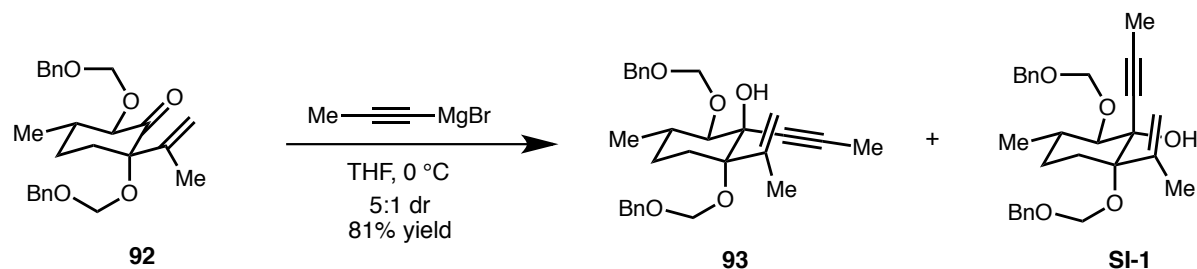


To a 500-mL, flame-dried flask was added diol **10** (9.14 g, 49.6 mmol, 1.0 equiv), tetrabutylammonium iodide (36.6 g, 99.2 mmol, 2.0 equiv), and anhydrous CH_2Cl_2 (200 mL). The solution was cooled to 0 $^\circ\text{C}$ in an ice/water bath and $t\text{Pr}_2\text{NEt}$ (69 mL, 400 mmol, 8.0 equiv) was added rapidly via syringe. After 10 minutes, chloromethyl benzyl ether (34.4 mL, 248 mmol, 5.0 equiv) was added dropwise via syringe. The cold bath was subsequently removed and the solution was allowed to warm to 20 $^\circ\text{C}$ over 45 minutes. The flask was equipped with an oven-dried reflux condenser and then submerged into a preheated oil bath at 55 $^\circ\text{C}$ (internal temp. 50 $^\circ\text{C}$), resulting in gentle reflux of the pale yellow solution. As the reaction proceeds, the color of the solution changes to a deep red. After 40 h, the solution was cooled to ambient temperature, poured into a 1-liter separatory funnel, diluted with additional CH_2Cl_2 (250 mL), and washed sequentially with sat. aq. NaHCO_3 (250 mL) and sat. aq. NH_4Cl (3 x 200 mL). The combined aqueous

washings were then extracted with CH₂Cl₂ (2 x 100 mL), then the combined organic layers were washed with 0.2 N NaOH (300 mL) and brine (300 mL), dried over anhydrous MgSO₄, filtered, and concentrated *in vacuo* to afford a thick red slurry. EtOAc (100 mL) was added and the suspension vigorously agitated to ensure suspension of the solids. The suspension was then treated with hexanes (400 mL) resulting in the additional precipitation of ammonium salts, and the solids removed via filtration over Celite, rinsing with hexanes/EtOAc (4:1, 200 mL). Concentration *in vacuo* resulted in isolation of a homogeneous red oil. Purification by silica gel chromatography (7 to 9 to 12% EtOAc in hexanes) afforded ketone **92** as a thick, colorless oil (13.6 g, 32.1 mmol, 65% yield).

Notes: A similar yield was obtained albeit at longer reaction times in the absence of Bu₄NI.

TLC (10% EtOAc/Hexanes), R_f: 0.23 (UV, *p*-anisaldehyde). **¹H NMR (500 MHz, CDCl₃):** δ 7.38 – 7.26 (m, 10H), 5.20 (app. p, *J* = 1.4 Hz, 1H), 5.05 (app. t, *J* = 1.0 Hz, 1H), 4.84 (d, *J* = 7.1 Hz, 1H), 4.80 (d, *J* = 11.9 Hz, 1H), 4.78 (d, *J* = 7.1 Hz, 1H), 4.78 (d, *J* = 7.1 Hz, 1H), 4.74 (d, *J* = 11.7 Hz, 1H), 4.72 (d, *J* = 7.1 Hz, 1H), 4.66 (d, *J* = 11.7 Hz, 1H), 4.65 (d, *J* = 10.9 Hz, 1H), 4.64 (d, *J* = 11.9 Hz, 1H), 2.29 (dt, *J* = 14.4, 2.9 Hz, 1H), 1.96 – 1.77 (m, 3H), 1.74 – 1.67 (m, 1H), 1.71 (app. q, *J* = 0.7 Hz, 3H), 1.20 (d, *J* = 6.1 Hz, 3H). **¹³C NMR (126 MHz, CDCl₃):** δ 142.8, 137.8, 137.5, 128.5, 128.5, 128.4, 127.9, 127.8, 127.8, 127.6, 116.4, 94.3, 90.4, 87.8, 83.0, 71.1, 69.9, 41.8, 34.2, 27.6, 19.7, 19.5. **FTIR (NaCl, thin film):** 2890, 1734, 1454, 1379, 1157, 1057, 1015 cm⁻¹; **HRMS:** calc'd for [M+Na]⁺: 447.2142, found: 447.2126. **[α]_D²⁵:** +58 (*c* = 1.0, CHCl₃).

Preparation of Enyne 93:

To a 1-liter, flame-dried round-bottomed flask was charged ketone **11** (13.3 g, 31.3 mmol, 1.0 equiv) and THF (310 mL). The solution was placed in an ice/water bath at 0 °C and stirred for 25 minutes for adequate cooling, then a solution of propynylmagnesium bromide (0.5 M solution, 125 mL, 62.5 mmol, 2.0 equiv) was added dropwise by cannula transfer over 45 min. The reaction was stirred for an additional 30 min and then carefully quenched by the addition of sat. aq. NH_4Cl (300 mL). The mixture was diluted with Et_2O (300 mL) and washed with sat. aq. NH_4Cl (2 x 100 mL), then the combined aqueous layers extracted with Et_2O (200 mL). The combined organic layers were then washed with brine (300 mL), dried over anhydrous MgSO_4 , filtered, and concentrated *in vacuo* to afford a thick, light yellow oil. ^1H NMR analysis of the crude product indicated that the reaction occurs with complete consumption of starting material in a 5:1 diastereomeric ratio. Purification by silica gel chromatography (15 to 20 EtOAc in hexanes) afforded enyne **93** as a viscous oil that slowly solidifies into colorless, semicrystalline needles (11.8 g, 25.4 mmol, 81% yield) in addition to minor diastereomer **SI-1** (1.75 g, 3.76 mmol, 12% yield).

Major Diastereomer (93):

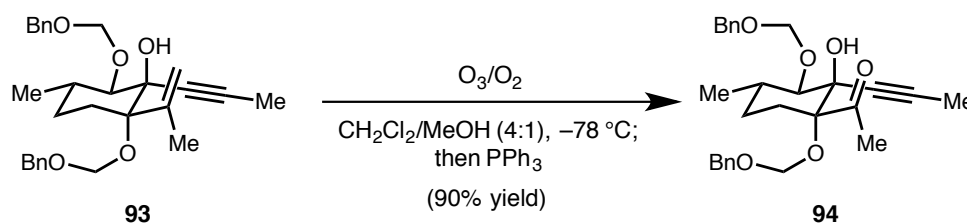
TLC (20% EtOAc/Hexanes), R_f : 0.38 (*p*-anisaldehyde); **^1H NMR (500 MHz, CDCl_3):** δ 7.40 – 7.33 (m, 8H), 7.32 – 7.27 (m, 2H), 5.24 (p, J = 1.5 Hz, 1H), 5.20 (d, J = 6.9 Hz, 1H), 5.20 (dd, J = 1.8, 0.8 Hz, 1H), 4.96 (d, J = 6.8 Hz, 1H), 4.89 (d, J = 12.0 Hz, 1H), 4.82 (d, J = 11.8 Hz, 1H), 4.77 (d, J = 6.8 Hz, 1H), 4.74 (d, J = 6.8 Hz, 1H), 4.63 (d, J = 12.0 Hz, 1H), 4.58 (d, J = 11.8 Hz, 1H), 3.64 (d, J = 10.6 Hz, 1H), 2.72 (s, 1H), 2.17 – 2.08 (m, 1H), 1.96 – 1.92 (m, 3H), 1.90 – 1.78 (m, 1H), 1.81 (s, 3H), 1.74 (dt, J = 14.4, 3.1 Hz, 1H), 1.55 – 1.48 (m, 2H), 1.09 (d, J = 6.5 Hz, 3H); **^{13}C NMR (126 MHz, CDCl_3):** δ 144.7, 138.0, 137.9, 128.4, 128.4, 127.8, 127.7, 127.6, 117.0, 96.7, 90.3, 86.4, 85.3, 82.0, 80.9, 75.3, 70.7, 70.5, 31.8, 27.6, 27.1, 22.0, 19.0, 3.8; **FTIR (NaCl, thin film):** 3401, 2952, 2927, 2240, 1497, 1453, 1379, 1022 cm^{-1} ; **HRMS:** calc'd for $[\text{M}+\text{Na}]^+$: 487.2445, found: 487.2438; **$[\alpha]_D^{25}$:** +84 (c = 1.1, CHCl_3).

Minor Diastereomer (SI-1):

TLC (20% EtOAc/Hexanes), R_f : 0.31 (*p*-anisaldehyde); **^1H NMR (500 MHz, CDCl_3):** δ 7.39 – 7.31 (m, 8H), 7.31 – 7.26 (m, 2H), 5.24 (p, J = 1.4 Hz, 1H), 5.16 (dd, J = 1.6, 0.8 Hz, 1H), 5.10 (d, J = 7.0 Hz, 1H), 4.86 (d, J = 7.0 Hz, 1H), 4.85 (d, J = 12.0 Hz, 1H), 4.81 (d, J = 11.8 Hz, 1H), 4.81 (d, J = 7.2 Hz, 1H), 4.77 (d, J = 7.2 Hz, 1H), 4.70 (d, J = 12.0 Hz, 1H), 4.55 (d, J = 11.9 Hz, 1H), 4.05 (s, 1H), 3.58 (d, J = 10.5 Hz, 1H), 2.19 – 2.11 (m, 1H), 1.96 (q, J = 0.7 Hz, 3H), 1.95 – 1.87 (m, 2H), 1.87 (s, 3H), 1.59 – 1.54 (m, 2H), 1.06 (d, J = 6.5 Hz, 3H); **^{13}C NMR (126 MHz, CDCl_3):** δ 144.5, 137.8, 137.5, 128.4, 128.4, 127.8, 127.8, 127.7, 127.7, 117.5, 97.0, 91.1, 89.2, 86.4, 83.2, 78.3, 77.5, 71.1, 70.2, 35.3, 29.9, 27.9, 22.4, 18.6, 3.9; **FTIR (NaCl, thin film):** 2952, 2927, 2240,

1454, 1380, 1023 cm^{-1} ; **HRMS**: calc'd for $[\text{M}+\text{Na}]^+$: 487.2445, found: 487.2456; $[\alpha]_{\text{D}}^{25}$: +61 ($c = 0.90$, CHCl_3).

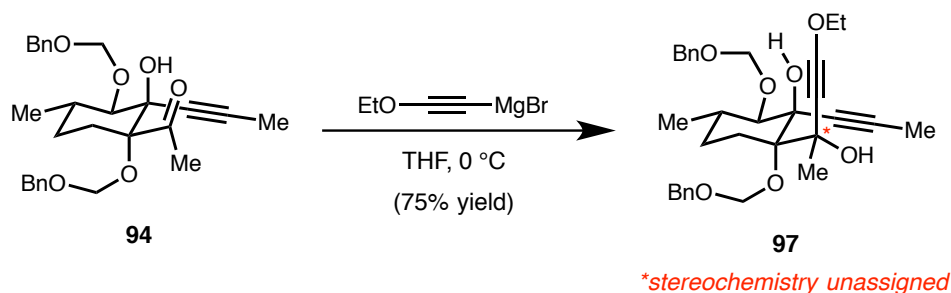
Preparation of Methyl Ketone **94**:



To a 1-liter, round-bottomed flask was charged enyne **93** (11.7 g, 25.2 mmol, 1.0 equiv), followed by CH_2Cl_2 (400 mL) and MeOH (100 mL). The solution was purged with O_2 by means of a gas dispersion tube while cooling to $-78\text{ }^\circ\text{C}$ in a dry ice/acetone bath. A mixture of O_3/O_2 [Caution! Ozone is an extremely hazardous chemical! Proper training and use in a well-ventilated fume hood are necessary] was then passed through the solution and the reaction carefully monitored by TLC to track disappearance of the starting material. After 4.5 h, the solution slowly changed from a colorless solution to a very slight, pale blue color. O_2 (g) was sparged through the solution at an increased rate to purge out excess ozone, followed by N_2 (g) for 10 minutes. Triphenylphosphine (6.61 g, 25.2 mmol, 1.0 equiv) was then added in a single portion to the mixture at $-78\text{ }^\circ\text{C}$. The mixture was allowed to warm to $23\text{ }^\circ\text{C}$ with efficient stirring under N_2 over the course of 1 h, then concentrated *in vacuo* to afford a thick oil. Purification by silica gel chromatography (20 to 30 to 35% EtOAc in hexanes, sample loaded in 10 mL of CH_2Cl_2) afforded methyl ketone **94** as a white amorphous solid (10.6 g, 22.7 mmol, 90% yield).

Notes: The product readily precipitates from hexanes/EtOAc solutions. To ensure quantitative transfer and prevent streaking, complete dissolution in CH₂Cl₂ (10 mL) is necessary for loading the silica gel column. Furthermore, although triphenylphosphine oxide could be removed by careful trituration from the reaction mixture, purification in this manner was undesirable due to the risk of product loss.

TLC (40% EtOAc/Hexanes), R_f: 0.50 (UV, *p*-anisaldehyde); **¹H NMR (500 MHz, CDCl₃):** δ 7.38 – 7.33 (m, 8H), 7.33 – 7.27 (m, 2H), 5.17 (d, *J* = 7.0 Hz, 1H), 4.93 (d, *J* = 7.0 Hz, 1H), 4.89 (d, *J* = 6.8 Hz, 1H), 4.88 (d, *J* = 11.9 Hz, 1H), 4.77 (d, *J* = 11.9 Hz, 1H), 4.76 (d, *J* = 6.8 Hz, 1H), 4.64 (d, *J* = 11.9 Hz, 1H), 4.62 (d, *J* = 11.9 Hz, 1H), 3.57 (d, *J* = 10.6 Hz, 1H), 3.08 (s, 1H), 2.40 (s, 3H), 2.26 (ddd, *J* = 15.0, 13.8, 4.3 Hz, 1H), 1.96 – 1.85 (m, 1H), 1.83 (s, 3H), 1.77 (dt, *J* = 15.0, 3.2 Hz, 1H), 1.57 (dtd, *J* = 13.6, 4.3, 2.9 Hz, 1H), 1.36 (tdd, *J* = 13.7, 12.5, 3.5 Hz, 1H), 1.06 (d, *J* = 6.5 Hz, 3H); **¹³C NMR (126 MHz, CDCl₃):** δ 209.4, 137.8, 137.4, 128.4, 128.4, 127.8, 127.7, 127.7, 127.7, 96.5, 91.1, 88.1, 85.7, 82.9, 80.1, 72.5, 70.8, 70.6, 31.5, 28.1, 27.1, 24.6, 18.7, 3.8; **FTIR (NaCl, thin film):** 3402, 2951, 2927, 2235, 1713, 1453, 1020 cm⁻¹; **HRMS:** calc'd for [M+Na]⁺: 489.2248, found: 489.2246; **[α]_D²⁵:** +97 (*c* = 1.0, CHCl₃).

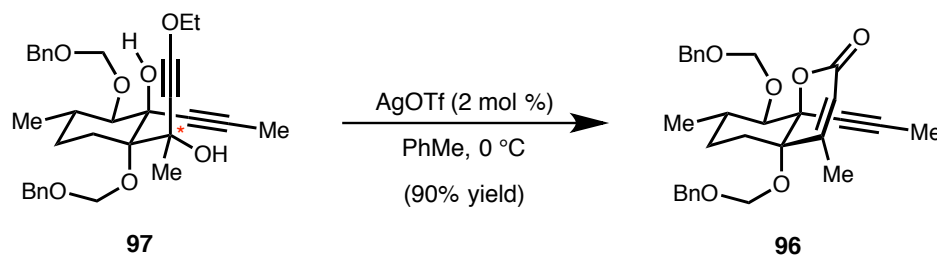
Preparation of Diyne 98:

To a 1-liter, oven-dried, round-bottomed flask was added ethylmagnesium bromide (1.0 M in THF, 114 mL, 114 mmol, 5.0 equiv) and THF (114 mL). The solution was cooled to 0 °C in an ice/water bath and ethoxyacetylene (50 wt % in hexanes, 23.8 mL, 6.0 equiv) added dropwise by syringe. The resulting brown solution was stirred at 0 °C for 15 minutes, then removed from the ice bath and allowed to warm to room temperature over 30 minutes. The dark brown solution was then recooled to 0 °C in an ice/water bath, and a solution of ketone **94** (10.6 g, 22.7 mmol, 1.0 equiv) in THF (100 mL) was added via cannula transfer over 30 minutes. Upon completion of the addition, the dark brown solution was stirred for an additional 20 minutes, then quenched by the addition of sat. aq. NH_4Cl (300 mL), diluted with EtOAc (300 mL), and washed with additional sat. aq. NH_4Cl (2 x 200 mL). The combined organic layers were extracted with additional EtOAc (250 mL), and the combined organic layers were washed with brine (300 mL), dried over anhydrous MgSO_4 , filtered, and concentrated *in vacuo*. ^1H NMR analysis of the mixture reveals approximately 85% conversion. Purification of the resulting brown oil, twice, by silica gel chromatography (30 to 35% EtOAc in hexanes) afforded diyne **97** (9.13 g, 17.0 mmol, 75% yield) as a light yellow oil that very slowly solidified to a slightly yellow amorphous solid under high vacuum, along with a mixture

of recovered starting material and product (2.2 g) that could be resubjected for further material throughput.

Notes: Incomplete conversion is typically observed. Removal of starting material can be challenging on larger scale. 1,2-Addition into the methyl ketone appears to occur with complete diastereoselectivity, although the absolute configuration at the newly formed (albeit inconsequential given the subsequent step) stereocenter could not be unambiguously assigned via 2D-NMR spectroscopic techniques.

TLC (40% EtOAc/Hexanes), R_f : 0.40 (UV, *p*-anisaldehyde); **^1H NMR (500 MHz, CDCl_3):** δ 7.40 – 7.27 (m, 10H), 5.13 (d, J = 6.9 Hz, 1H), 5.11 (d, J = 6.8 Hz, 1H), 4.99 (d, J = 6.8 Hz, 1H), 4.95 (d, J = 6.9 Hz, 1H), 4.88 (d, J = 11.9 Hz, 1H), 4.81 (d, J = 11.7 Hz, 1H), 4.74 (d, J = 11.6 Hz, 1H), 4.60 (d, J = 11.9 Hz, 1H), 4.50 (s, 1H), 4.03 (q, J = 7.1 Hz, 2H), 3.70 (s, 1H), 3.56 (d, J = 10.6 Hz, 1H), 2.27 (dt, J = 15.6, 3.4 Hz, 1H), 2.12 (ddd, J = 15.4, 13.8, 4.3 Hz, 1H), 1.88 – 1.81 (m, 1H), 1.84 (s, 3H), 1.80 (s, 3H), 1.55 (dq, J = 11.8, 4.1 Hz, 1H), 1.35 – 1.25 (m, 1H), 1.31 (t, J = 7.1 Hz, 3H), 1.03 (d, J = 6.5 Hz, 3H); **^{13}C NMR (126 MHz, CDCl_3):** 137.9, 137.7, 128.4, 128.3, 128.0, 127.7, 127.6, 127.6, 97.0, 94.4, 89.2, 87.5, 84.1, 83.3, 81.7, 75.4, 74.8, 74.2, 70.6, 70.2, 42.5, 31.6, 28.9, 27.0, 22.8, 18.7, 14.5, 3.9.; **FTIR (NaCl, thin film):** 3402, 2983, 2929, 2262, 1457, 1022 cm^{-1} ; **HRMS:** calc'd for $[\text{M}+\text{Na}]^+$: 559.2666, found: 559.2662; **$[\alpha]_D^{25}$:** +11 (c = 1.1, CHCl_3).

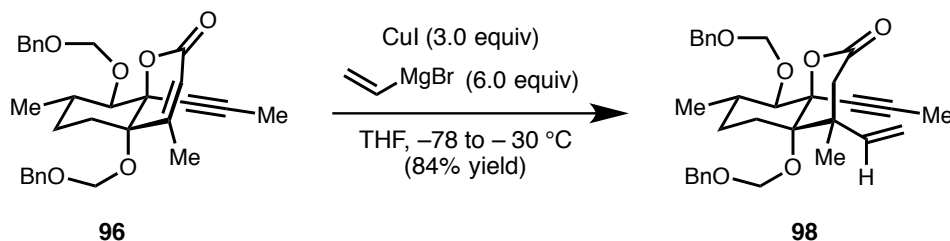
Preparation of Lactone 96:

To a 200 mL, round-bottomed flask was added diyne **97** (8.97 g, 16.7 mmol, 1.0 equiv) and anhydrous PhMe (84 mL). The solution was stirred vigorously at 23 °C for 15 minutes to ensure complete dissolution of the starting material, then the flask was submerged in an ice/water bath and allowed to cool over 15 minutes. AgOTf (85.6 mg, 0.334 mmol, 0.02 equiv) was weighed into a 1-dram vial in a nitrogen-filled glovebox and then added directly to the solution against a positive pressure of Argon, and the resulting mixture stirred vigorously at 0 °C for 20 min. The entire cold solution was then directly and rapidly loaded onto a silica gel column pre-equilibrated with 20% EtOAc in hexanes, and the compound purified by silica gel chromatography (20 to 30 to 40% EtOAc in hexanes) to provide lactone **96** as a pale yellow oil (7.38 g, 15.0 mmol, 90% yield).

Notes: The reaction is challenging to monitor by TLC since the product and starting material have nearly identical R_f 's. Since the reaction is purified directly by chromatography on scale, it is recommended that preparation of the silica gel column is performed prior to the addition of AgOTf so that the reaction can be immediately purified. Prolonged reaction times (>1 h) can result in the acid-catalyzed, hydrolytic cleavage of the benzyloxymethyl groups.

TLC (40% EtOAc/Hexanes), R_f : 0.40 (UV, *p*-anisaldehyde); **^1H NMR (500 MHz, CDCl_3):** δ 7.39 – 7.27 (m, 10H), 5.85 (q, J = 1.5 Hz, 1H), 5.12 (d, J = 7.3 Hz, 1H), 5.08 (d, J = 6.6 Hz, 1H), 5.06 (d, J = 6.6 Hz, 1H), 4.91 (d, J = 7.3 Hz, 1H), 4.84 (d, J = 11.9 Hz, 1H), 4.76 (d, J = 11.7 Hz, 1H), 4.65 (d, J = 11.7 Hz, 1H), 4.59 (d, J = 12.0 Hz, 1H), 3.70 (d, J = 10.1 Hz, 1H), 2.07 (tdd, J = 9.3, 6.7, 4.6 Hz, 1H), 2.01 (d, J = 1.5 Hz, 3H), 2.02 – 1.96 (m, 1H), 1.77 (s, 3H), 1.71 – 1.47 (m, 3H), 1.12 (d, J = 6.6 Hz, 3H); **^{13}C NMR (126 MHz, CDCl_3):** δ 162.5, 138.1, 137.4, 128.5, 128.4, 127.9, 127.8, 127.7, 127.5, 118.6, 96.8, 91.5, 85.2, 83.8, 81.4, 80.6, 76.6, 70.6, 70.5, 32.4, 32.3, 27.2, 18.5, 17.9, 3.8; **FTIR (NaCl, thin film):** 2954, 2927, 2245, 1727, 1247, 1167, 1025 cm^{-1} ; **HRMS:** calc'd for $[\text{M}+\text{Na}]^+$: 513.2248, found: 513.2236; $[\alpha]_D^{25}$: +34 (c = 0.50, CHCl_3).

Preparation of Enyne 98:



To a flame-dried, 1-liter, round-bottomed flask was charged CuI (8.46 g, 44.4 mmol, 3.0 equiv) and THF (400 mL). The suspension was cooled to $-78\text{ }^\circ\text{C}$ in a dry ice/acetone bath and vinylmagnesium bromide (1 M in THF, 89 mL, 89 mmol, 6.0 equiv) was added dropwise by syringe. Upon completion of the addition, the mixture was stirred for an additional 15 minutes, then a solution of lactone **96** (7.26 g, 14.8 mmol, 1.0 equiv) in THF (100 mL) was added dropwise by cannula transfer. The resulting mixture was

maintained at $-78\text{ }^{\circ}\text{C}$ for 15 minutes, then the mixture was gradually warmed to $-30\text{ }^{\circ}\text{C}$ over 30 minutes, and stirring maintained at $-30\text{ }^{\circ}\text{C}$ for 30 minutes. The reaction was then carefully quenched by the addition of sat. aq. NH_4Cl (300 mL) and warmed to ambient temperature. The reaction was then diluted with Et_2O (400 mL) and the biphasic mixture filtered through a short pad of Celite to remove precipitated red copper solids. The resulting mixture was then poured into a separatory funnel and washed with sat. aq. NH_4Cl (2 x 200 mL), and the combined aqueous layers extracted with additional Et_2O (2 x 200 mL). The combined organic layers were then washed with brine (400 mL), dried over anhydrous MgSO_4 and filtered over a short pad of silica gel to remove additional red copper-based precipitates, and the resultant solution concentrated *in vacuo* to afford a colorless oil. Purification of the crude residue by silica gel chromatography (20 to 30% EtOAc in hexanes) afforded enyne **98** as a slightly yellow oil (6.45 g, 12.4 mmol, 84% yield).

TLC (40% EtOAc /Hexanes), R_f : 0.53 (UV, *p*-anisaldehyde); **^1H NMR (500 MHz, CDCl_3):** δ 7.39 – 7.27 (m, 10H), 6.81 (dd, $J = 17.7, 10.8\text{ Hz}$, 1H), 5.16 (d, $J = 7.2\text{ Hz}$, 1H), 5.09 (dd, $J = 4.0, 0.8\text{ Hz}$, 1H), 5.08 – 5.05 (m, 1H), 4.99 (d, $J = 7.2\text{ Hz}$, 1H), 4.89 (d, $J = 11.9\text{ Hz}$, 1H), 4.82 (d, $J = 7.1\text{ Hz}$, 1H), 4.77 (d, $J = 11.7\text{ Hz}$, 1H), 4.71 (d, $J = 7.1\text{ Hz}$, 1H), 4.60 (d, $J = 11.9\text{ Hz}$, 1H), 4.51 (d, $J = 11.8\text{ Hz}$, 1H), 3.66 (d, $J = 10.7\text{ Hz}$, 1H), 3.49 (d, $J = 15.6\text{ Hz}$, 1H), 2.13 (d, $J = 15.6\text{ Hz}$, 1H), 2.07 – 1.94 (m, 2H), 1.91 (s, 3H), 1.56 – 1.46 (m, 3H), 1.26 (s, 3H), 1.08 (d, $J = 6.5\text{ Hz}$, 3H); **^{13}C NMR (126 MHz, CDCl_3):** δ 170.6, 144.9, 138.0, 137.4, 128.4, 128.4, 127.8, 127.8, 127.8, 127.6, 111.6, 97.6, 90.5, 86.0, 85.8, 83.3, 81.3, 77.2, 71.0, 70.5, 44.2, 43.7, 31.0, 27.4, 26.7, 24.1, 18.8, 3.9; **FTIR**

(NaCl, thin film): 2954, 2928, 2871, 1752, 1454, 1237, 1026 cm^{-1} ; HRMS: calc'd for $[\text{M}+\text{Na}]^+$: 541.2561, found: 541.2539; $[\alpha]_{\text{D}}^{25}$: +76 ($c = 1.0$, CHCl_3).

Evaluation of Pauson–Khand Reaction Conditions

Evaluation of Pauson–Khand reaction conditions were performed with enyne **14** on 0.20 mmol scale (104 mg). A variety of conditions employing cobalt,^{17,34} molybdenum,^{18,35} and rhodium¹⁹ complexes were surveyed following literature precedent. Isolated yields are indicated for the combined mixture of diastereomers, and were obtained after purification by silica gel chromatography. In entries **1** and **2** (cobalt-mediated), the diastereomeric ratios were obtained by ^1H NMR after silica gel purification due to the presence of paramagnetic Co-species, whereas in the remainder of the entries, diastereomeric ratios were obtained by ^1H NMR of the crude reaction mixtures.

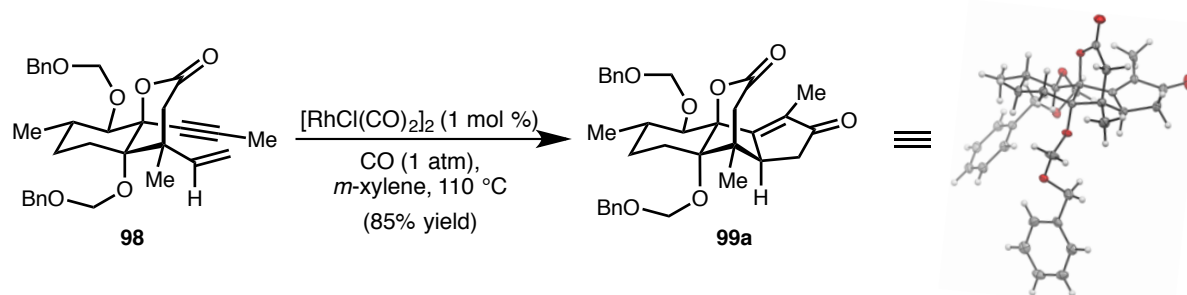
Table S1. Evaluation of Pauson–Khand Reaction Conditions

Conditions	dr	Yield 15	
1. $\text{Co}_2(\text{CO})_8$ (1.2 equiv), THF, 12 h; then DMSO, 65 °C	2.2 :1	46%	
2. $\text{Co}_2(\text{CO})_8$ (1.2 equiv), CH_2Cl_2 , 9 h; then NMO, 23 °C	4.5 :1	78%	
3. $\text{Mo}(\text{CO})_6$ (1.2 equiv), DMSO, PhMe, 110 °C	--	trace	
4. $\text{Mo}(\text{CO})_3(\text{DMF})_3$ (1.1 equiv), CH_2Cl_2 , 23 °C	>20:1	67%	
5. $[\text{RhCl}(\text{CO})_2]_2$ (1 mol %), CO (1 atm), <i>m</i> -xylene, 110 °C	>20:1	85%	

A sample of the minor diastereomer (**99b**) was obtained via purification of entry **2** for characterization purposes.

Minor Diastereomer (99b):

TLC (70% EtOAc/Hexanes), R_f : 0.52 (UV, *p*-anisaldehyde). **^1H NMR (500 MHz, CDCl_3):** δ 7.38 – 7.26 (m, 8H), 7.25 – 7.20 (m, 2H), 5.24 (d, J = 5.9 Hz, 1H), 5.06 (d, J = 6.0 Hz, 1H), 4.83 (d, J = 6.8 Hz, 1H), 4.77 (d, J = 11.8 Hz, 1H), 4.70 (d, J = 6.8 Hz, 1H), 4.64 (d, J = 11.8 Hz, 1H), 4.47 (d, J = 11.5 Hz, 1H), 4.41 (d, J = 11.5 Hz, 1H), 4.02 (d, J = 11.0 Hz, 1H), 2.83 (ddt, J = 7.4, 5.0, 2.5 Hz, 1H), 2.69 (dd, J = 18.6, 1.0 Hz, 1H), 2.65 (dd, J = 16.4, 6.7 Hz, 1H), 2.63 (d, J = 18.7 Hz, 1H), 2.35 – 2.23 (m, 1H), 2.33 (dd, J = 16.4, 5.1 Hz, 1H), 2.08 (d, J = 2.4 Hz, 3H), 2.02 – 1.91 (m, 1H), 1.79 – 1.64 (m, 2H), 1.63 – 1.52 (m, 1H), 1.19 (d, J = 6.5 Hz, 3H), 1.11 (s, 3H); **^{13}C NMR (126 MHz, CDCl_3):** δ 208.8, 172.3, 168.0, 137.9, 136.4, 135.9, 128.6, 128.3, 128.2, 128.1, 127.7, 127.6, 91.8, 90.6, 89.3, 89.0, 78.2, 70.5, 70.5, 51.1, 48.0, 42.8, 41.8, 30.0, 28.7, 21.9, 18.5, 16.7, 9.4; **FTIR (NaCl, thin film):** 2929, 1748, 1707, 1453, 1234, 1025, 1008 cm^{-1} ; **HRMS:** calc'd for $[\text{M}+\text{Na}]^+$: 569.2510, found: 569.2510; **$[\alpha]_D^{25}$:** -140 (c = 0.20, CHCl_3).

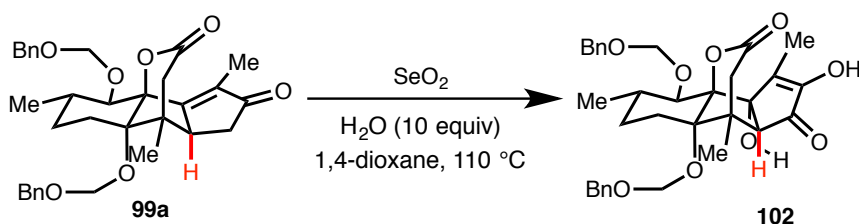
Preparation of Enone 15:

To a 500-mL, round-bottomed flask containing enyne **98** (6.33 g, 12.2 mmol, 1.0 equiv) was added $[\text{RhCl}(\text{CO})_2]_2$ (47.4 mg, 0.122 mmol, 0.01 equiv) in a nitrogen-filled glovebox. The flask was capped with a rubber septum, removed from the glovebox, and anhydrous *m*-xylene (120 mL) was added via syringe. The flask was equipped with an outlet needle and dry argon was bubbled through the solution for five minutes, followed by carbon monoxide for five minutes [Caution! Carbon monoxide is highly toxic. This reaction must be run in an efficient fume hood!]. The vent needle was removed and a CO atmosphere was maintained in the flask by means of a double-walled balloon, then the flask was submerged into a preheated oil bath at 110 °C. After heating for 2 h, the reaction was cooled to ambient temperature, sparged with N_2 to thoroughly expel excess CO gas, then the solvent was removed *in vacuo* (an efficient rotovap was utilized with a bath temperature at 50 °C) to afford a thick, dark orange oil. ^1H NMR analysis of the unpurified reaction mixture could not identify traces of the undesired diastereomer, **99b**. Purification by silica gel chromatography (30 to 50 to 70 % EtOAc in hexanes) afforded enone **99a** as a crunchy foam. Dissolution of the resulting foam in Et_2O followed by reevaporation (2 x 100 mL) affords enone **99a** as an off-white powder (5.66 g, 10.4

mmol, 85% yield). Single crystals suitable for X-ray diffraction were obtained from this material by crystallization from Et₂O (See S30 for Data).

TLC (70% EtOAc/Hexanes), R_f: 0.60 (UV, *p*-anisaldehyde); **¹H NMR (500 MHz, CDCl₃):** δ 7.37 – 7.27 (m, 10H), 5.02 (d, *J* = 6.9 Hz, 1H), 4.98 (d, *J* = 6.9 Hz, 1H), 4.85 (d, *J* = 11.9 Hz, 1H), 4.85 (d, *J* = 6.7 Hz, 1H), 4.78 (d, *J* = 6.8 Hz, 1H), 4.70 (d, *J* = 11.7 Hz, 1H), 4.63 (d, *J* = 11.7 Hz, 1H), 4.59 (d, *J* = 11.9 Hz, 1H), 4.13 (d, *J* = 10.4 Hz, 1H), 3.63 (dtd, *J* = 8.7, 3.4, 1.7 Hz, 1H), 2.48 (dd, *J* = 18.4, 6.6 Hz, 1H), 2.32 (dd, *J* = 19.5, 1.3 Hz, 1H), 2.28 – 2.21 (m, 1H), 2.25 (d, *J* = 19.6 Hz, 1H), 2.06 (dd, *J* = 18.4, 3.3 Hz, 1H), 2.03 – 1.96 (m, 1H), 1.93 (d, *J* = 2.7 Hz, 3H), 1.75 (dtd, *J* = 11.5, 4.3, 2.6 Hz, 1H), 1.71 – 1.57 (m, 2H), 1.16 (d, *J* = 6.6 Hz, 3H), 1.14 (s, 3H); **¹³C NMR (126 MHz, CDCl₃):** δ 209.2, 174.1, 168.8, 140.9, 137.6, 137.0, 128.5, 128.4, 128.0, 127.9, 127.7, 127.6, 95.5, 90.1, 89.3, 87.1, 79.2, 71.2, 70.7, 51.0, 45.4, 37.3, 35.6, 32.1, 28.5, 20.6, 18.8, 18.2, 10.1; **FTIR (NaCl, thin film):** 2954, 2872, 1748, 1707, 1454, 1209, 1154, 1042, 1025 cm⁻¹; **HRMS:** calc'd for [M+Na]⁺: 569.2510, found: 569.2523; [α]_D²⁵: +180 (*c* = 1.0, CHCl₃).

Preparation of Diosphenol 102:



110 °C for 1 h. The vial was then cooled to ambient temperature, diluted with EtOAc (50 mL) and washed with sat. aq. NaHCO₃ (2 x 50 mL). The combined aqueous layers were then extracted with EtOAc (15 mL), the combined organics dried over anhydrous Na₂SO₄, and the solution filtered and concentrated *in vacuo* to afford a dark orange foam. Purification by silica gel chromatography (2% MeOH in CH₂Cl₂) affords an orange foam that was used in the subsequent reaction without additional purification.

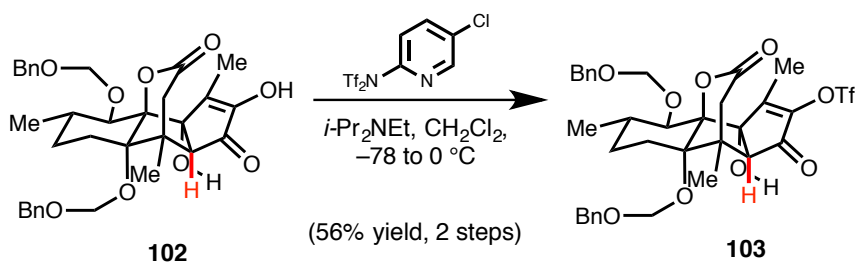
Notes: Large amounts of Se-based byproducts (both selenium black and selenium red) are produced during the course of this reaction. Although material post-chromatography appears to be spectroscopically pure by ¹H NMR spectroscopy, integration of purified material against an internal standard indicates that a significant amount of selenium red (colloidal) is co-eluted during silica gel chromatography, and thus a two-step yield is obtained after triflation (see next step).

A sample of diosphenol **102** was further purified by repeated chromatography to remove Se-based byproducts to afford an analytically pure sample for characterization purposes, affording **102** as a colorless foam.

TLC (70% EtOAc/Hexanes), R_f: 0.50 (UV, KMnO₄); **¹H NMR (500 MHz, CDCl₃):** δ 7.40 – 7.27 (m, 10H), 5.39 (s, 1H), 5.09 (d, *J* = 5.4 Hz, 1H), 5.01 (d, *J* = 6.8 Hz, 1H), 4.97 (d, *J* = 6.8 Hz, 1H), 4.84 (d, *J* = 5.4 Hz, 1H), 4.76 (d, *J* = 11.7 Hz, 1H), 4.71 (d, *J* = 11.7 Hz, 1H), 4.71 (d, *J* = 12.2 Hz, 1H), 4.64 (d, *J* = 12.2 Hz, 1H), 4.55 (s, 1H), 3.99 (d, *J* = 10.5 Hz, 1H), 2.92 (s, 1H), 2.29 (dd, *J* = 19.9, 1.2 Hz, 1H), 2.24 (d, *J* = 19.9 Hz, 1H),

2.11 – 2.03 (m, 1H), 2.10 (s, 3H), 1.96 – 1.88 (m, 1H), 1.69 – 1.47 (m, 3H), 1.28 (s, 3H), 1.05 (d, $J = 6.6$ Hz, 3H); ^{13}C NMR (126 MHz, CDCl_3): δ 200.1, 166.9, 150.0, 143.9, 137.0, 136.9, 128.7, 128.6, 128.2, 128.1, 128.0, 127.7, 97.0, 91.4, 90.6, 89.8, 87.1, 80.0, 71.1, 70.3, 64.4, 45.1, 39.1, 33.3, 27.9, 21.3, 19.9, 18.5, 11.2; FTIR (NaCl, thin film): 3350, 2926, 1744, 1707, 1405, 1240, 1157, 1034 cm^{-1} ; HRMS: calc'd for $[\text{M}+\text{NH}_4]^+$: 596.2871, found: 596.2854; $[\alpha]_{\text{D}}^{25}$: +79 ($c = 0.55$, CHCl_3).

Preparation of Triflate **103**:

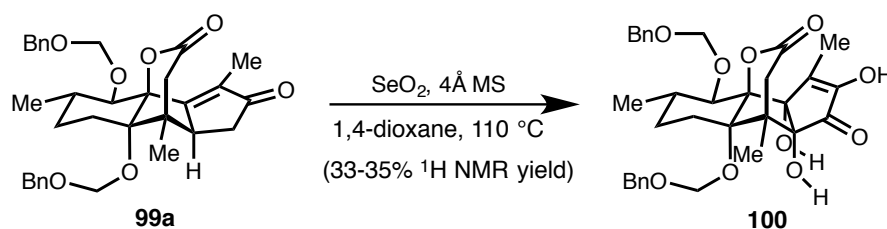


To a 25-mL, round-bottomed flask was added **102** (material directly isolated from the previous reaction) and anhydrous CH_2Cl_2 (4.0 mL). $i\text{-Pr}_2\text{NEt}$ (0.18 mL) was added and then solution cooled to -78°C in a dry ice/acetone bath. N -(5-chloro-2-pyridyl)bis(trifluoromethanesulfonylimide) (Comins' reagent, 78.5 mg, 0.20 mmol, 1.0 equiv) was then added in a single portion and the solution stirred for 5 minutes, then the cold bath removed and replaced with an ice/water bath at 0°C . After 1 h, the solution was directly loaded onto a silica gel column (30 to 40% EtOAc in hexanes) to afford triflate **103** as a colorless foam (79.4 mg, 0.111 mmol, 56% yield).

TLC (40% EtOAc/Hexanes), R_f : 0.40 (UV, KMnO_4); ^1H NMR (CDCl_3 , 400 MHz): δ 7.41 – 7.29 (m, 11H), 5.33 (s, 1H), 5.05 (d, $J = 4.7$ Hz, 1H), 4.99 (d, $J = 6.8$ Hz, 1H),

4.95 (d, $J = 6.9$ Hz, 1H), 4.79 (d, $J = 4.8$ Hz, 1H), 4.77 (d, $J = 11.8$ Hz, 1H), 4.71 (d, $J = 11.7$ Hz, 1H), 4.64 (s, 2H), 4.01 (d, $J = 10.5$ Hz, 1H), 3.03 (d, $J = 1.5$ Hz, 1H), 2.49 (d, $J = 19.9$ Hz, 1H), 2.31 (dd, $J = 19.9, 1.5$ Hz, 1H), 2.26 (s, 3H), 2.15 – 2.05 (m, 1H), 1.96 – 1.88 (m, 1H), 1.70 – 1.46 (m, 3H), 1.30 (s, 3H), 1.01 (d, $J = 6.5$ Hz, 3H); ^{13}C NMR (126 MHz, CDCl_3): δ 195.5, 166.0, 164.0, 144.8, 137.0, 136.1, 128.8, 128.7, 128.4, 128.2, 128.0, 127.8, 118.3 (q, $J_{\text{C-F}} = 321$ Hz), 96.6, 90.5, 90.5, 89.5, 86.0, 79.5, 70.8, 70.0, 63.6, 45.7, 38.8, 33.2, 27.8, 21.2, 19.8, 18.2, 12.6; FTIR (NaCl, thin film): 3368, 2930, 2875, 1756, 1732, 1426, 1216, 1038 cm^{-1} ; HRMS: calc'd for $[\text{M}+\text{NH}_4]^+$: 728.2347, found 728.2359; $[\alpha]_{\text{D}}^{25}$: +83 ($c = 1.0$ CHCl_3).

Preparation of Diosphenol 100:



To an oven-dried, 48-mL, heavy-walled pressure vessel equipped with a magnetic stirbar was charged enone **99a** (1.09 g, 2.00 mmol, 1.0 equiv), anhydrous SeO_2 (2.22 g, 20.0 mmol, 10.0 equiv), and freshly activated 4 Å molecular sieves (prepared via vigorous flame-drying at <200 mTorr for 10 minutes, 2.18 g, 200 wt % relative to substrate) in a nitrogen-filled glovebox. Anhydrous 1,4-dioxane (20 mL) was then added and the vessel was tightly sealed, removed from the glovebox, and submerged in a preheated oil bath at 110 °C. After 9.0 h, the vessel was allowed to cool to ambient temperature, diluted with EtOAc (100 mL), and filtered through a short pad of Celite, rinsing with additional EtOAc (50 mL). The resulting filtrate was then washed with sat. aq. NaHCO_3 (2 x 50

mL), H₂O (50 mL), and the combined aqueous layers back extracted with EtOAc (2 x 25 mL). The combined organics were then dried over anhydrous Na₂SO₄, filtered, and concentrated *in vacuo* to afford an orange foam. ¹H NMR analysis of this crude reaction mixture, integrating an external standard of phenyltrimethylsilane, indicated that **100** had been produced in 34% ¹H NMR yield. The crude residue was purified via silica gel chromatography (slurry packed column, 2% MeOH in CH₂Cl₂) to afford a pale orange-tan foam. The isolated material (typically ~575 mg) was carried to the next reaction without further purification.

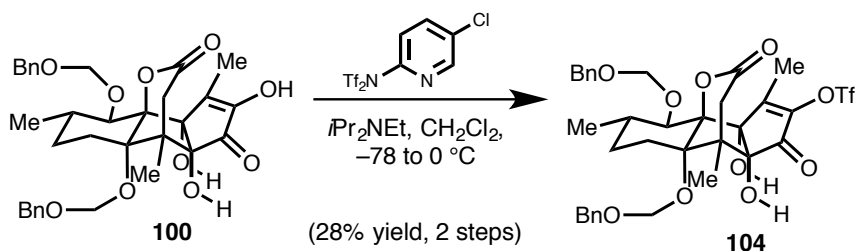
Notes: It is critical that the reaction is rigorously anhydrous. Strictly anhydrous solvent and adequately activated 4Å molecular sieves are necessarily for complete conversion to **100**. Failure to use rigorously anhydrous solvent or adequately flame-dried 4Å molecular sieves can result in contaminated material (containing up to ~7% **102**), which is extremely challenging to separate by silica gel chromatography. Furthermore, failure to remove residual **102** from samples carried through the triflation results in an inseparable mixture of vinyl triflates **103** and **104**.

As above, amounts of Se-based byproducts (both selenium black and selenium red) are produced during the course of this reaction. Although material post-chromatography appears to be spectroscopically pure by ¹H NMR spectroscopy, integration of purified material against an internal standard indicates that a significant amount of red selenium (colloidal) is co-eluted during silica gel chromatography, and thus a two-step yield is obtained after triflation (see next step).

A sample of this material was further purified by repeated silica gel chromatography for characterization purposes:

TLC (70% EtOAc/Hexanes), R_f : 0.36 (UV, KMnO_4); **^1H NMR (500 MHz, CDCl_3):** δ 7.40 – 7.27 (m, 10H), 5.66 (br s, 1H), 5.15 (d, $J = 5.7$ Hz, 1H), 4.96 (d, $J = 6.1$ Hz, 1H), 4.93 (d, $J = 6.2$ Hz, 1H), 4.89 (d, $J = 5.7$ Hz, 1H), 4.76 (d, $J = 12.1$ Hz, 1H), 4.70 (s, 1H), 4.70 (s, 1H), 4.65 (d, $J = 12.1$ Hz, 1H), 4.60 (s, 1H), 4.08 (s, 1H), 4.00 (d, $J = 10.5$ Hz, 1H), 2.41 (d, $J = 19.8$ Hz, 1H), 2.25 (d, $J = 19.9$ Hz, 1H), 2.14 (s, 3H), 2.13 – 2.00 (m, 1H), 1.92 – 1.81 (m, 1H), 1.64 (dtd, $J = 6.7, 4.6, 2.1$ Hz, 1H), 1.56 – 1.42 (m, 2H), 1.27 (s, 3H), 1.08 (d, $J = 6.6$ Hz, 3H); **^{13}C NMR (126 MHz, CDCl_3):** δ 197.2, 166.7, 149.3, 146.0, 137.0, 136.4, 128.7, 128.6, 128.4, 128.1, 128.0, 127.8, 97.1, 91.2, 90.6, 90.2, 86.6, 84.6, 79.9, 71.7, 70.4, 47.3, 40.8, 33.1, 27.9, 21.5, 18.6, 15.1, 11.3; **FTIR (NaCl, thin film):** 3368, 2928, 1747, 1717, 1659, 1454, 1405, 1360, 1155, 1035 cm^{-1} ; **HRMS:** calc'd for $[\text{M}+\text{Na}]^+$: 617.2357, found: 617.2367; **$[\alpha]_D^{25}$:** +120 ($c = 0.86$, CHCl_3).

Preparation of Vinyl Triflate **104**:

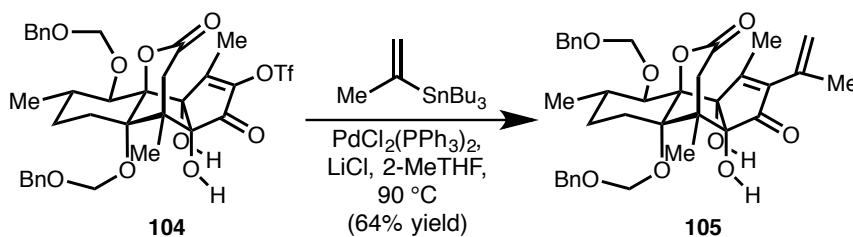


To a 50-mL, round-bottomed flask was added **100** (directly from the previous reaction, approximately 575 mg) and anhydrous CH_2Cl_2 (20 mL). $i\text{Pr}_2\text{NEt}$ (0.89 mL) was added, and then the solution was cooled to -78 °C in a dry ice/acetone bath. *N*-(5-chloro-2-pyridyl) bis(trifluoromethanesulfonimide) (Comins' reagent, 589 mg, 1.50 mmol) was

then added in a single portion and the solution stirred for five minutes, then the cold bath removed and replaced with an ice/water bath at 0 °C. After 1 h, the solution was directly purified by silica gel chromatography (30 to 40% EtOAc in Hexanes) to afford triflate **104** as a slightly off white foam (413 mg, 0.568 mmol, 28% yield, 2 steps).

TLC(40% EtOAc/Hexanes), R_f : 0.36 (UV, KMnO_4); **^1H NMR (CDCl_3 , 400 MHz):** δ 7.41 – 7.28 (m, 10H), 5.09 (d, J = 5.4 Hz, 1H), 4.98 (s, 1H), 4.95 (d, J = 6.2 Hz, 1H), 4.93 (d, J = 6.2 Hz, 1H), 4.88 (d, J = 5.4 Hz, 1H), 4.73 (d, J = 12.2 Hz, 1H), 4.69 (m, 2H), 4.65 (d, J = 12.0 Hz, 1H), 4.21 (s, 1H), 3.98 (d, J = 10.5 Hz, 1H), 2.53 (d, J = 20.3 Hz, 1H), 2.44 (d, J = 20.2 Hz, 1H), 2.30 (s, 3H), 2.08 (tdd, J = 13.8, 7.0, 3.9 Hz, 1H), 1.93 – 1.83 (m, 1H), 1.70 – 1.60 (m, 1H), 1.54 – 1.44 (m, 2H), 1.28 (s, 3H), 1.07 (d, J = 6.6 Hz, 3H); **^{13}C NMR (126 MHz, CDCl_3):** δ 192.9, 165.6, 164.6, 144.4, 136.6, 136.2, 128.8, 128.7, 128.5, 128.2, 128.1, 127.8, 118.3 (q, $J_{\text{C-F}}$ = 321 Hz), 96.8, 90.6, 90.4, 90.2, 85.7, 84.4, 79.5, 71.8, 70.4, 47.6, 40.1, 33.0, 27.8, 21.4, 18.4, 15.1, 12.7; **FTIR (NaCl, thin film):** 3368, 2931, 1743, 1650, 1429, 1243, 1216, 1040 cm^{-1} ; **HRMS:** calc'd for $[\text{M}+\text{NH}_4]^+$: 744.2313, found: 744.2296; **$[\alpha]_D^{25}$:** +58 (c = 0.74, CHCl_3).

Preparation of Enone **105**:



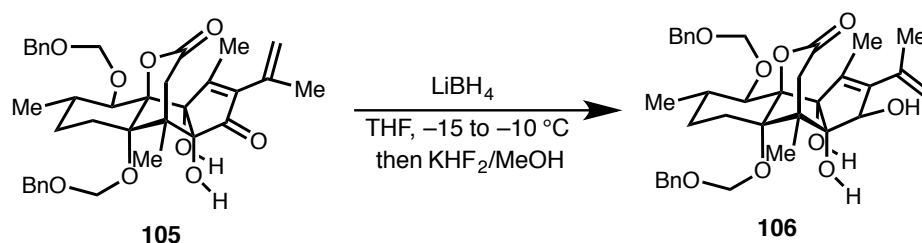
In a nitrogen-filled glovebox, an oven-dried, 48-mL capacity heavy-walled pressure vessel was charged with vinyl triflate **104** (413 mg, 0.568 mmol, 1.0 equiv),

$\text{PdCl}_2(\text{PPh}_3)_2$ (159 mg, 0.227 mmol, 40 mol %), anhydrous LiCl (192 mg, 4.54 mmol, 8.0 equiv), tributyl(2-propenyl)stannane (752 mg, 2.27 mmol, 4.0 equiv), and anhydrous 2-methyltetrahydrofuran (11 mL). The vial was sealed with a PTFE-lined cap, and submerged in a preheated oil bath at 90 °C. After 14 h, the vial was removed from the bath and allowed to cool to ambient temperature, then sat. aq. KF (15 mL) was added. The solution was stirred for 45 minutes, diluted with EtOAc (50 mL) and washed with sat. aq. KF (20 mL). The combined aqueous layers were extracted with additional EtOAc (25 mL), and the combined organics washed with brine (50 mL), dried over anhydrous Na_2SO_4 , filtered over Celite, and concentrated *in vacuo* to afford a red-brown oil. Purification by silica gel chromatography (30 to 40% EtOAc in hexanes) afforded the desired product **105** as an off-white foam (224 mg, 0.363 mmol, 64% yield).

TLC (40% EtOAc/Hexanes), R_f : 0.32 (UV, KMnO_4); **^1H NMR (CDCl_3 , 400 MHz):** 7.40 – 7.27 (m, 10H), 5.24 (p, $J = 1.6$ Hz, 1H), 5.15 (d, $J = 5.9$ Hz, 1H), 4.96 (d, $J = 6.3$ Hz, 1H), 4.94 (d, $J = 6.3$ Hz, 1H), 4.92 (d, $J = 5.9$ Hz, 1H), 4.82 (dq, $J = 2.0, 1.0$ Hz, 1H), 4.78 (d, $J = 12.1$ Hz, 1H), 4.70 (s, 2H), 4.64 (d, $J = 12.1$ Hz, 1H), 4.27 (s, 1H), 4.01 (d, $J = 10.5$ Hz, 1H), 3.94 (s, 1H), 2.42 (d, $J = 19.8$ Hz, 1H), 2.32 (d, $J = 19.8$ Hz, 1H), 2.25 (s, 3H), 2.14 – 2.01 (m, 1H), 1.89 – 1.82 (m, 1H), 1.87 (q, $J = 1.5$ Hz, 3H), 1.65 (dt, $J = 7.9, 4.9, 2.2$ Hz, 1H), 1.54 – 1.46 (m, 2H), 1.26 (s, 3H), 1.10 (d, $J = 6.5$ Hz, 3H); **^{13}C NMR (126 MHz, CDCl_3):** δ 202.1, 171.0, 166.8, 143.7, 137.3, 136.5, 135.6, 128.7, 128.5, 128.4, 128.1, 127.9, 127.7, 118.2, 97.1, 91.3, 91.2, 90.3, 88.1, 85.5, 79.9, 71.8, 70.5, 47.6, 40.9, 33.1, 27.9, 21.6, 21.4, 18.7, 15.0, 15.0; **FTIR (NaCl, thin film):** 3412, 2953, 2925,

1749, 1709, 1037, 1026 cm⁻¹; **HRMS**: calc'd for [M+Na]⁺: 641.2721, found: 641.2729; **[α]_D²⁵**: +100 (*c* = 0.67, CHCl₃).

Preparation of 106:

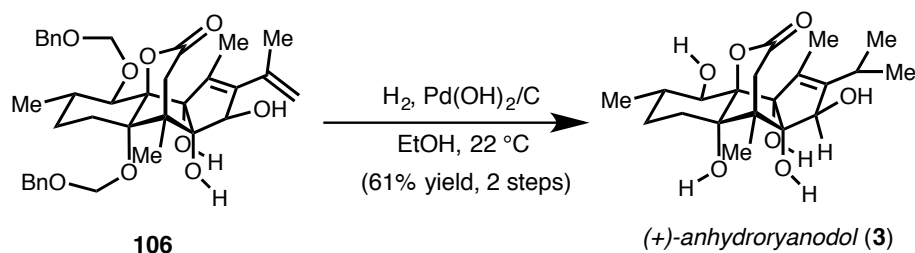


To an oven-dried, 2-dram vial was added enone **105** (250 mg, 0.404 mmol, 1.00 equiv), and anhydrous THF (16 mL). The solution was cooled to $-15\text{ }^{\circ}\text{C}$ in an ice/MeOH bath and solid LiBH_4 (132 mg, 6.06 mmol, 15 equiv) was added in a single portion. The temperature was carefully maintained between -10 and $-15\text{ }^{\circ}\text{C}$. After 2 h, TLC analysis indicated full consumption of the starting material. Sat. aq. NH_4Cl was then slowly added to the reaction [Caution! Vigorous evolution of H_2 gas occurs, particularly in the initial stages of addition. Careful, controlled dropwise addition is advised in order to avoid a violent reaction]. The mixture was diluted with EtOAc (30 mL), and washed thoroughly with sat. aq. NH_4Cl (2 x 20 mL), and the combined organic layers extracted with additional EtOAc (20 mL). The solution was then concentrated *in vacuo*, redissolved in MeOH (45 mL) and KHF_2 (3 M in H_2O , 3 mL) was then added and the solution vigorously swirled for two minutes and the entire mixture concentrated *in vacuo* [rotary evaporator bath temperature at $35\text{ }^{\circ}\text{C}$]. The resultant residue was suspended in EtOAc (50 mL), anhydrous Na_2SO_4 added, then filtered through a short pad of silica gel to remove

salts, and rinsed with additional EtOAc (25 mL), concentrated *in vacuo*. The resulting off-white foam was carried onto the next step without further purification.

A sample of allylic alcohol **106** could be additionally purified by preparative thin-layer chromatography (30% EtOAc in CH₂Cl₂) for characterization purposes.

TLC (40% EtOAc/Hexanes), R_f : 0.12 (UV, KMnO₄); **¹H NMR (CDCl₃, 400 MHz):** δ 7.42 – 7.26 (m, 11H), 5.17 (d, J = 6.5 Hz, 1H), 5.16 – 5.14 (m, 1H), 4.99 (d, J = 5.9 Hz, 1H), 4.95 (d, J = 5.8 Hz, 1H), 4.87 (d, J = 6.3 Hz, 1H), 4.87 (m, 1H), 4.86 – 4.83 (m, 1H), 4.79 (d, J = 12.3 Hz, 1H), 4.73 (d, J = 11.8 Hz, 1H), 4.69 (d, J = 11.8 Hz, 1H), 4.61 (d, J = 12.2 Hz, 1H), 4.41 (s, 1H), 3.91 (d, J = 10.3 Hz, 1H), 3.89 (s, 1H), 3.53 (d, J = 19.8 Hz, 1H), 2.26 (d, J = 19.8 Hz, 1H), 2.13 – 2.03 (m, 1H), 2.08 (d, J = 4.6 Hz, 1H), 1.85 (d, J = 2.3 Hz, 3H), 1.85 – 1.83 (m, 3H), 1.79 (ddd, J = 14.9, 4.4, 2.1 Hz, 1H), 1.71 – 1.63 (m, 1H), 1.60 (s, 3H), 1.56 (ddd, J = 14.9, 12.9, 4.6 Hz, 1H), 1.38 – 1.27 (m, 1H), 1.30 (s, 3H), 1.09 (d, J = 6.5 Hz, 3H); **¹³C NMR (126 MHz, CDCl₃):** δ 168.5, 143.4, 138.4, 137.7, 136.6, 136.4, 128.7, 128.4, 128.2, 127.7, 127.7, 117.0, 97.3, 91.5, 91.2, 91.1, 90.4, 88.7, 83.0, 80.6, 72.1, 70.5, 49.2, 39.6, 33.2, 28.3, 21.3, 21.2, 18.9, 16.0, 13.0; **FTIR (NaCl, thin film):** 3453, 2923, 2872, 1742, 1026 cm⁻¹; **HRMS:** calc'd for [M+Na]⁺: 643.2878, found: 643.2886; **$[\alpha]_D^{25}$:** –29 (c = 0.33, CHCl₃).

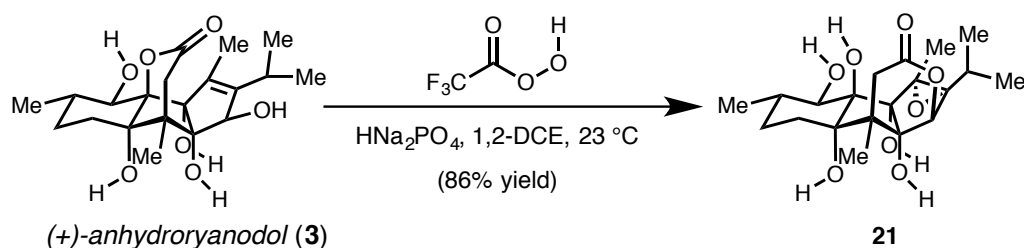
Preparation of Anhydroryanodol (3):

To a 25-mL, round-bottomed flask was charged crude triol **106**. $\text{Pd(OH)}_2/\text{C}$ (20 wt %, 375 mg) was added, followed by absolute EtOH (16 mL). The suspension was sparged with N_2 for five minutes, then H_2 for 5 minutes via a double-walled balloon. The suspension was subsequently stirred for 2 h at $20\text{ }^\circ\text{C}$ under H_2 , sparged with N_2 to remove excess hydrogen gas, then diluted with EtOAc (50 mL), filtered through a short pad of Celite and concentrated *in vacuo*. Purification of the crude residue by silica gel chromatography (slurry packed column, 4% MeOH in CHCl_3) affords (+)-anhydroryanodol (**3**) (94.1 mg, 0.246 mmol, 61% yield) as a colorless foam.

Note: Soda-lime (Flint) disposable culture tubes were purchased from Kimble Chase and used during silica gel chromatography for fraction collection in order to prevent formation of borate complexes formed with leached B_2O_3 from borosilicate (Pyrex) glassware. In some instances, leached B_2O_3 from use of borosilicate glass resulted in up to 10% of a stable borate. Treatment with aq. 3 M KHF_2 in MeOH followed by dilution with EtOAc and filtration over silica gel allowed for clean liberation of the reactive triol (as described above). The chloroform employed for silica gel chromatography contains 0.75 % EtOH as a stabilizer.

TLC (10% MeOH/CH₂Cl₂), R_f: 0.32 (KMnO₄); ¹H NMR (500 MHz, CD₃OD): δ 4.71 (q, *J* = 2.3 Hz, 1H), 3.98 (d, *J* = 10.4 Hz, 1H), 3.62 (d, *J* = 19.9 Hz, 1H), 2.75 (hept, *J* = 7.0 Hz, 1H), 2.30 (d, *J* = 19.8 Hz, 1H), 1.84 – 1.74 (m, 1H), 1.77 (d, *J* = 2.4 Hz, 3H), 1.62 – 1.43 (m, 4H), 1.18 (s, 3H), 1.15 (d, *J* = 7.0 Hz, 3H), 1.11 (d, *J* = 7.0 Hz, 3H), 1.08 (d, *J* = 6.5 Hz, 3H); ¹³C NMR (126 MHz, CD₃OD): δ 173.2, 148.3, 134.2, 93.4, 92.8, 90.3, 84.7, 84.0, 72.8, 48.9, 40.3, 35.2, 28.8, 28.5, 26.1, 21.6, 19.3, 18.8, 14.7, 12.2; **FTIR (NaCl, thin film):** 3450, 1735 cm⁻¹; **HRMS:** calc'd for [M-H]⁻: 381.1919, found: 381.2045; [α]_D²⁵: +54 (*c* = 0.45, MeOH).

Preparation of Epianhydroryanodol Epoxide (21):



Deslongchamps et. al reported the use of a 1.09 M solution of trifluoroperacetic acid in 1,2-dichloroethane, prepared according to the procedure of Emmons and Pagano.²⁸ In this report, trifluoroperacetic acid is prepared from 90% H₂O₂ (aq.) and trifluoroacetic anhydride. Given the high hazards of preparing and handling 90% H₂O₂, which has been known detonate explosively during its preparation, we prepared trifluoroperacetic acid utilizing commercially available urea hydrogen peroxide.

An approximately 1M solution of trifluoroperacetic acid was prepared according to the following procedure: to a 25-mL, round-bottomed flask was added urea hydrogen peroxide (940 mg, 10.0 mmol, 1.00 equiv) and anhydrous 1,2-dichloroethane (10.0 mL).

The suspension was cooled to 0 °C in an ice/water bath and trifluoroacetic anhydride (1.56 mL, 11 mmol, 1.1 equiv) added dropwise by syringe. The solution was stirred at 0 °C for 1 h, then the ice bath removed and stirred at 20 °C for 1 h, by which time the white suspension had changed into a biphasic mixture. Stirring was stopped to allow the layers to separate before addition.

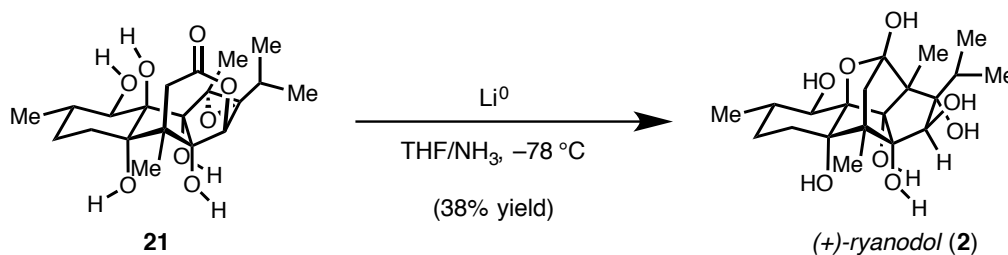
To a 100-mL, round-bottomed flask was added anhydroryanodol (76.4 mg, 0.200 mmol, 1.00 equiv), HNa_2PO_4 (170 mg, 1.20 mmol, 6.0 equiv) and 1,2-dichloroethane (30 mL). The suspension was stirred vigorously at 20 °C, then trifluoroperacetic acid (1M solution in 1,2-DCE, as prepared above, 0.40 mL, ~0.40 mmol, ~2 equiv) was added dropwise by syringe. The solution was stirred for 3 h at 20 °C, by which time TLC analysis had indicated consumption of the starting material, then filtered over a short pad of Celite to remove solids, rinsing with 1,2-dichloroethane (20 mL) and concentrated *in vacuo* to afford a white foam [Caution! Trifluoroperacetic acid, like other organic peroxides, is potentially explosive and should be used with caution. Although no incidents involving this peroxide were encountered during these studies, rotary evaporation was conducted behind a blast shield as a precaution]. Purification of the crude foam by silica gel chromatography (5% MeOH in CHCl_3) afforded epianhydroryanodol epoxide **21** as a colorless semicrystalline solid (68.5 mg, 0.172 mmol, 86% yield).

Note: Soda-lime (Flint) disposable culture tubes were purchased from Kimble Chase and used during silica gel chromatography for fraction collection in order to prevent formation of borate complexes formed with leached B_2O_3 from borosilicate (Pyrex)

glassware. The chloroform employed for silica gel chromatography contains 0.75 % EtOH as a stabilizer.

TLC (5% MeOH/CH₂Cl₂), R_f 0.20 (KMnO₄); ¹H NMR (CDCl₃, 400 MHz): δ 4.58 (s, 1H), 4.07 (d, *J* = 10.1 Hz, 1H), 3.66 (d, *J* = 16.0 Hz, 1H), 2.18 (d, *J* = 16.1 Hz, 1H), 1.87 – 1.76 (m, 2H), 1.73 – 1.64 (m, 1H), 1.63 (s, 3H), 1.59 – 1.41 (m, 3H), 1.29 (ddd, *J* = 13.0, 4.5, 2.1 Hz, 1H), 1.22 (d, *J* = 7.0 Hz, 3H), 1.06 (d, *J* = 7.3 Hz, 4H), 1.06 (d, *J* = 6.3 Hz, 3H), 1.01 (s, 3H); ¹³C NMR (CDCl₃, 400 MHz): 174.2, 94.7, 89.8, 89.1, 88.1, 85.1, 77.4, 74.8, 74.3, 51.0, 38.4, 34.6, 30.6, 28.5, 24.7, 19.1, 18.3, 17.4, 17.1, 15.2; **FTIR (NaCl, thin film):** 3462, 1736 cm⁻¹; **HRMS:** calc'd for [M+H]⁺: 399.2013, found: 399.2034. [α]_D²⁵: –39 (*c* = 0.40, MeOH).

Preparation of (+)-Ryanodol (2):



An oven-dried, 100-mL, three-necked, round-bottomed flask containing a borosilicate glass-coated magnetic stirbar was equipped with an oven-dried cold-finger condenser and allowed to cool under dry Argon. While cooling, the flask was directly connected to a gas cylinder of ammonia (Matheson anhydrous ammonia) by means of a gas inlet adapter connected to a piece of dry Tygon tubing. Once the glassware had completely cooled, the flask was submerged into a dry-ice/acetone bath (–78 °C) and the

cold finger filled with dry-ice/acetone. Ammonia was carefully condensed into the flask by opening the tank, until ~50 mL had accumulated, and both the ammonia inlet and cold finger condenser were removed and replaced with rubber septa. Freshly cut sodium metal (200 mg cut into six pieces, hexanes washed) was then added piecewise to the ammonia, which resulted immediately in a deep blue solution. This solution was maintained at -78°C for 30 min for drying.

A separate oven-dried, 100-mL, three-necked, round-bottomed flask containing a borosilicate glass coated magnetic stirbar was equipped with an oven-dried cold-finger condenser, and was allowed to cool under an Ar atmosphere. The distilling flask prepared above was then connected by means of a dry piece of Tygon tubing under a positive pressure of Argon. The receiving flask was submerged into a dry-ice/acetone bath, and the cold finger condenser filled with dry ice/acetone. The distilling flask was then removed from the cold bath, allowing for the slow distillation of anhydrous ammonia from sodium metal, until ~20 mL of ammonia had condensed into the receiving flask (approximately 30 minutes). A solution of epianhydroryanodol epoxide (**21**, 15.3 mg, $38.7\text{ }\mu\text{mol}$, 1.0 equiv) in THF (4.0 mL) was then added dropwise by syringe to the freshly distilled ammonia, which was allowed to stir for an additional 15 minutes -78°C .

A fresh piece of lithium(0)-wire (30.5 mg, stored in mineral oil), was rinsed with hexanes, then cut into a pre-tared 25-mL beaker containing hexanes (15 mL). Immediately prior to addition, this piece of wire was further cut into four pieces (~ 7-8 mg each) and added to the flask above within two minutes, and the deep blue mixture stirred for 60 min at -78°C . Ammonium chloride (solid, 750 mg) was then added slowly as a solid. The deep blue color faded within 90 seconds, producing a colorless

suspension. The cold bath was then removed and the flask was opened to atmosphere, allowing for the evaporation of ammonia as the flask warmed to ambient temperature (45 min). The resulting slurry, consisting primarily of some residual THF, LiCl, and NH₄Cl salts, was then carefully diluted with H₂O (20 mL), and additional THF (5 mL). The mixture was extracted with CH₂Cl₂ (3 x 15 mL), and the combined organics concentrated *in vacuo*. ¹H NMR analysis of this organic layer indicated the presence of a carbonyl reduction product and a small amount of starting material.

Carbon dioxide (g) was then bubbled through the aqueous layer (20 mL) for 10 minutes to neutralize the pH below 8 and the aqueous layer saturated with NaCl. This aqueous solution was then transferred into a continuous extraction apparatus equipped with an efficient reflux condenser and 100 mL round bottomed flask that had been pre-filled with CHCl₃ (50 mL in the flask, 100 mL in the extraction body). The round-bottomed flask was then heated in an oil bath at 100 °C, allowing for vigorous reflux of the chloroform, and the apparatus maintained for 40 h under a nitrogen atmosphere. The flask was then removed from the apparatus and the solvent removed *in vacuo* affording a solid residue. ¹H NMR analysis of this organic residue indicated that it was ~90% pure by NMR. The residue was again dissolved in H₂O (20 mL) and THF (5 mL) and washed with CH₂Cl₂ (3 x 15 mL). Concentration of the aqueous layer (rotovap temperature at 50 °C) and drying under high vacuum affords (+)-ryanodol (**2**) as a white solid (95% purity by ¹H NMR, 7.4 mg, 47% yield) that contains minor salt impurities and is further purified by silica gel chromatography (3 g of slurry packed silica, 10% MeOH in CHCl₃) to afford ryanodol (**2**) as a white film (5.9 mg, 14.8 μmol, 38% yield).

Notes: Deslongchamps and coworkers report a detailed procedure for this reductive cyclization on 20 mg scale, to produce 12 mg of (+)-ryanodol, isolated in pure fashion directly after continuous extraction.⁵ In our hands, the reaction profile of this transformation was determined to be highly dependent on the purity of the ammonia, particularly with respect to trace iron impurities and water. Control experiments with added H₂O (10 equiv) after distillation from sodium indicates that proton sources, as may be expected, favor the formation of carbonyl reduction products, whereas the addition of Fe-salts and direct condensation from the ammonia cylinder result in diminished reactivity, presumably due to the rapid formation of LiNH₂ catalyzed by trace metal impurities. Fresh distillation of the ammonia to aid in drying of the solvent and removal of trace impurities yielded the most reproducible results. Despite these precautions, an identical reaction profile to that described by Deslongchamps was not obtained.

A continuous extractor consisting of a 14/20 ground glass attachment was used for the extraction process. This particular extractor had a volume of approximately 120 mL, allowing for an aqueous phase of approximately 20 mL and a heavy-organic phase of 100 mL. Material obtained after continuous extraction was typically of ~90% purity by ¹H NMR. Most organic impurities were readily removed by washing with THF/DCM, as described above. However, dissolution of this material in MeOH typically left trace inorganic residues (potentially trace salts from the aqueous phase) that affect an accurate mass. The material obtained after column chromatography does not produce the same residue, lending further evidence to trace inorganic salt impurities.

¹H NMR (CDCl₃, 400 MHz): δ 4.12 (s, 1H), 3.78 (d, *J* = 10.2 Hz, 1H), 2.51 (d, *J* = 13.4 Hz, 1H), 2.15 (hept, *J* = 6.7 Hz, 1H), 2.08 (td, *J* = 12.9, 5.3 Hz, 1H), 1.90 – 1.76 (m, 1H), 1.74 (d, *J* = 13.4 Hz, 1H), 1.53 (dtd, *J* = 12.7, 5.2, 1.6 Hz, 1H), 1.46 (qd, *J* = 12.9, 4.7 Hz, 1H), 1.33 (s, 3H), 1.26 (ddd, *J* = 12.7, 4.6, 2.0 Hz, 1H), 1.12 (s, 3H), 1.08 (d, *J* = 6.8 Hz, 3H), 1.01 (d, *J* = 6.5 Hz, 3H), 1.00 (d, *J* = 6.5 Hz, 3H). **¹³C NMR (CDCl₃, 400 MHz):** δ 103.1, 96.3, 92.6, 91.6, 87.3, 86.6, 84.9, 72.9, 65.4, 49.7, 41.5, 35.4, 30.7, 29.4, 26.6, 19.5, 19.4, 19.0, 13.2, 10.2; **HRMS:** calc'd for [M–H][–]: 399.2024, found: 399.2028; **[α]_D²⁵:** +37 (*c* = 0.30, MeOH).

Comparison Tables for Authentic vs. Synthetic (+)-Ryanodol*Table 2. Comparison of ¹H NMR data for Authentic vs. Synthetic (+)-Ryanodol*

Inoue et al. Report ³² Authentic (+)-Ryanodol ¹ H NMR, 400 MHz, CD ₃ OD	This Work, Synthetic (+)-Ryanodol ¹ H NMR, 500 MHz, CD ₃ OD
δ 4.12 (s, 1H)	δ 4.12 (s, 1H)
3.77 (d, <i>J</i> = 10.4 Hz, 1H)	3.78 (d, <i>J</i> = 10.2 Hz, 1H)
2.51 (d, <i>J</i> = 13.1, 1H)	2.51 (d, <i>J</i> = 13.4 Hz, 1H)
2.15 (qq, <i>J</i> = 6.8, 6.3 Hz, 1H)	2.15 (hept, <i>J</i> = 6.7 Hz, 1H)
2.08 (1H, ddd, <i>J</i> = 12.8, 12.8, 5.5 Hz, 1H)	2.08 (td, <i>J</i> = 12.9, 5.3 Hz, 1H)
1.83 (1H, ddqd, <i>J</i> = 13.2, 10.4, 6.3, 5.8 Hz, 1H)	1.90 – 1.76 (m, 1H)
1.73 (d, <i>J</i> = 13.1 Hz, 1H)	1.74 (d, <i>J</i> = 13.4 Hz, 1H)
1.51 (dddd, 13.2, 5.8, 5.5, 1.7 Hz, 1H)	1.53 (dtd, <i>J</i> = 12.7, 5.2, 1.6 Hz, 1H)
1.45 (dddd, <i>J</i> = 13.2, 13.2, 12.8, 4.6)	1.46 (qd, <i>J</i> = 12.9, 4.7 Hz, 1H)
1.33 (s, 3H)	1.33 (s, 3H)
1.26 (ddd, <i>J</i> = 12.8, 4.6, 1.7 Hz, 1H)	1.26 (ddd, <i>J</i> = 12.7, 4.6, 2.0 Hz, 1H)
1.12 (s, 3H)	1.12 (s, 3H)
1.08 (d, <i>J</i> = 6.8, 3H)	1.08 (d, <i>J</i> = 6.8 Hz, 3H)
1.01 (d, <i>J</i> = 6.3 Hz, 3H)	1.01 (d, <i>J</i> = 6.5 Hz, 3H)
1.00 (d, <i>J</i> = 6.3 Hz, 3H)	1.00 (d, <i>J</i> = 6.5 Hz, 3H)

Table 3. Comparison of ^{13}C NMR data for Authentic vs. Synthetic (+)-Ryanodol

Inoue et al. Report, ³² Authentic (+)-Ryanodol ^{13}C NMR, 100 MHz, CD_3OD	This Work, Synthetic (+)-Ryanodol ^{13}C NMR, 126 MHz, CD_3OD	Chemical Shift Difference, $\Delta\delta$
δ 103.1	δ 103.1	0
96.3	96.3	0
92.6	92.6	0
91.6	91.6	0
87.3	87.3	0
86.6	86.6	0
84.9	84.9	0
72.9	72.9	0
65.4	65.4	0
49.6	49.7	0.1
41.5	41.5	0
35.4	35.4	0
30.7	30.7	0
29.4	29.4	0
26.6	26.6	0
19.5	19.5	0
19.4	19.4	0
19.0	19.0	0
13.2	13.2	0
10.2	10.2	0

2.5 NOTES AND REFERENCES

- (1) Deslongchamps, P.; Bélanger, A.; Berney, D. J. F.; Borschberg, H.-J.; Brousseau, R.; Doutheau, A.; Durand, R.; Katayama, H.; Lapalme, R.; Leturc, D. M.; Liao, C.-C.; MacLachlan, F. N.; Maffrand, J.-P.; Marazza, F.; Martino, R.; Moreau, C.; Ruest, L.; Saint-Laurent, L.; Saintonge, R.; Soucy, P. *Can. J. Chem.* **1990**, *68* (1), 115.
- (2) Bélanger, A.; Berney, D.; Borschberg, H.-J.; Brousseau, R.; Doutheau, A.; Durand, R.; Katayama, H.; Lapalme, R.; Leturc, D. M.; Liao, C.-C.; MacLachlan, F. N.; Maffrand, J.-P.; Marazza, F.; Martino, R.; Moreau, C.; Saint-Laurent, L.; Saintonge, R.; Soucy, P.; Ruest, L.; Deslongchamps, P. *Can. J. Chem.* **1979**, *57*, 3348.
- (3) Deslongchamps, P.; Bélanger, A.; Berney, D. J. F.; Borschberg, H.-J.; Brousseau, R.; Doutheau, A.; Durand, R.; Katayama, H.; Lapalme, R.; Leturc, D. M.; Liao, C.-C.; MacLachlan, F. N.; Maffrand, J.-P.; Marazza, F.; Martino, R.; Moreau, C.; Ruest, L.; Saint-Laurent, L.; Saintonge, R.; Soucy, P. *Can. J. Chem.* **1990**, *69*, 127.
- (4) Deslongchamps, P.; Bélanger, A.; Berney, D. J. F.; Borschberg, H.-J.; Brousseau, R.; Doutheau, A.; Durand, R.; Katayama, H.; Lapalme, R.; Leturc, D. M.; Liao, C.-C.; MacLachlan, F. N.; Maffrand, J.-P.; Marazza, F.; Martino, R.; Moreau, C.; Ruest, L.; Saint-Laurent, L.; Saintonge, R.; Soucy, P. *Can. J. Chem.* **1990**, *68*, 153.
- (5) Deslongchamps, P.; Bélanger, A.; Berney, D. J. F.; Borschberg, H.-J.; Brousseau,

- R.; Doutheau, A.; Durand, R.; Katayama, H.; Lapalme, R.; Leturc, D. M.; Liao, C.-C.; MacLachlan, F. N.; Maffrand, J.-P.; Marazza, F.; Martino, R.; Moreau, C.; Ruest, L.; Saint-Laurent, L.; Saintonge, R.; Soucy, P. *Can. J. Chem.* **1990**, *68* (1), 186.
- (6) Corey, E. J.; Ensley, H. E.; Suggs, J. W. *J. Org. Chem.* **1976**, *41* (2), 380.
- (7) Ngo, K.-S.; Cheung, K.-K.; Brown, G. D. *J. Chem. Res.* **1998**, *2*, 80.
- (8) Reusch, W.; Anderson, D. F.; Johnson, C. K. *J. Am. Chem. Soc.* **1968**, *90* (18), 4988.
- (9) Vishwakarma, L. C.; Stringer, O. D.; Davis, F. A. *Org. Synth.* **2003**, 203.
- (10) Brodsky, B. H.; Bois, Du, J. *J. Am. Chem. Soc.* **2005**, *127* (44), 15391.
- (11) Davis, F. A.; Towson, J. C.; Vashi, D. B.; ThimmaReddy, R.; McCauley, J. P.; Harakal, M. E.; Gosciniaik, D. J. *J. Org. Chem.* **1990**, *55* (4), 1254.
- (12) Towson, J. C.; Weismiller, M. C.; Lal, G. S.; Kumar, A.; Davis, F. A. *Org. Synth.* **1990**, *69*, 158.
- (13) Jung, M. E.; Davidov, P. *Org. Lett.* **2001**, *3* (4), 627.
- (14) Nahmany, M.; Melman, A. *Org. Lett.* **2001**, *3* (23), 3733.
- (15) Shelkov, R.; Nahmany, M.; Melman, A. *J. Org. Chem.* **2002**, *67*, 8975.
- (16) Egi, M.; Ota, Y.; Nishimura, Y.; Shimizu, K.; Azechi, K.; Akai, S. *Org. Lett.* **2013**, *15* (16), 4150.
- (17) Chung, Y. K.; Lee, B. Y.; Jeong, N.; Hudecek, M.; Pauson, P. L. *J. Am. Chem. Soc.* **1993**, *112* (1), 220.
- (18) Javier Adrio; Marta Rodríguez Rivero, A.; Carretero, J. C. *Org. Lett.* **2005**, *7* (3), 431.

- (19) Koga, Y.; Kobayashi, T.; Narasaka, K. *Chem. Lett.* **1998**, 3, 249.
- (20) Yu, J.-Q.; Corey, E. J. *J. Am. Chem. Soc.* **2003**, 125 (11), 3232.
- (21) Catino, A. J.; Forslund, R. E.; Doyle, M. P. *J. Am. Chem. Soc.* **2004**, 126 (42), 13622.
- (22) Wilde, N. C.; Isomura, M.; Mendoza, A.; Baran, P. S. *J. Am. Chem. Soc.* **2014**, 136, 4049.
- (23) Riley, H. L.; Morley, J. F.; Friend, N. A. C. *J. Chem. Soc. (Resumed)* **1932**, 1875.
- (24) Achenbach, H.; Hübner, H.; Vierling, W.; Brandt, W.; Reiter, M. *J. Nat. Prod.* **1995**, 58 (7), 1092.
- (25) Hübner, H.; Vierling, W.; Brandt, W.; Reiter, M.; Achenbach, H. *Phytochemistry* **2001**, 57 (2), 285.
- (26) Han, C.; Buchwald, S. L. *J. Am. Chem. Soc.* **2009**, 131 (22), 7532.
- (27) Li, L.; Wang, C.-Y.; Huang, R.; Biscoe, M. R. *Nat. Chem.* **2013**, 5 (7), 607.
- (28) Emmons, W. D.; Pagano, A. S. *J. Am. Chem. Soc.* **1955**, 77 (17), 4557.
- (29) Heaney, H.; Cardona, F.; Goti, A.; Frederick, A. L. *Hydrogen Peroxide-Urea*; John Wiley & Sons, Ltd: Chichester, UK, 2001.
- (30) Harvey, R. G.; Urberg, K. *J. Org. Chem.* **1968**, 33 (6), 2570.
- (31) Deslongchamps, P. *Pure Appl. Chem.* **1977**, 49 (9).
- (32) Nagatomo, M.; Koshimizu, M.; Masuda, K.; Tabuchi, T.; Urabe, D.; Inoue, M. *J. Am. Chem. Soc.* **2014**, 136, 5916.
- (33) Hill, A. J.; Keach, D. T. *J. Am. Chem. Soc.* **1926**, 48 (1), 257.
- (34) Shambayani, S.; Crowe, W. E.; Schreiber, S. L. *Tetrahedron Lett.* **1990**, 31 (37), 5289.

- (35) Jeong, N.; Lee, S. J.; Lee, B. Y.; Chung, Y. K. *Tetrahedron Lett.* **1993**, 34 (25), 4027.

Appendix 1

X-Ray Crystallography Report Relevant to Chapter 2

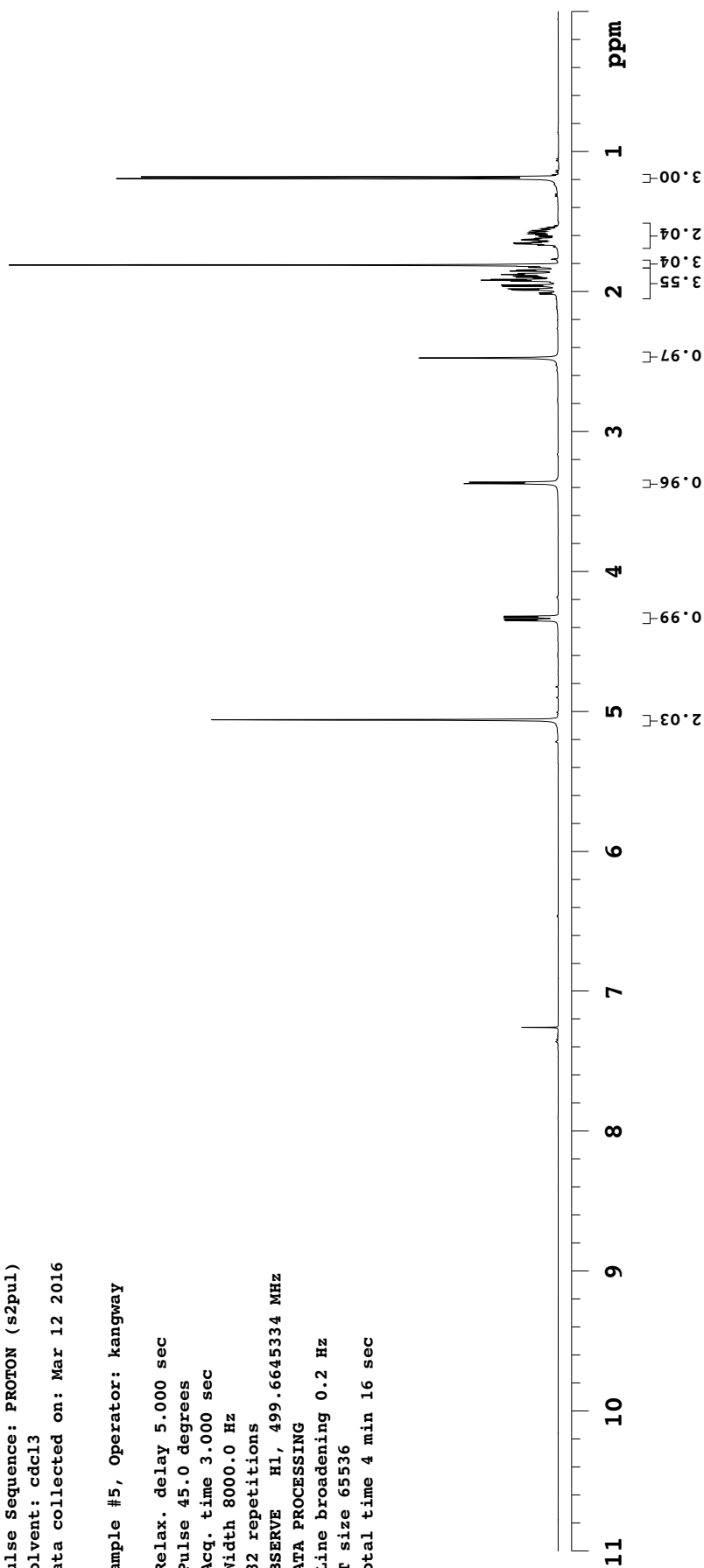
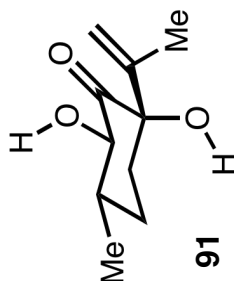
KVC25-169-Repurified

Sample Name:
 KVC25-169-Repurified
 Data Collected on:
 indy.caltech.edu-inova500
 Archive directory:
 /home/kangway/vnmrsys/data
 Sample directory:
 KVC25-169-Repurified
 FidFile: PROTON01

Pulse Sequence: PROTON (s2pul)
 Solvent: cdcl3
 Data collected on: Mar 12 2016

Sample #5, Operator: kangway

Relax. delay 5.000 sec
 Pulse 45.0 degrees
 Acq. time 3.000 sec
 Width 8000.0 Hz
 32 repetitions
 OBSERVE H1, 499.6645334 MHz
 DATA PROCESSING
 Line broadening 0.2 Hz
 FT size 65536
 Total time 4 min 16 sec



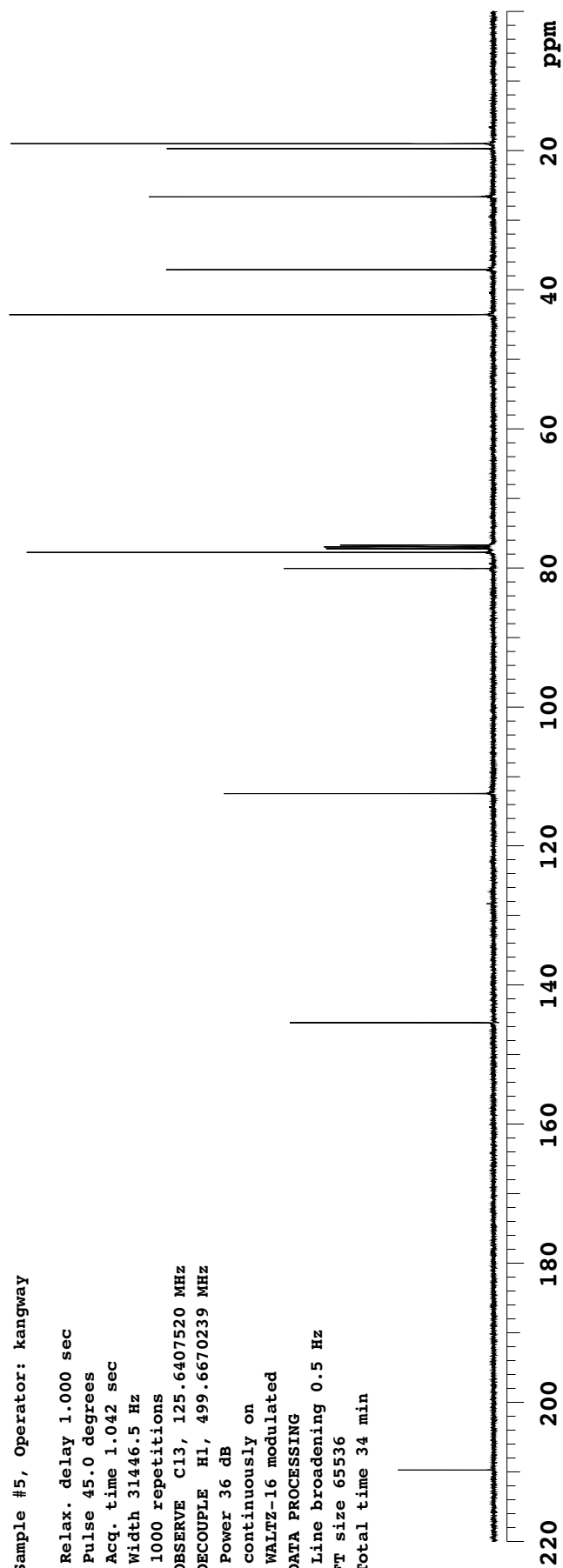
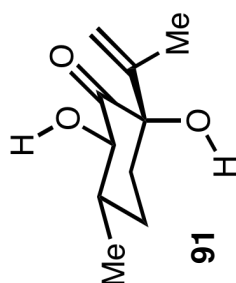
KVC25-169-Repurified

Sample Name:
KVC25-169-Repurified
Data Collected on:
indy.caltech.edu-inova500
Archive directory:
/home/kangway/vnmrsys/data
Sample directory:
KVC25-169-Repurified
FidFile: CARBON01

Pulse Sequence: CARBON (s2pul)
Solvent: cdcl3
Data collected on: Mar 12 2016

Sample #5, Operator: kangway

Relax. delay 1.000 sec
Pulse 45.0 degrees
Acq. time 1.042 sec
Width 31446.5 Hz
1000 repetitions
OBSERVE C13, 125.6407520 MHz
DECOUPLE H1, 499.6670239 MHz
Power 36 dB
continuously on
WALTZ-16 modulated
DATA PROCESSING
Line broadening 0.5 Hz
FT size 65536
Total time 34 min



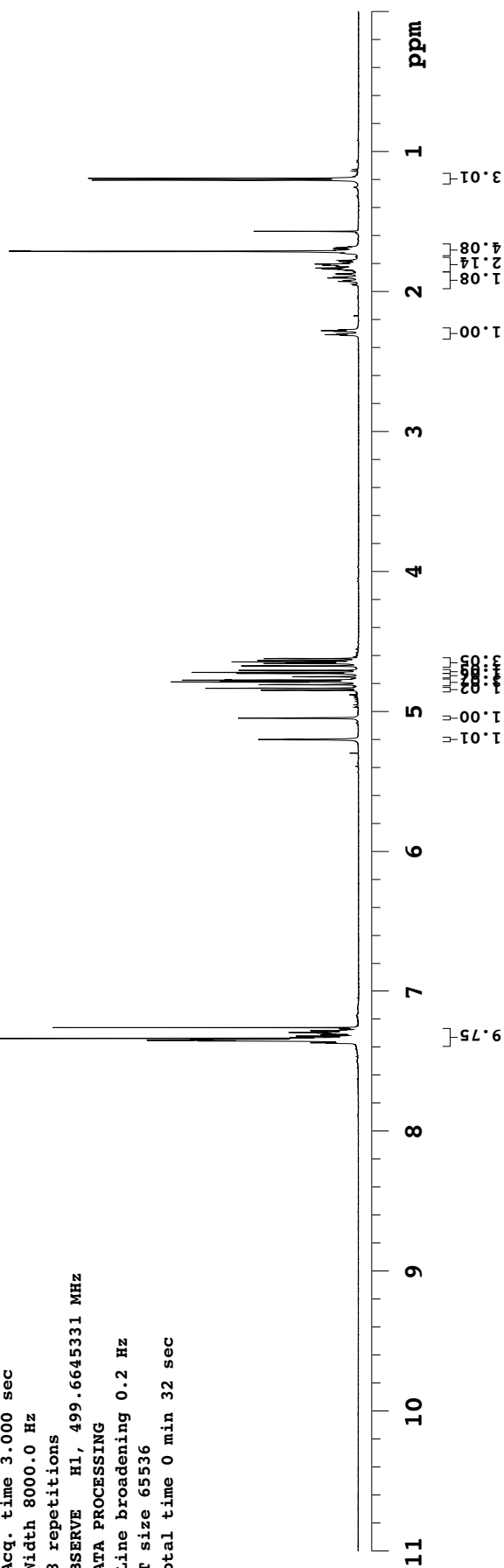
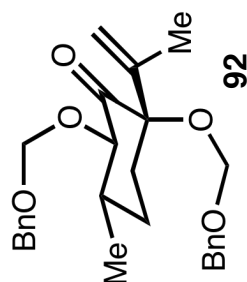
KVC25-171

Sample Name:
KVC25-171
Data Collected on:
indy.caltech.edu-inova500
Archive directory:
/home/kangway/vnmrsys/data
Sample directory:
KVC25-171
FidFile: PROTON02

Pulse Sequence: PROTON (s2pul)
Solvent: cdcl3
Data collected on: Jan 20 2016

Sample #28, Operator: kangway

Relax. delay 1.000 sec
Pulse 45.0 degrees
Acq. time 3.000 sec
Width 8000.0 Hz
8 repetitions
OBSERVE H1, 499.6645331 MHz
DATA PROCESSING
Line broadening 0.2 Hz
FT size 65536
Total time 0 min 32 sec



KVC25-171

Sample Name:

KVC25-171

Data Collected on:

indy.caltech.edu-inova500

Archive directory:

/home/kangway/vnmrsys/data

Sample directory:

KVC25-171

FidFile: CARBON01

Pulse Sequence: CARBON (s2pul)

Solvent: cdcl3

Data collected on: Jan 19 2016

Sample #28, Operator: kangway

Relax. delay 1.000 sec

Pulse 45.0 degrees

Acq. time 1.042 sec

Width 31446.5 Hz

1000 repetitions

OBSERVE C13, 125.6407491 MHz

DECOUPLE H1, 499.6670239 MHz

Power 36 dB

continuously on

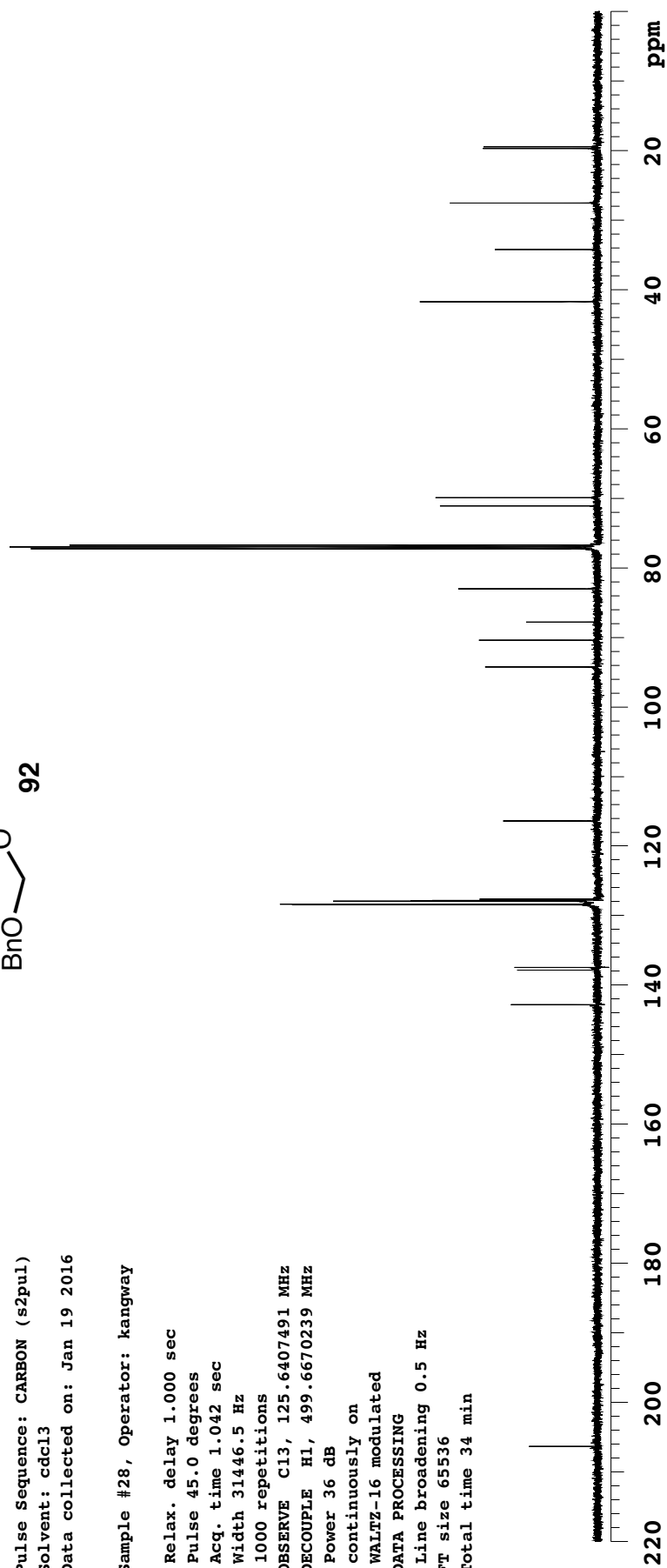
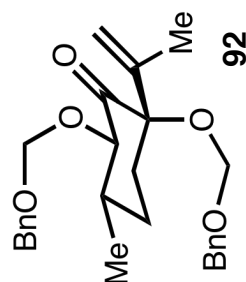
WALTZ-16 modulated

DATA PROCESSING

Line broadening 0.5 Hz

FT size 65536

Total time 34 min



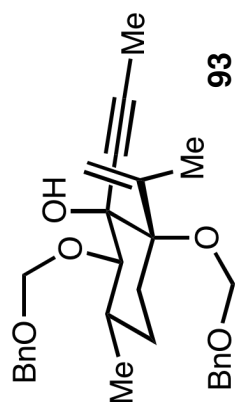
Major Diastereomer

Sample Name:
KVC25-173-Major
Data Collected on:
indy.caltech.edu-inova500
Archive directory:
/home/kangway/vnmrsys/data
Sample directory:
KVC25-173-Major
FidFile: PROTON01

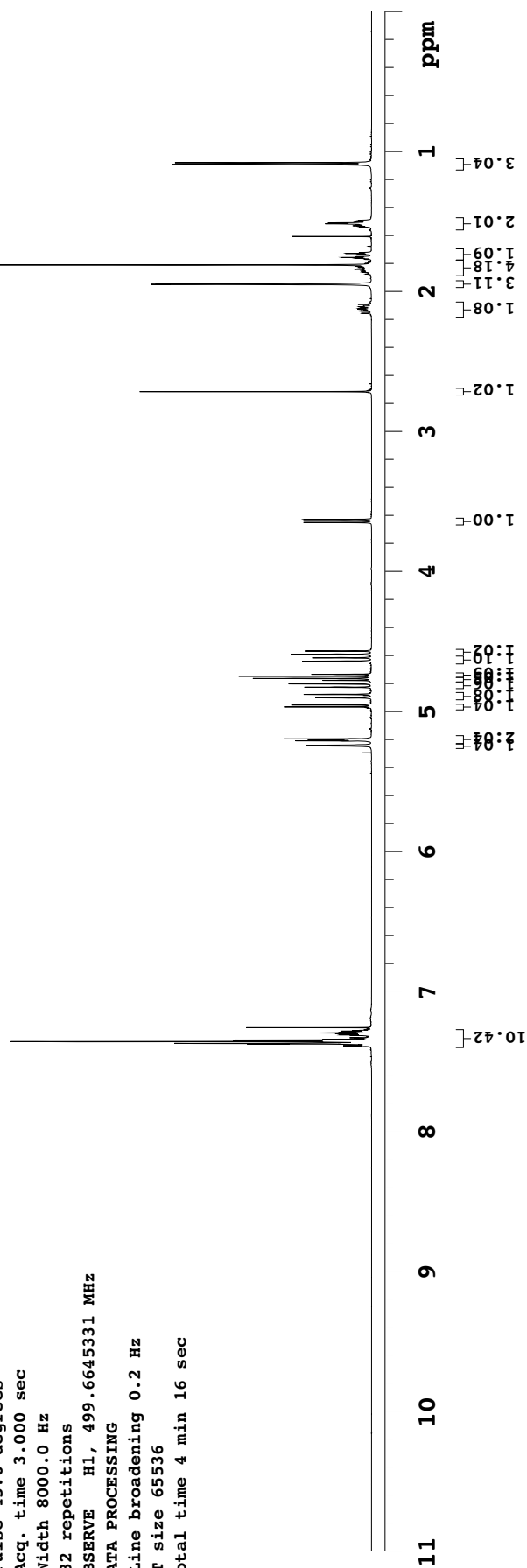
Pulse Sequence: PROTON (s2pul)
Solvent: cdcl3
Data collected on: Jan 21 2016

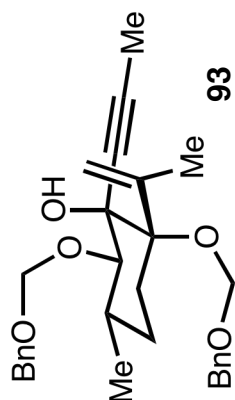
Sample #6, Operator: kangway

Relax. delay 5.000 sec
Pulse 45.0 degrees
Acq. time 3.000 sec
Width 8000.0 Hz
32 repetitions
OBSERVE H1, 499.6645331 MHz
DATA PROCESSING
Line broadening 0.2 Hz
FT size 65536
Total time 4 min 16 sec



93





93

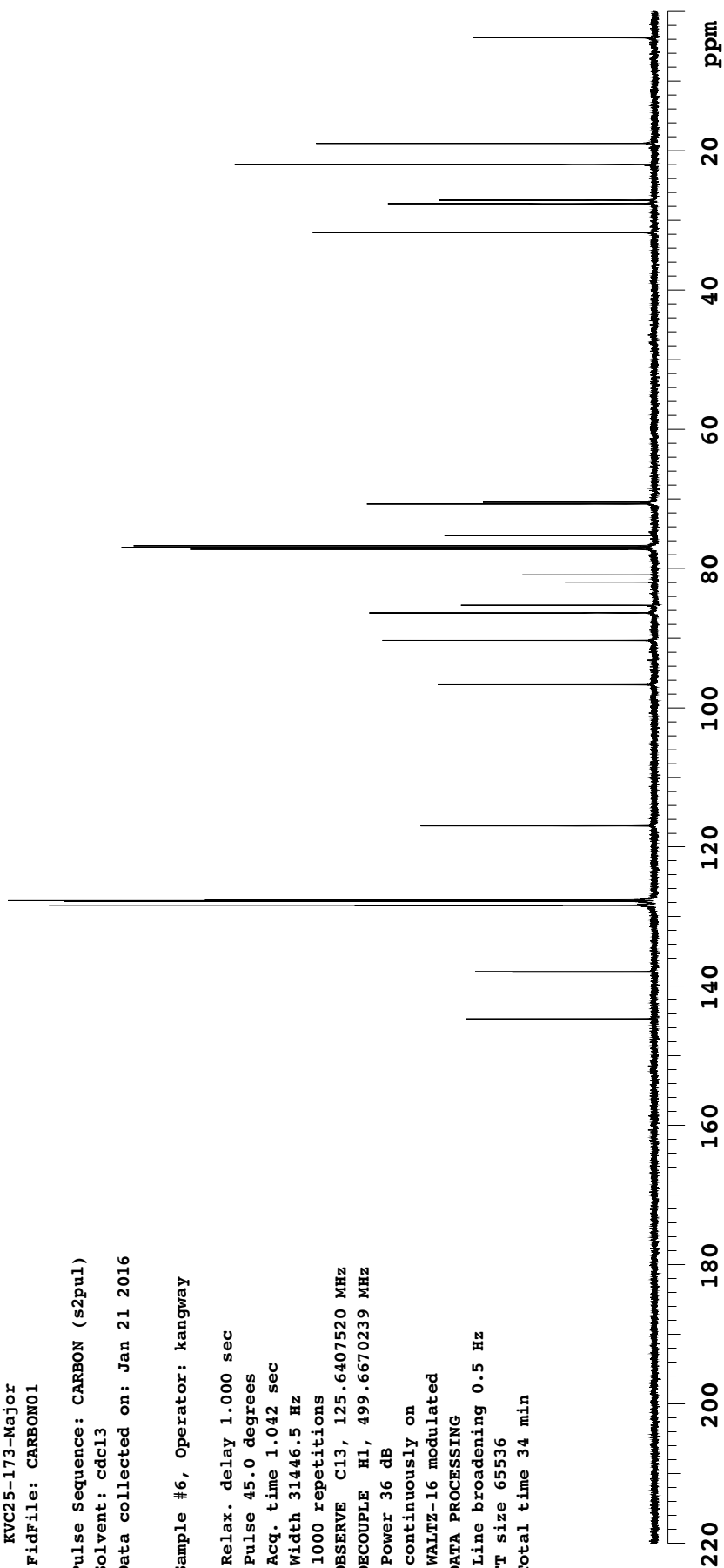
Major Diastereomer

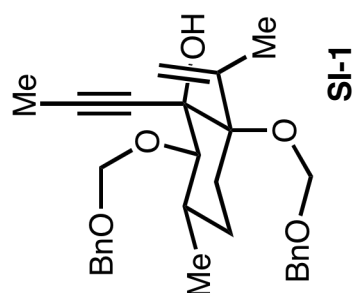
Sample Name:
KVC25-173-Major
Data Collected on:
indy.caltech.edu-inova500
Archive directory:
/home/kangway/vnmrsys/data
Sample directory:
KVC25-173-Major
FidFile: CARBON01

Pulse Sequence: CARBON (s2pul)
Solvent: cdcl3
Data collected on: Jan 21 2016

Sample #6, Operator: kangway

Relax. delay 1.000 sec
Pulse 45.0 degrees
Acq. time 1.042 sec
Width 31446.5 Hz
1000 repetitions
OBSERVE C13, 125.6407520 MHz
DECOUPLE H1, 499.6670239 MHz
Power 36 dB
continuously on
WALTZ-16 modulated
DATA PROCESSING
Line broadening 0.5 Hz
FT size 65536
Total time 34 min





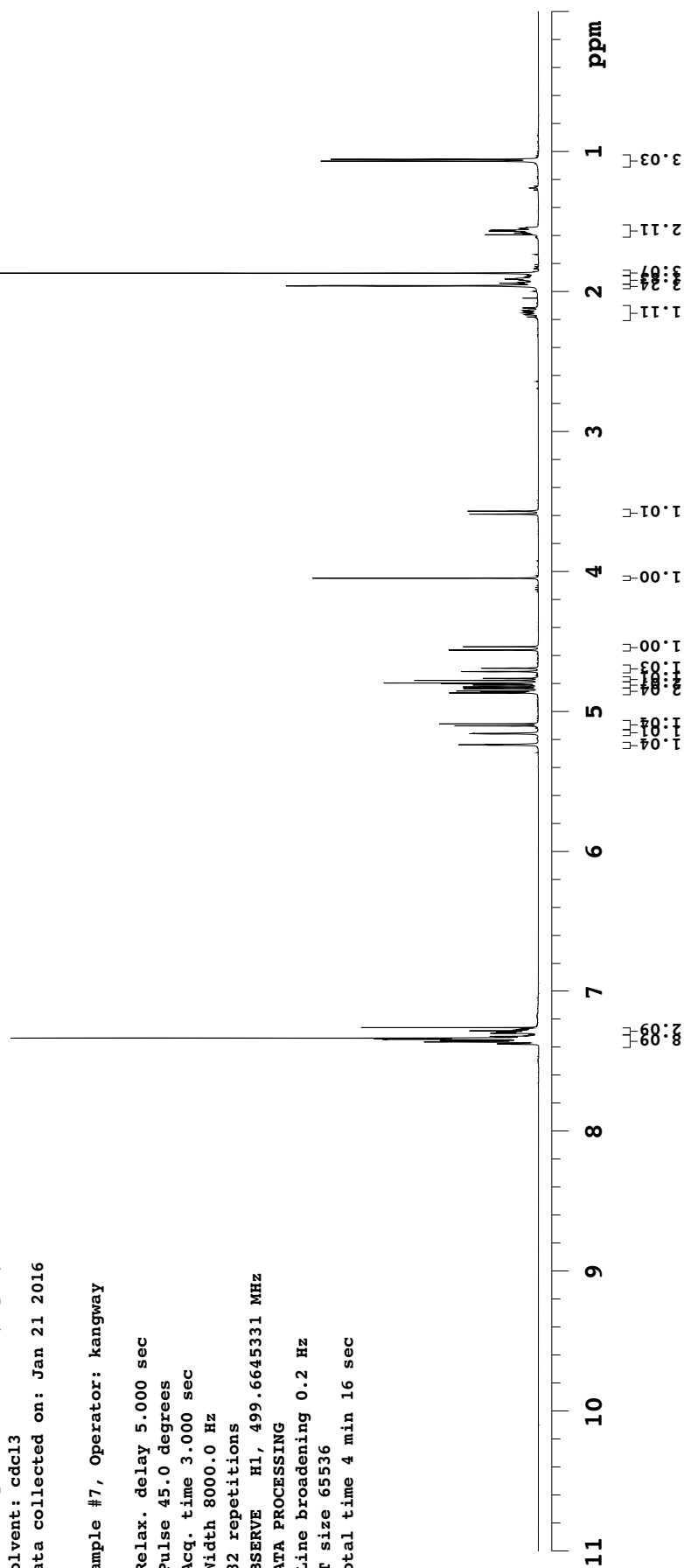
Minor Diastereomer

Sample Name:
KVC25-173-Minor
Data Collected on:
indy.caltech.edu-inova500
Archive directory:
/home/kangway/vnmrsys/data
Sample directory:
KVC25-173-Minor
FidFile: PROTON01

Pulse Sequence: PROTON (s2pul)
Solvent: cdcl3
Data collected on: Jan 21 2016

Sample #7, Operator: kangway

Relax. delay 5.000 sec
Pulse 45.0 degrees
Acq. time 3.000 sec
Width 8000.0 Hz
32 repetitions
OBSERVE H1, 499.6645331 MHz
DATA PROCESSING
Line broadening 0.2 Hz
FT size 65536
Total time 4 min 16 sec



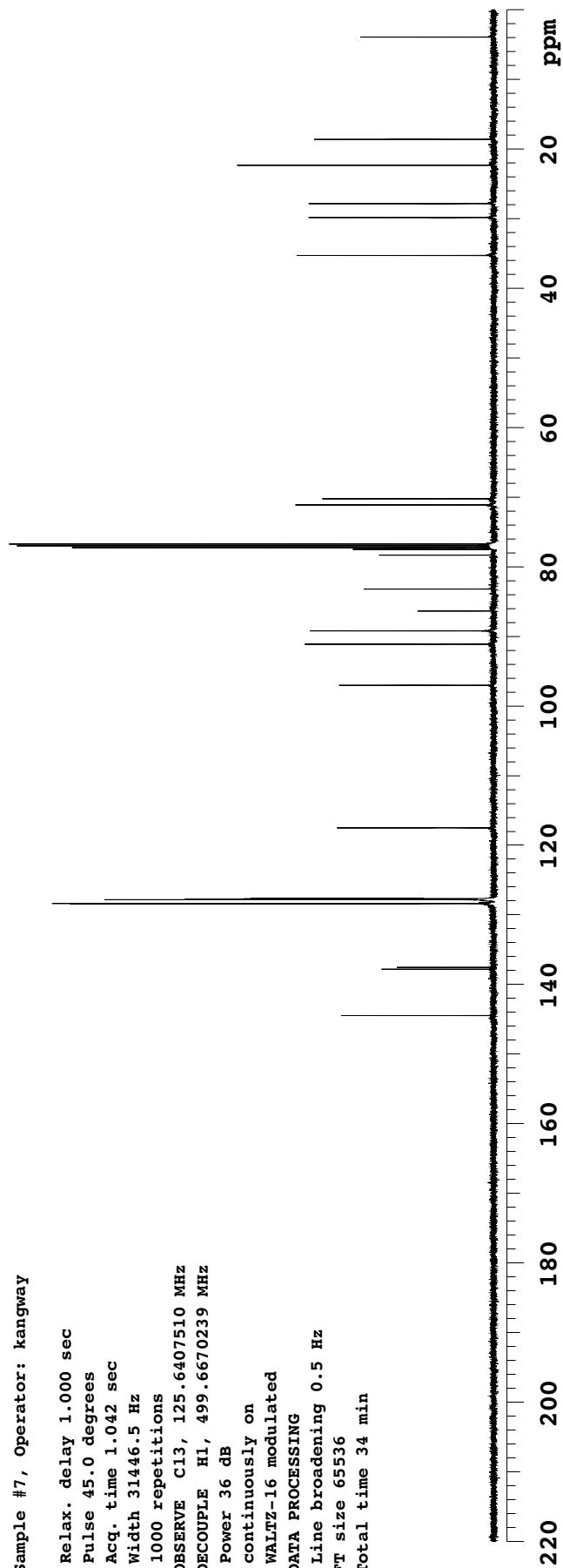
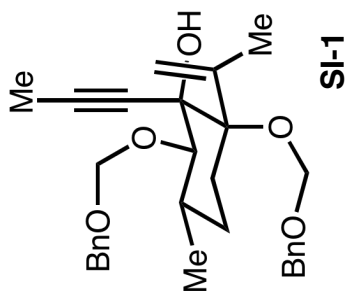
Minor Diastereomer

Sample Name:
KVC25-173-Minor
Data Collected on:
indy.caltech.edu-inova500
Archive directory:
/home/kangway/vnmrsys/data
Sample directory:
KVC25-173-Minor
FidFile: CARBON01

Pulse Sequence: CARBON (s2pul)
Solvent: cdcl3
Data collected on: Jan 21 2016

Sample #7, Operator: kangway

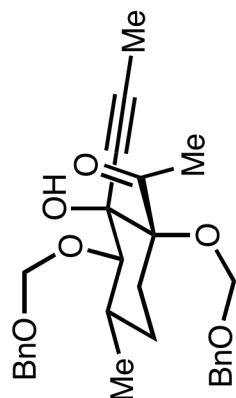
Relax. delay 1.000 sec
Pulse 45.0 degrees
Acq. time 1.042 sec
Width 31446.5 Hz
1000 repetitions
OBSERVE C13, 125.6407510 MHz
DECOUPLE H1, 499.6670239 MHz
Power 36 dB
continuously on
WALTZ-16 modulated
DATA PROCESSING
Line broadening 0.5 Hz
FT size 65536
Total time 34 min



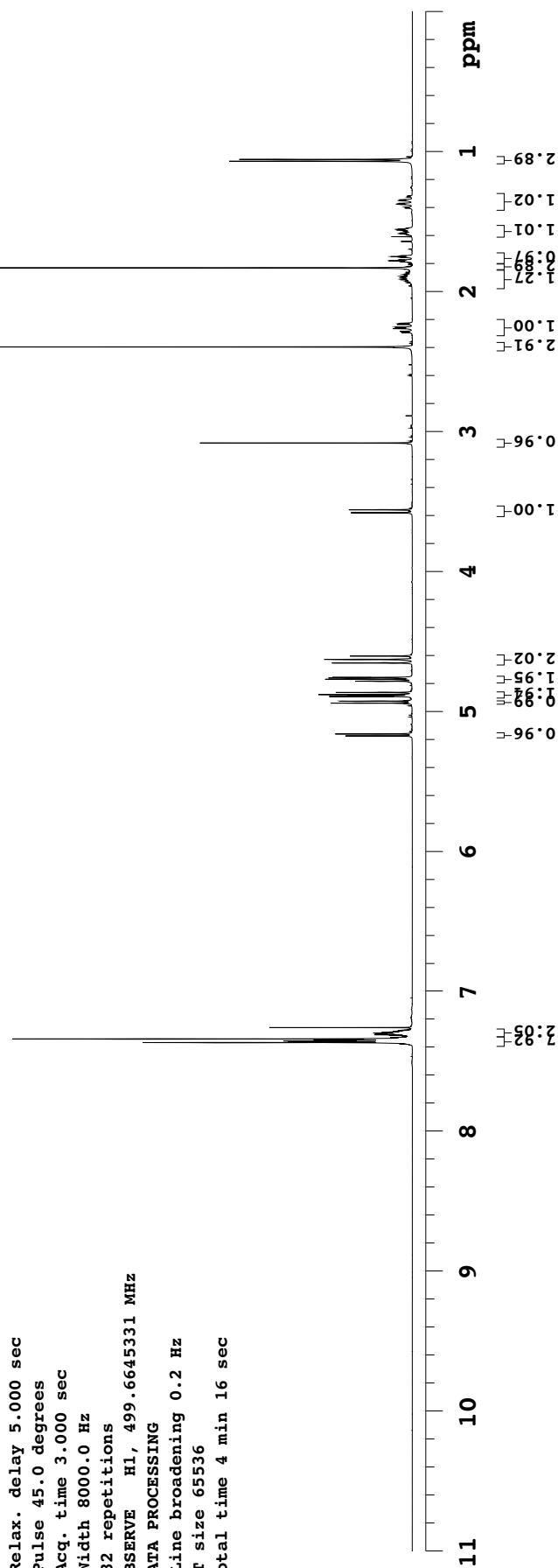
KVC25-175

Sample Name:
KVC25-175
Data Collected on:
indy.caltech.edu-inova500
Archive directory:
/home/kangway/vnmrsys/data
Sample directory:
KVC25-175
FidFile: PROTON01
Pulse Sequence: PROTON (s2pul)
Solvent: cdcl3
Data collected on: Jan 21 2016

Sample #16, Operator: kangway
Relax. delay 5.000 sec
Pulse 45.0 degrees
Acq. time 3.000 sec
Width 8000.0 Hz
32 repetitions
OBSERVE H1, 499.6645331 MHz
DATA PROCESSING
Line broadening 0.2 Hz
FT size 65536
Total time 4 min 16 sec



94



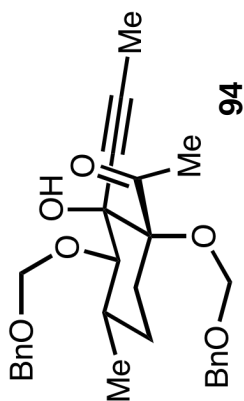
KVC25-175

Sample Name:
KVC25-175
Data Collected on:
indy.caltech.edu-inova500
Archive directory:
/home/kangway/vnmrsys/data
Sample directory:
KVC25-175
FidFile: CARBON01

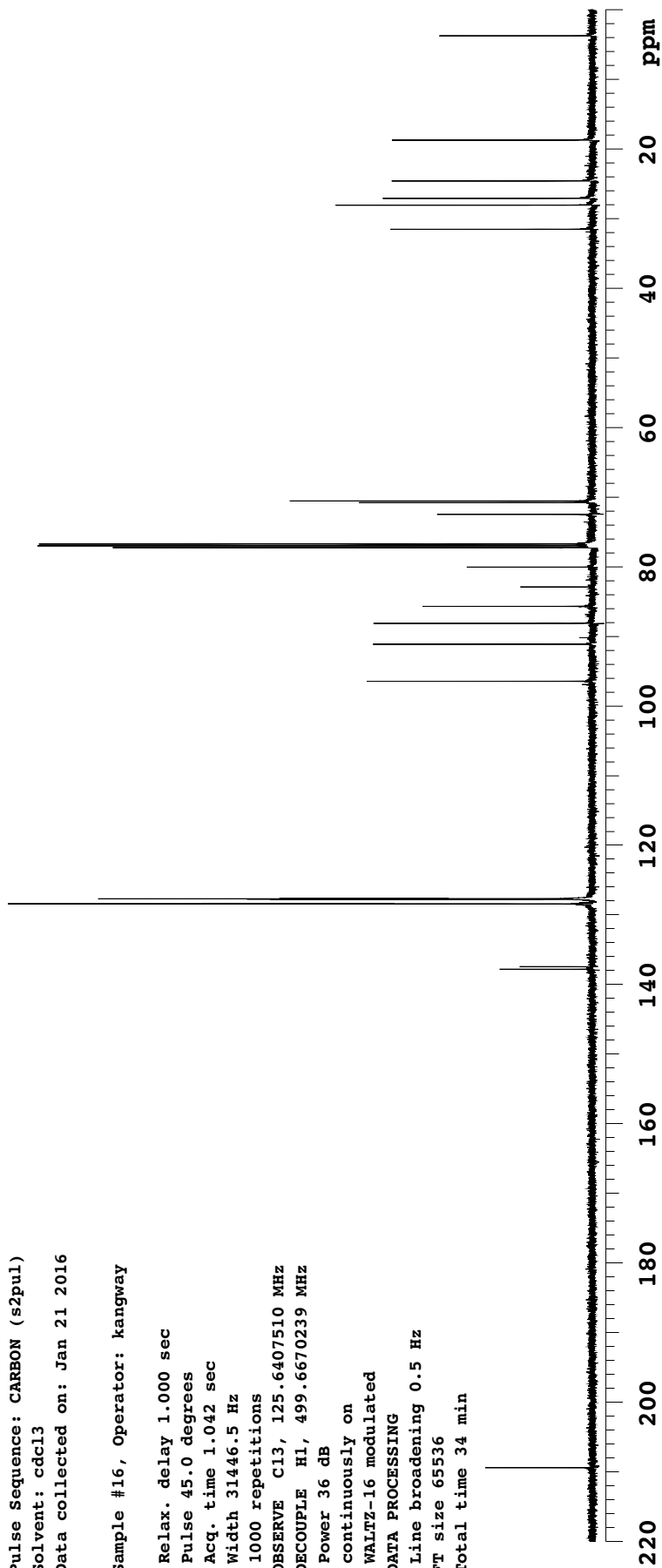
Pulse Sequence: CARBON (s2pul)
Solvent: cdcl3
Data collected on: Jan 21 2016

Sample #16, Operator: kangway

Relax. delay 1.000 sec
Pulse 45.0 degrees
Acq. time 1.042 sec
Width 31446.5 Hz
1000 repetitions
OBSERVE C13, 125.6407510 MHz
DECOUPLE H1, 499.6670239 MHz
Power 36 dB
continuously on
WALTZ-16 modulated
DATA PROCESSING
Line broadening 0.5 Hz
FT size 65536
Total time 34 min



94



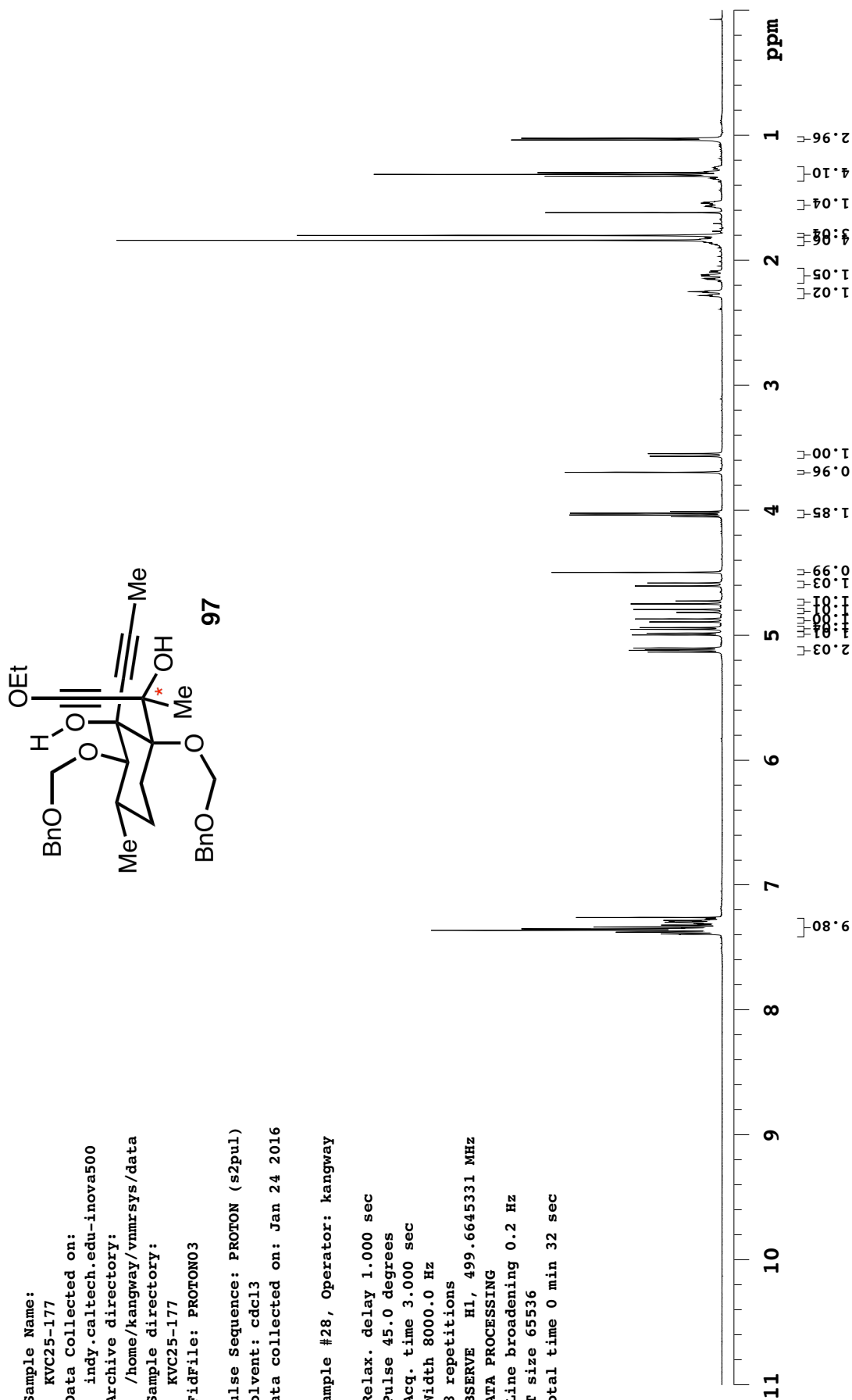
KVC25-177

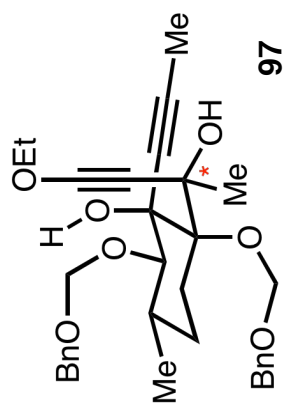
Sample Name:
KVC25-177
Data Collected on:
indy.caltech.edu-inova500
Archive directory:
/home/kangway/vnmrsys/data
Sample directory:
KVC25-177
FidFile: PROTON03

Pulse Sequence: PROTON (s2pul)
Solvent: cdcl3
Data collected on: Jan 24 2016

Sample #28, Operator: kangway

Relax. delay 1.000 sec
Pulse 45.0 degrees
Acq. time 3.000 sec
Width 8000.0 Hz
8 repetitions
OBSERVE H1, 499.6645331 MHz
DATA PROCESSING
Line broadening 0.2 Hz
FT size 65536
Total time 0 min 32 sec





97

KVC25-177

Sample Name:

KVC25-177

Data Collected on:

indy.caltech.edu-inova500

Archive directory:

/home/kangway/vnmrsys/data

Sample directory:

KVC25-177

FidFile: CARBON01

Pulse Sequence: CARBON (s2pul)

Solvent: cdcl3

Data collected on: Jan 21 2016

Sample #48, Operator: kangway

Relax. delay 1.000 sec

Pulse 45.0 degrees

Acq. time 1.042 sec

Width 31446.5 Hz

1000 repetitions

OBSERVE C13, 125.6407520 MHz

DECOUPLE H1, 499.6670239 MHz

Power 36 dB

continuously on

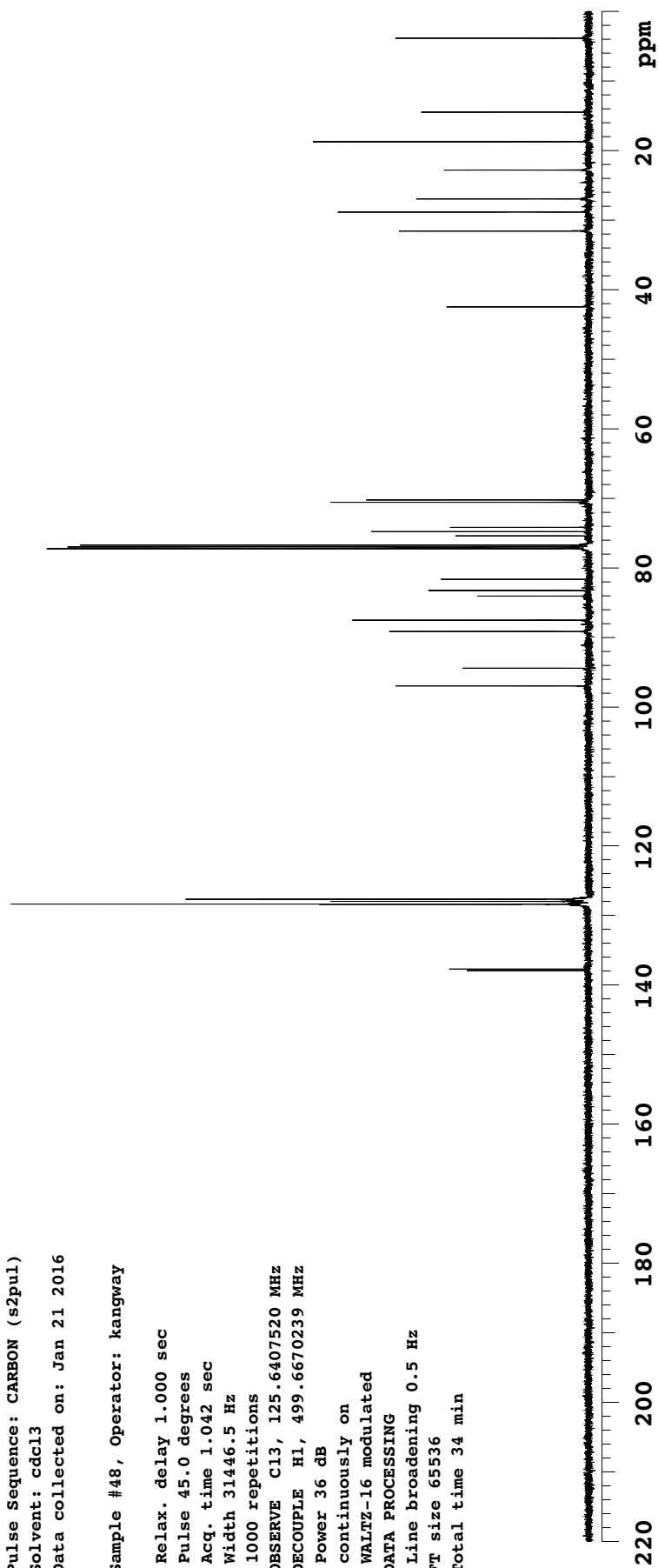
WALTZ-16 modulated

DATA PROCESSING

Line broadening 0.5 Hz

FT size 65536

Total time 34 min



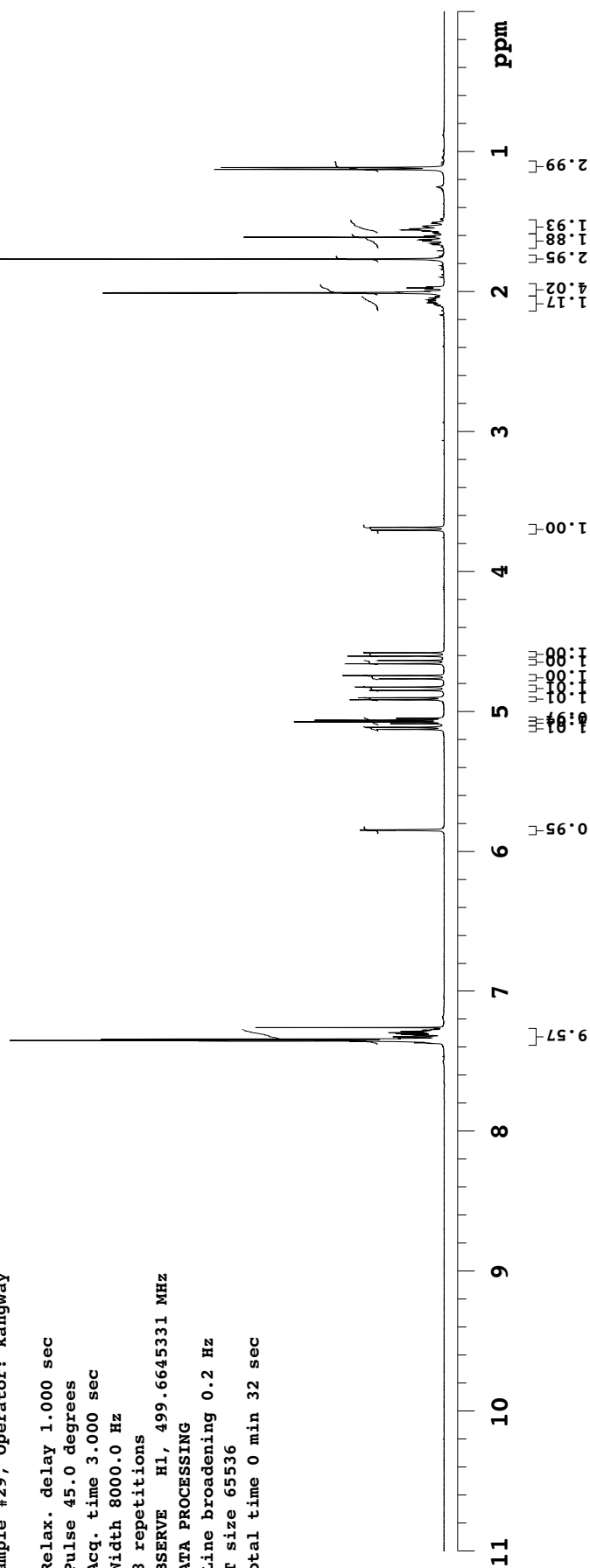
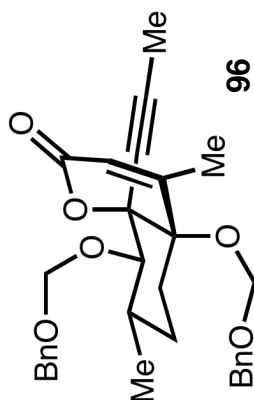
KVC25-179

Sample Name:
KVC25-179
Data Collected on:
indy.caltech.edu-inova500
Archive directory:
/home/kangway/vnmrsys/data
Sample directory:
KVC25-179
FidFile: PROTON03

Pulse Sequence: PROTON (s2pul)
Solvent: cdcl3
Data collected on: Jan 24 2016

Sample #29, Operator: kangway

Relax. delay 1.000 sec
Pulse 45.0 degrees
Acq. time 3.000 sec
Width 8000.0 Hz
8 repetitions
OBSERVE H1, 499.6645331 MHz
DATA PROCESSING
Line broadening 0.2 Hz
FT size 65536
Total time 0 min 32 sec



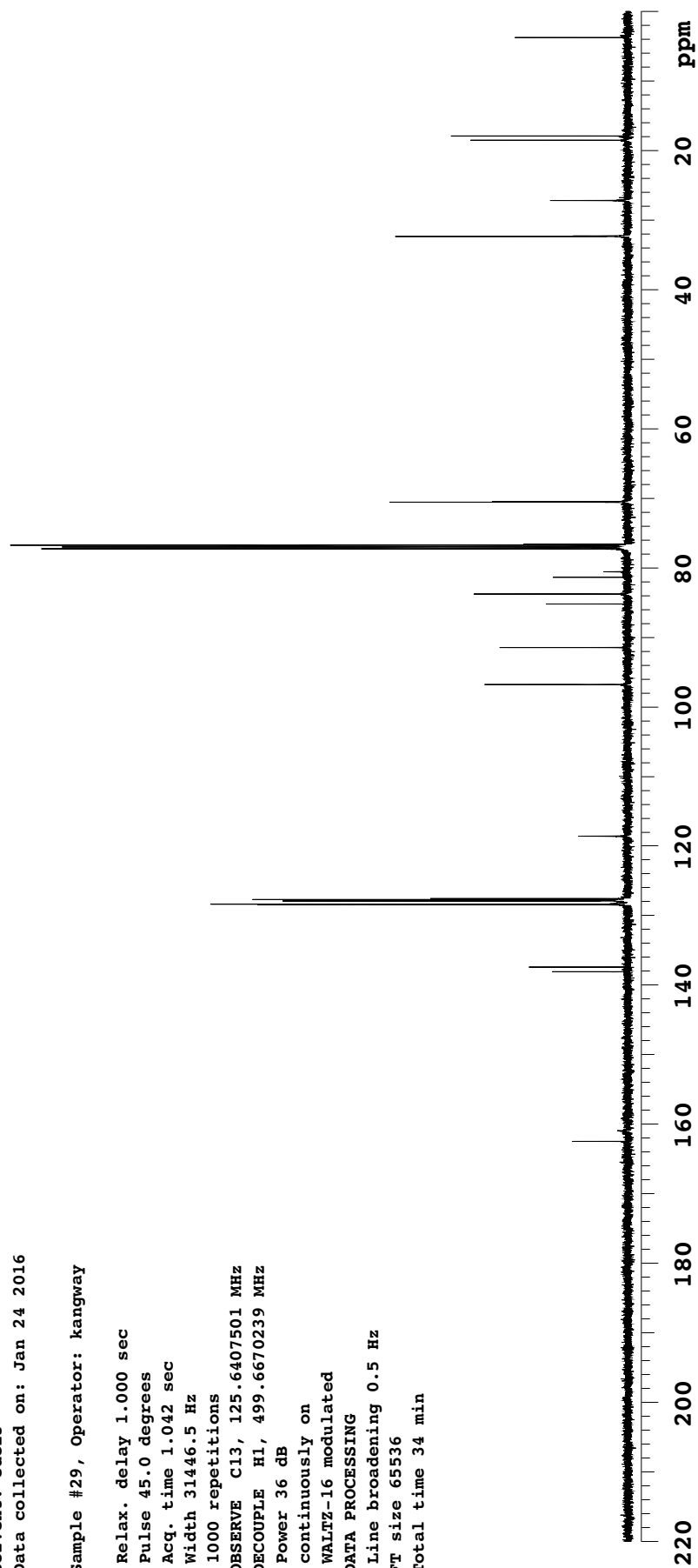
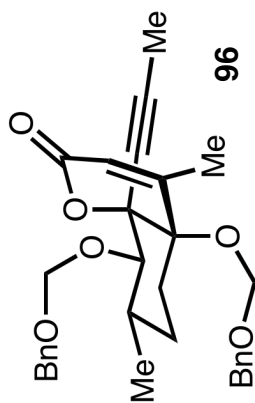
KVC25-179

Sample Name:
KVC25-179
Data Collected on:
indy.caltech.edu-inova500
Archive directory:
/home/kangway/vnmrsys/data
Sample directory:
KVC25-179
FidFile: CARBON02

Pulse Sequence: CARBON (s2pul)
Solvent: cdcl3
Data collected on: Jan 24 2016

Sample #29, Operator: kangway

Relax. delay 1.000 sec
Pulse 45.0 degrees
Acq. time 1.042 sec
Width 31446.5 Hz
1000 repetitions
OBSERVE C13, 125.6407501 MHz
DECOUPLE H1, 499.6670239 MHz
Power 36 dB
continuously on
WALTZ-16 modulated
DATA PROCESSING
Line broadening 0.5 Hz
FT size 65536
Total time 34 min



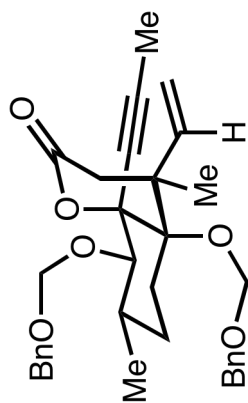
KVC25-181

Sample Name:
KVC25-181
Data Collected on:
indy.caltech.edu-inova500
Archive directory:
/home/kangway/vnmrsys/data
Sample directory:
KVC25-181
FidFile: PROTON01

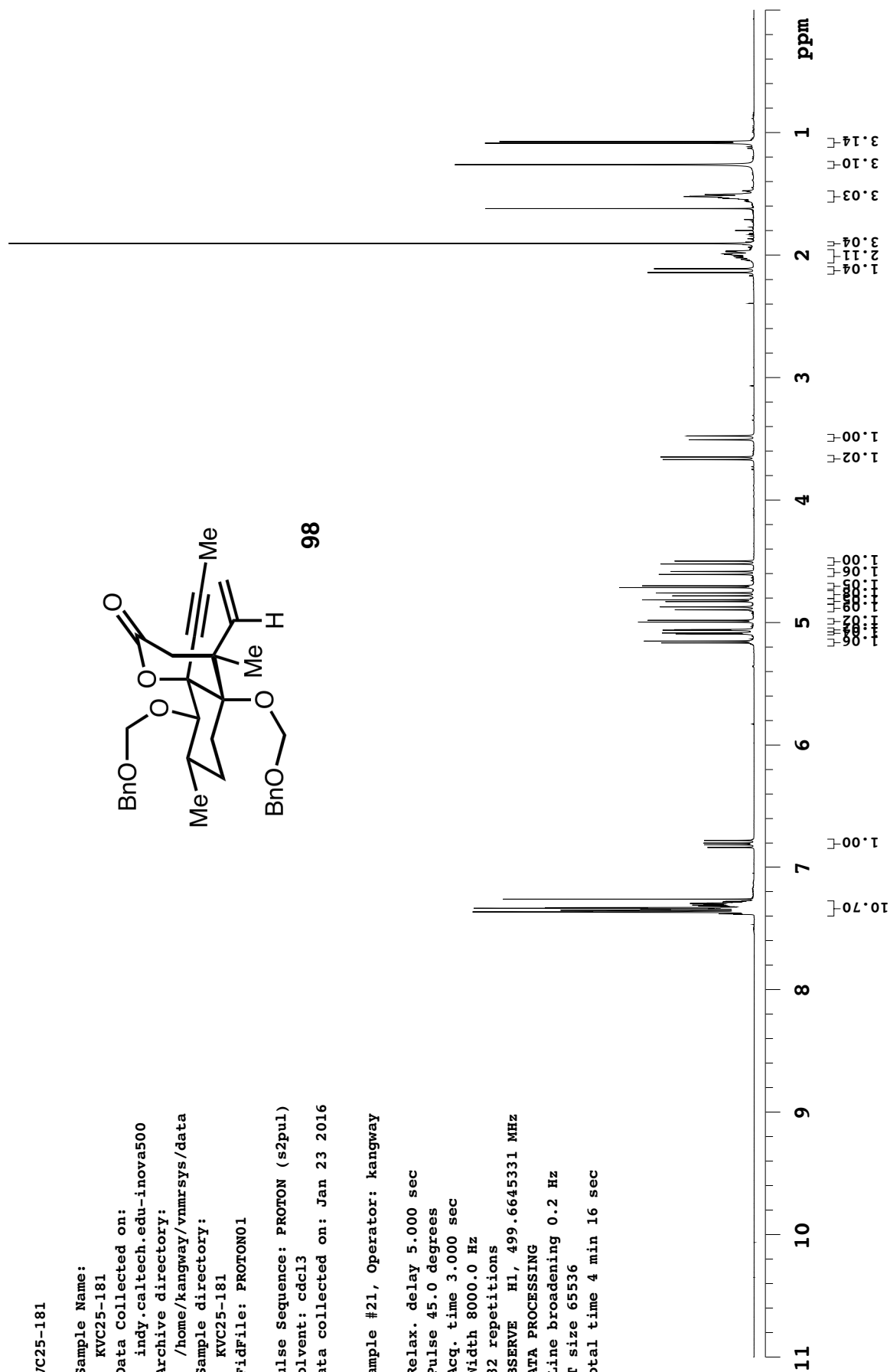
Pulse Sequence: PROTON (s2pul)
Solvent: cdcl3
Data collected on: Jan 23 2016

Sample #21, Operator: kangway

Relax. delay 5.000 sec
Pulse 45.0 degrees
Acq. time 3.000 sec
Width 8000.0 Hz
32 repetitions
OBSERVE H1, 499.6645331 MHz
DATA PROCESSING
Line broadening 0.2 Hz
FT size 65536
Total time 4 min 16 sec



98



KVC25-181

Sample Name:

KVC25-181

Data Collected on:

indy.caltech.edu-inova500

Archive directory:

/home/kangway/vnmrsys/data

Sample directory:

KVC25-181

FidFile: CARBON01

Pulse Sequence: CARBON (s2pul)

Solvent: cdcl3

Data collected on: Jan 23 2016

Sample #21, Operator: kangway

Relax. delay 1.000 sec

Pulse 45.0 degrees

Acq. time 1.042 sec

Width 31446.5 Hz

1000 repetitions

OBSERVE C13, 125.6407510 MHz

DECOUPLE H1, 499.6670239 MHz

Power 36 dB

continuously on

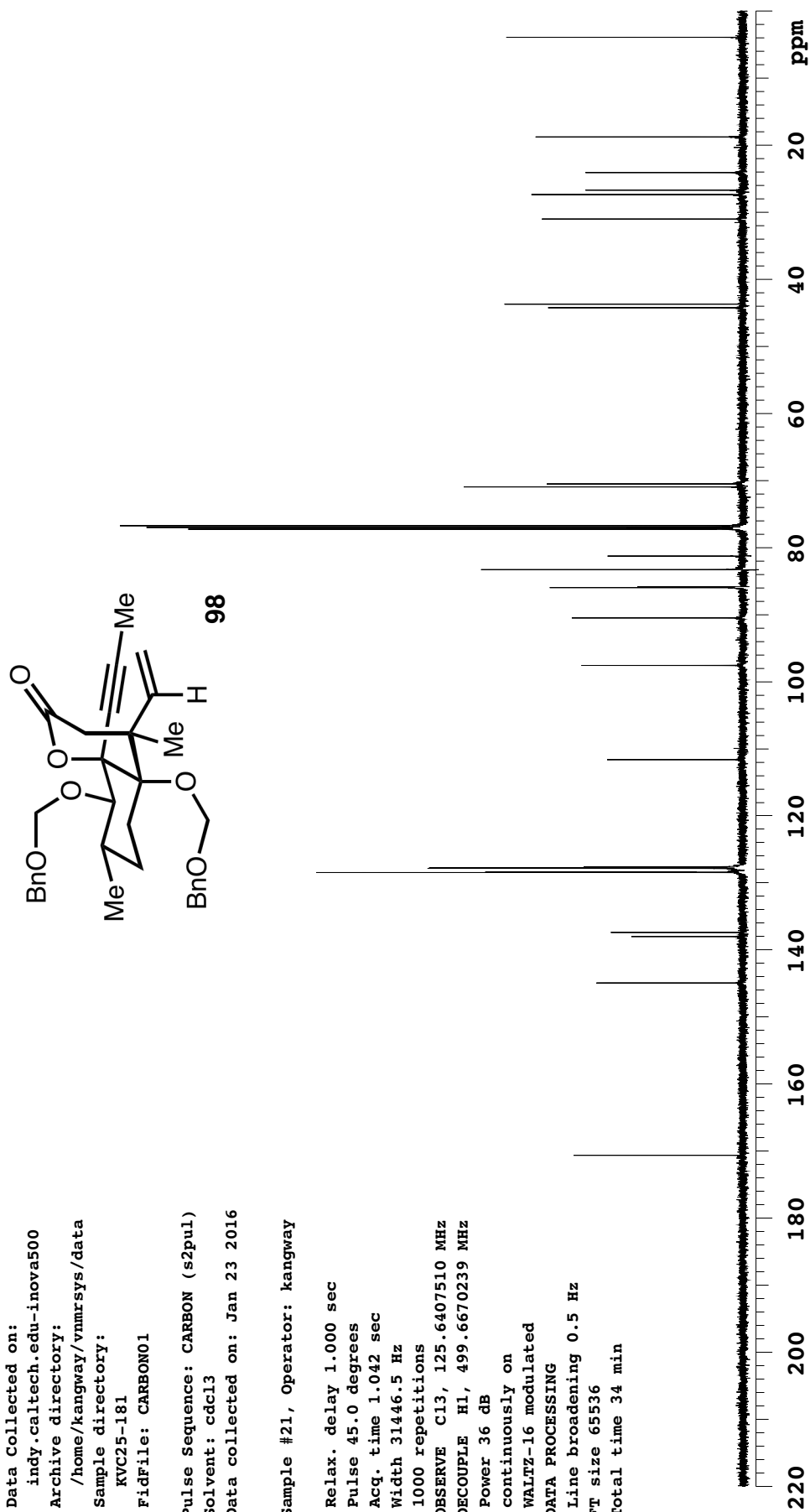
WALTZ-16 modulated

DATA PROCESSING

Line broadening 0.5 Hz

FT size 65536

Total time 34 min

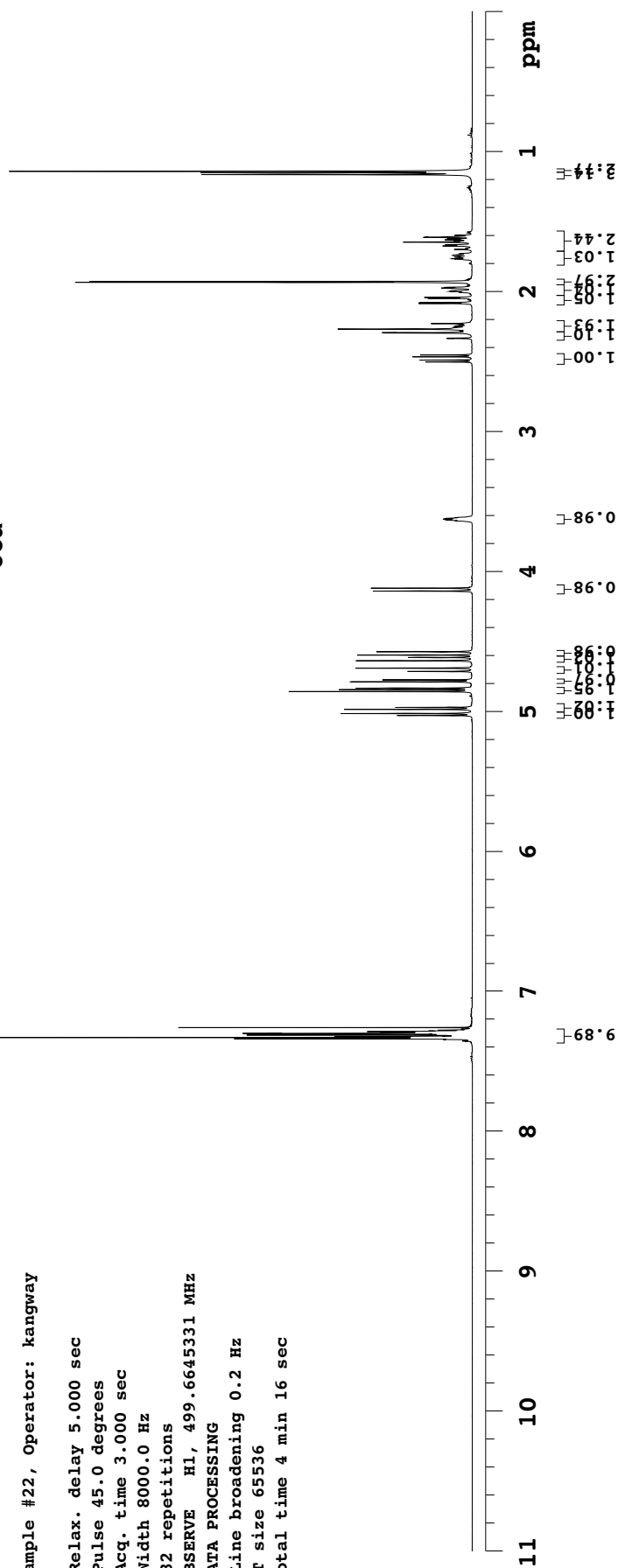
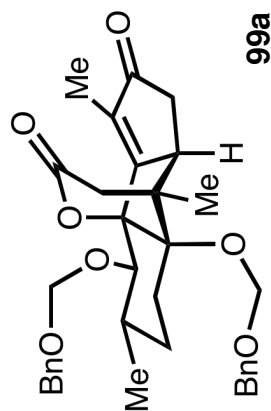


```

Sample #22, Operator: kangway

Relax. delay 5.000 sec
Pulse 45.0 degrees
Acq. time 3.000 sec
Width 8000.0 Hz
32 repetitions
OBSERVE H1, 499.6645331 MHz
DATA PROCESSING
Line broadening 0.2 Hz
FFT size 65536
Total time 4 min 16 sec

```



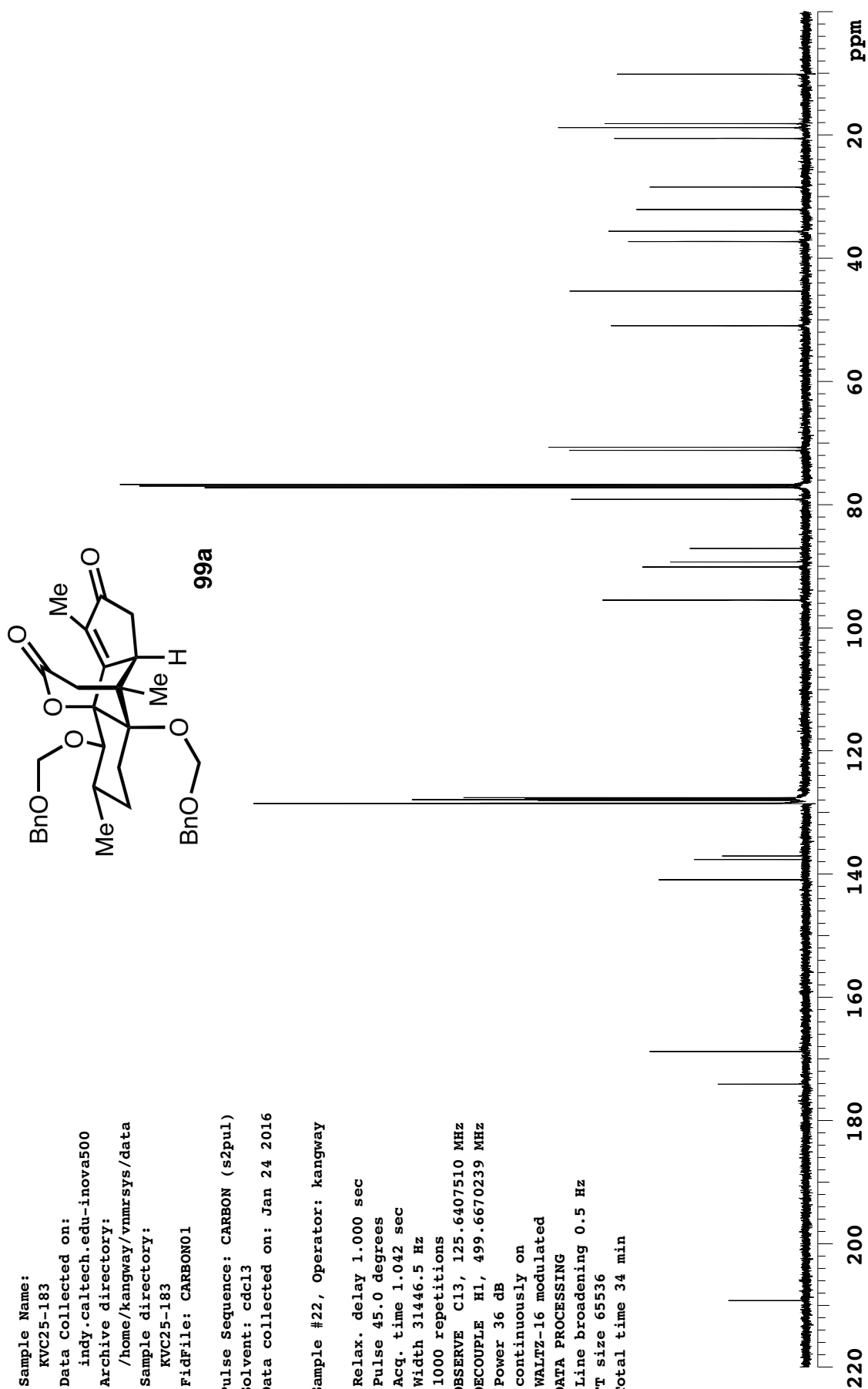
KVC25-183

Sample Name:
KVC25-183
Data Collected on:
indy.caltech.edu-inova500
Archive directory:
/home/kangway/vnmrsys/data
Sample directory:
KVC25-183
FidFile: CARBON01

Pulse Sequence: CARBON (s2pul)
Solvent: cdcl3
Data collected on: Jan 24 2016

Sample #22, Operator: kangway

Relax. delay 1.000 sec
Pulse 45.0 degrees
Acq. time 1.042 sec
Width 31446.5 Hz
1000 repetitions
OBSERVE C13, 125.6407510 MHz
DECOUPLE H1, 499.6670239 MHz
Power 36 dB
continuously on
WALTZ-16 modulated
DATA PROCESSING
Line broadening 0.5 Hz
FT size 65536
Total time 34 min



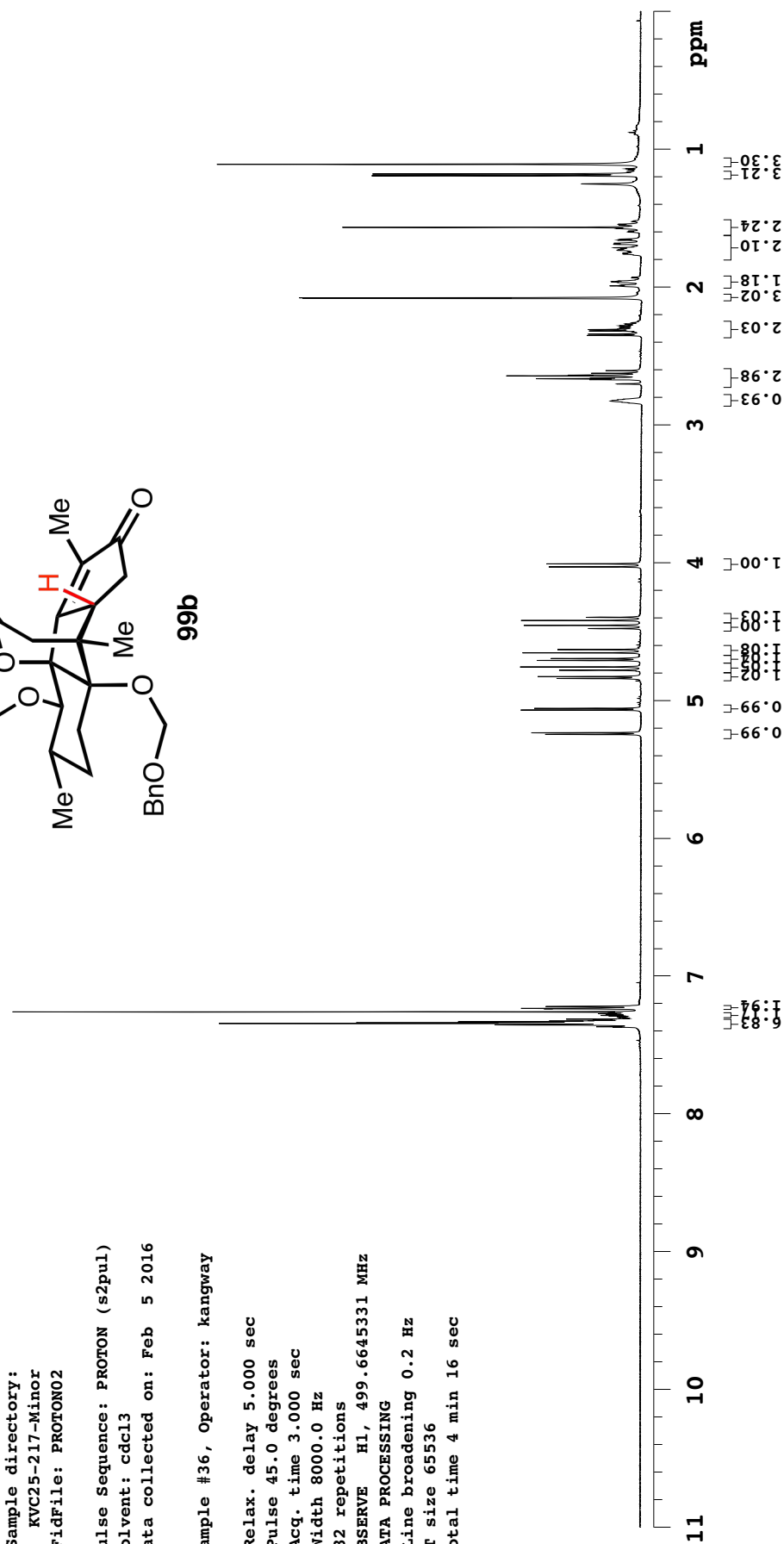
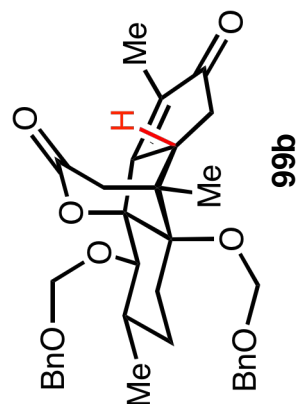
KVC25-217-Minor

Sample Name:
KVC25-217-Minor
Data Collected on:
indy.caltech.edu-inova500
Archive directory:
/home/kangway/vnmrsys/data
Sample directory:
KVC25-217-Minor
FidFile: PROTON02

Pulse Sequence: PROTON (s2pul)
Solvent: cdcl3
Data collected on: Feb 5 2016

Sample #36, Operator: kangway

Relax. delay 5.000 sec
Pulse 45.0 degrees
Acq. time 3.000 sec
Width 8000.0 Hz
32 repetitions
OBSERVE H1, 499.6645331 MHz
DATA PROCESSING
Line broadening 0.2 Hz
FT size 65536
Total time 4 min 16 sec



KVC25-217-Minor

Sample Name:

KVC25-217-Minor

Data Collected on:

indy.caltech.edu-inova500

Archive directory:

/home/kangway/vnmrsys/data

Sample directory:

KVC25-217-Minor

FidFile: CARBON02

Pulse Sequence: CARBON (s2pul)

Solvent: cdcl3

Data collected on: Feb 5 2016

Sample #36, Operator: kangway

Relax. delay 1.000 sec

Pulse 45.0 degrees

Acq. time 1.042 sec

Width 31446.5 Hz

2000 repetitions

OBSERVE C13, 125.6407482 MHz

DECOUPLE H1, 499.6670239 MHz

Power 36 dB

continuously on

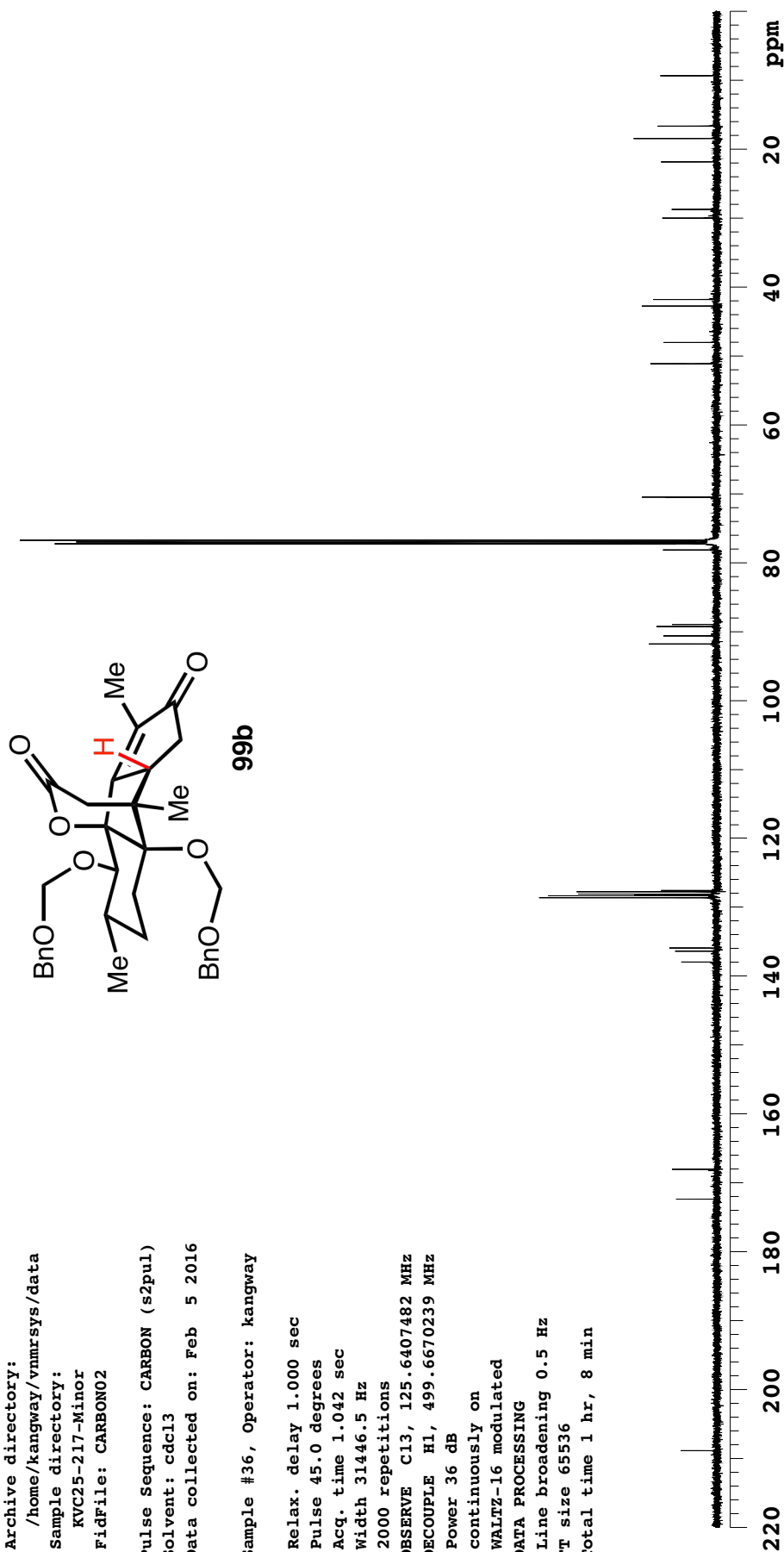
WALTZ-16 modulated

DATA PROCESSING

Line broadening 0.5 Hz

FT size 65536

Total time 1 hr, 8 min



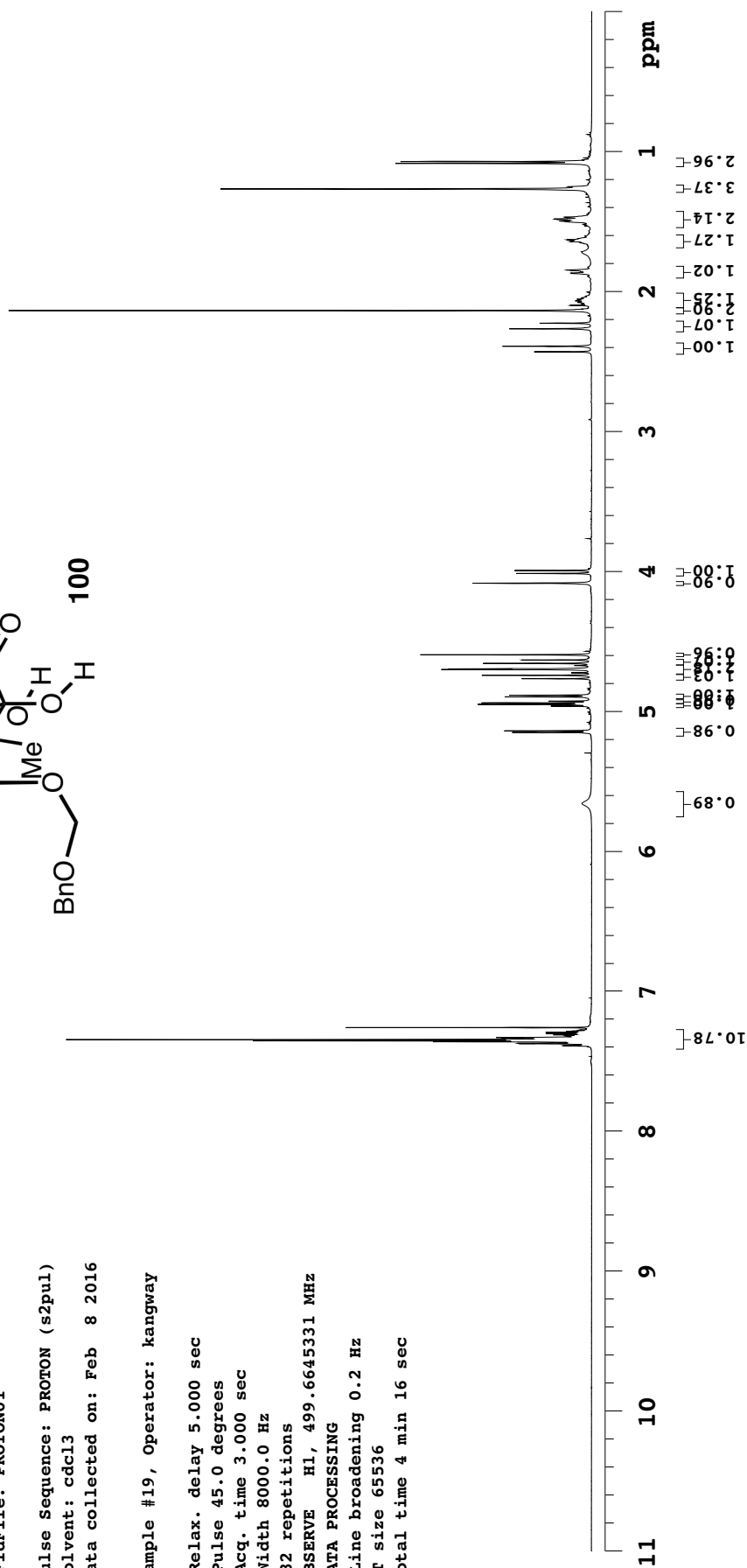
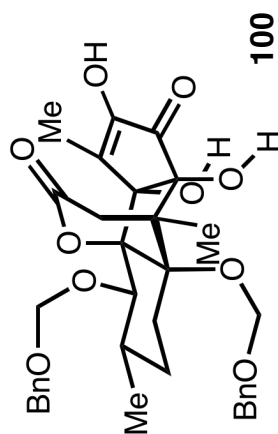
KVC25-221

Sample Name:
KVC25-221
Data Collected on:
indy.caltech.edu-inova500
Archive directory:
/home/kangway/vnmrsys/data
Sample directory:
KVC25-221
FidFile: PROTON01

Pulse Sequence: PROTON (s2pul)
Solvent: cdcl3
Data collected on: Feb 8 2016

Sample #19, Operator: kangway

Relax. delay 5.000 sec
Pulse 45.0 degrees
Acq. time 3.000 sec
Width 8000.0 Hz
32 repetitions
OBSERVE H1, 499.6645331 MHz
DATA PROCESSING
Line broadening 0.2 Hz
FT size 65536
Total time 4 min 16 sec



KVC25-221

Sample Name:

KVC25-221

Data Collected on:

indy.caltech.edu-inova500

Archive directory:

/home/kangway/vnmrsys/data

Sample directory:

KVC25-221

FidFile: CARBON01

Pulse Sequence: CARBON (s2pul)

Solvent: cdcl3

Data collected on: Feb 8 2016

Sample #19, Operator: kangway

Relax. delay 1.000 sec

Pulse 45.0 degrees

Acq. time 1.042 sec

Width 31446.5 Hz

2000 repetitions

OBSERVE C13, 125.6407501 MHz

DECOUPLE H1, 499.6670239 MHz

Power 36 dB

continuously on

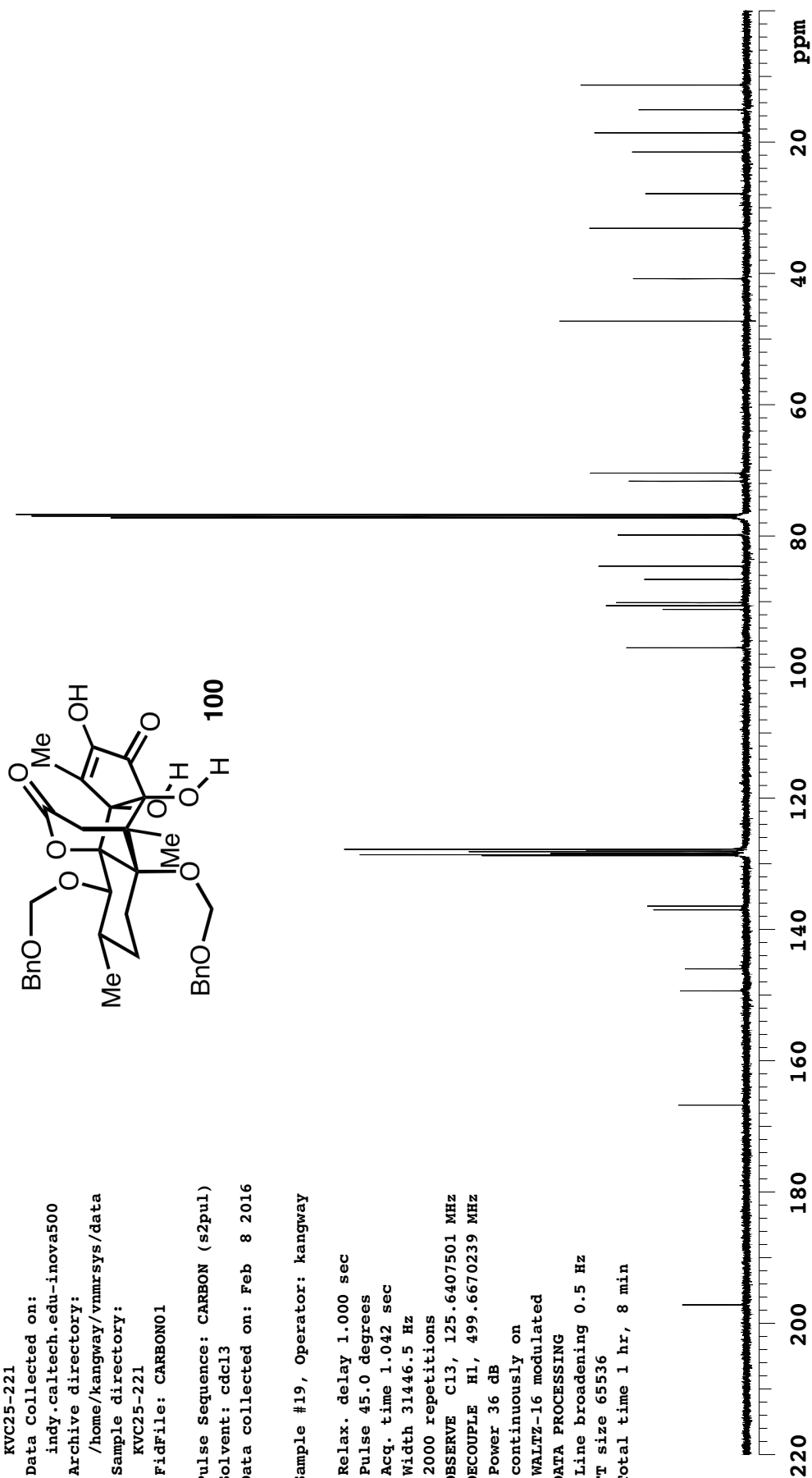
WALTZ-16 modulated

DATA PROCESSING

Line broadening 0.5 Hz

FT size 65536

Total time 1 hr, 8 min

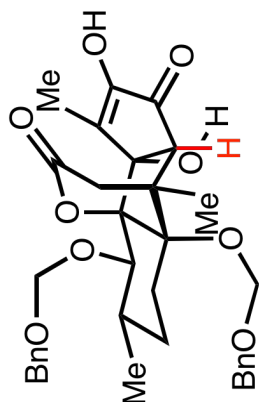


```

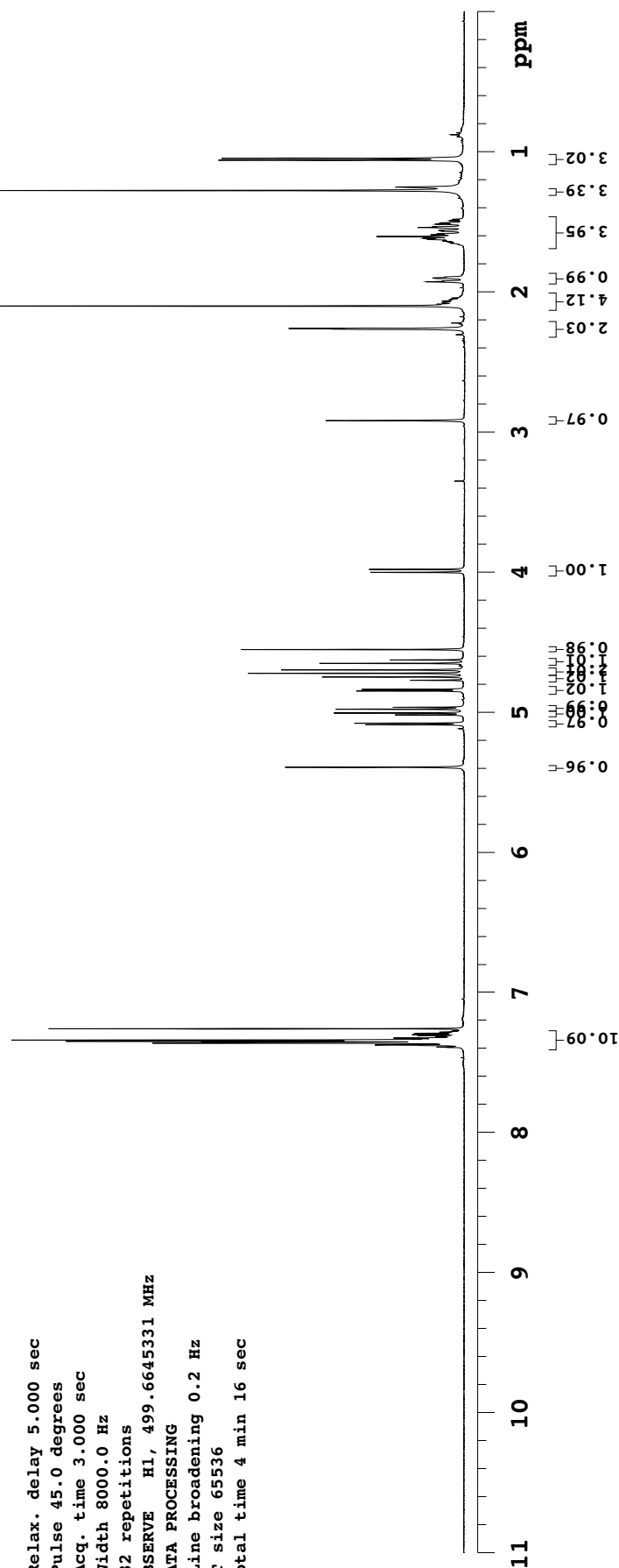
Sample #19, Operator: kangway

Relax. delay 5.000 sec
Pulse 45.0 degrees
Acq. time 3.000 sec
Width 8000.0 Hz
32 repetitions
OBSERVE H1, 499.6645331 MHz
DATA PROCESSING
Line broadening 0.2 Hz
FFT size 65536
Total time 4 min 16 sec

```



102



KVC25-227

Sample Name:

KVC25-227

Data Collected on:

indy.caltech.edu-inova500

Archive directory:

/home/kangway/vnmrsys/data

Sample directory:

KVC25-227

FidFile: CARBON01

Pulse Sequence: CARBON (s2pul)

Solvent: cdcl3

Data collected on: Feb 8 2016

Sample #19, Operator: kangway

Relax. delay 1.000 sec

Pulse 45.0 degrees

Acq. time 1.042 sec

Width 31446.5 Hz

1000 repetitions

OBSERVE C13, 125.6407482 MHz

DECOUPLE H1, 499.6670239 MHz

Power 36 dB

continuously on

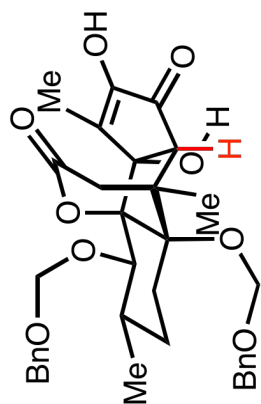
WALTZ-16 modulated

DATA PROCESSING

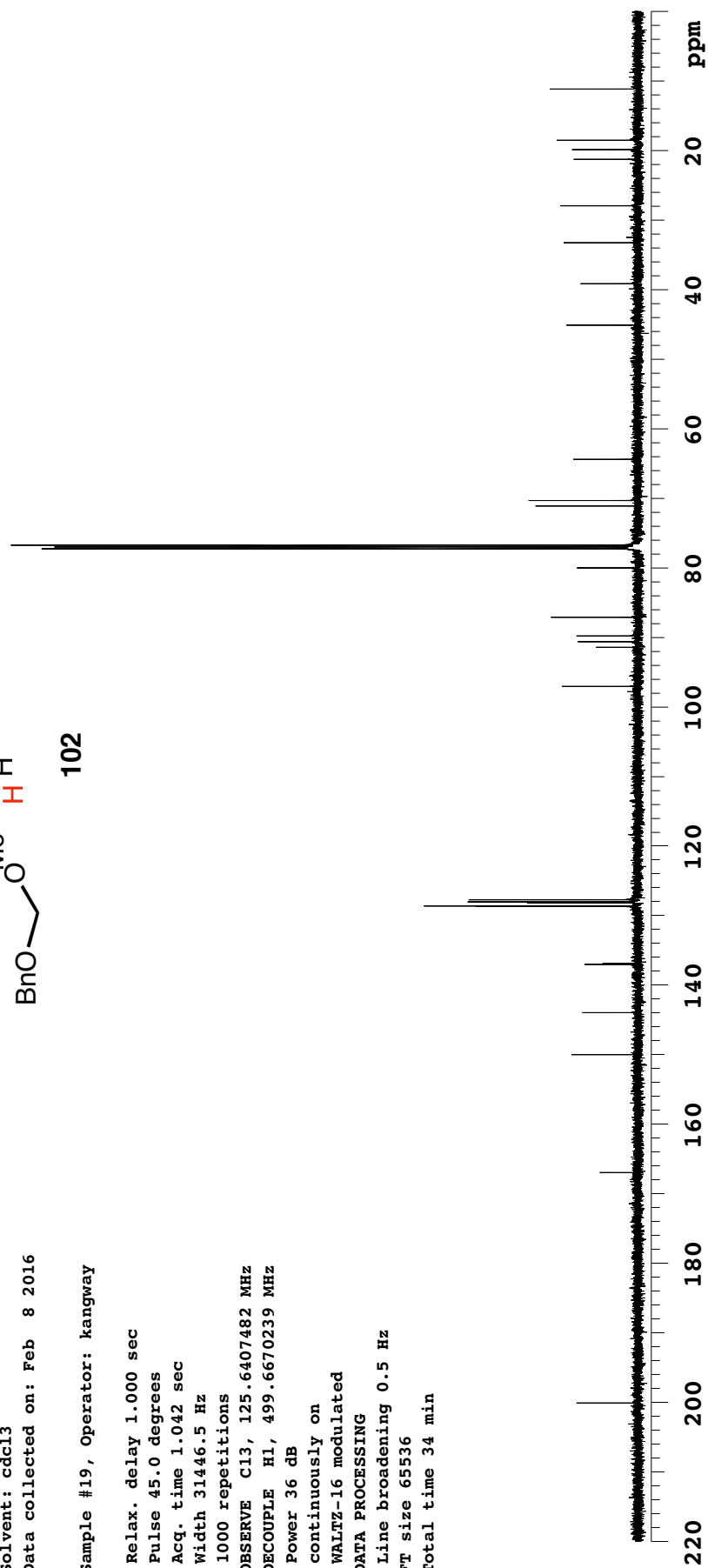
Line broadening 0.5 Hz

FT size 65536

Total time 34 min



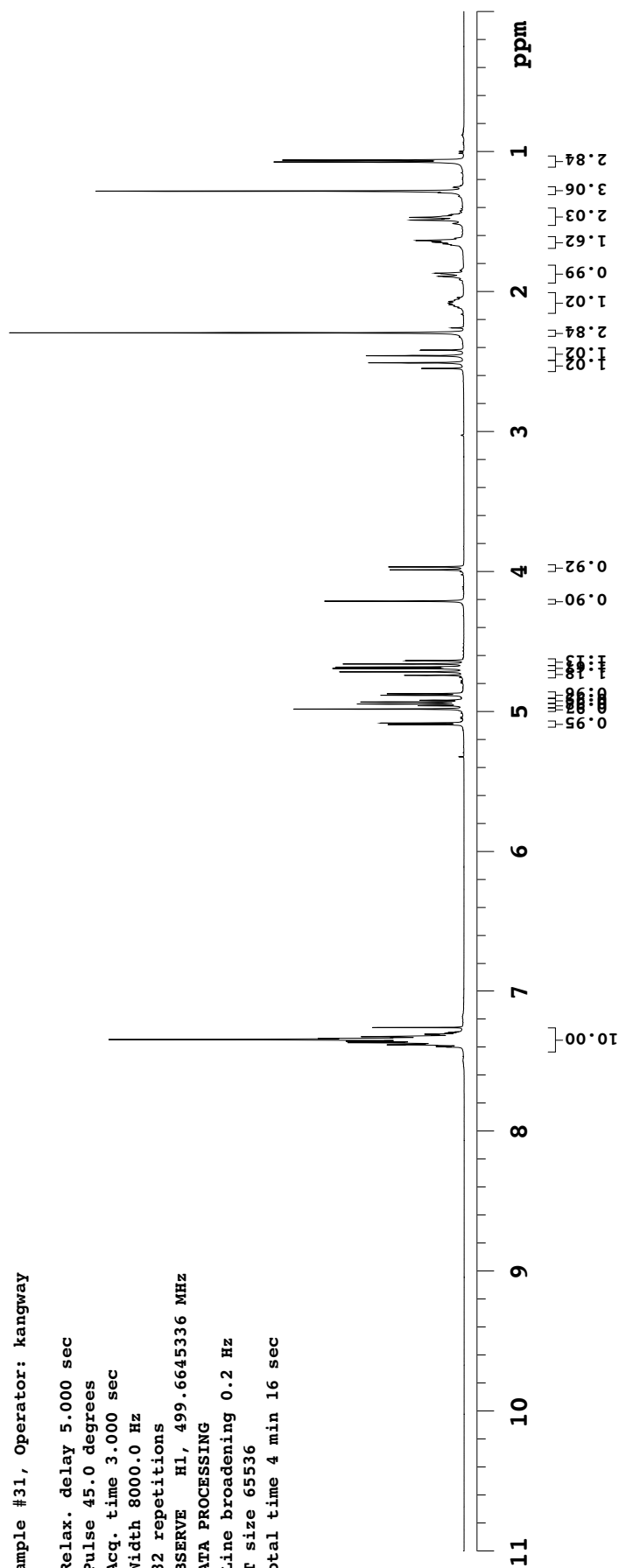
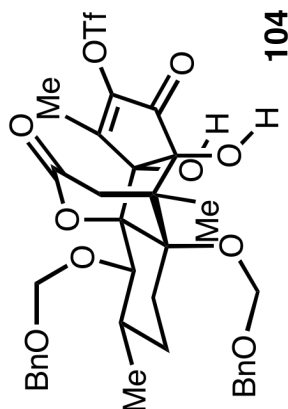
102



KVC25-255

Sample Name:
KVC25-255
Data Collected on:
indy.caltech.edu-inova500
Archive directory:
/home/kangway/vnmrsys/data
Sample directory:
KVC25-255
FidFile: PROTON01
Pulse Sequence: PROTON (s2pul)
Solvent: cdcl3
Data collected on: Mar 10 2016

Sample #31, Operator: kangway
Relax. delay 5.000 sec
Pulse 45.0 degrees
Acq. time 3.000 sec
Width 8000.0 Hz
32 repetitions
OBSERVE H1, 499.6645336 MHz
DATA PROCESSING
Line broadening 0.2 Hz
FT size 65536
Total time 4 min 16 sec



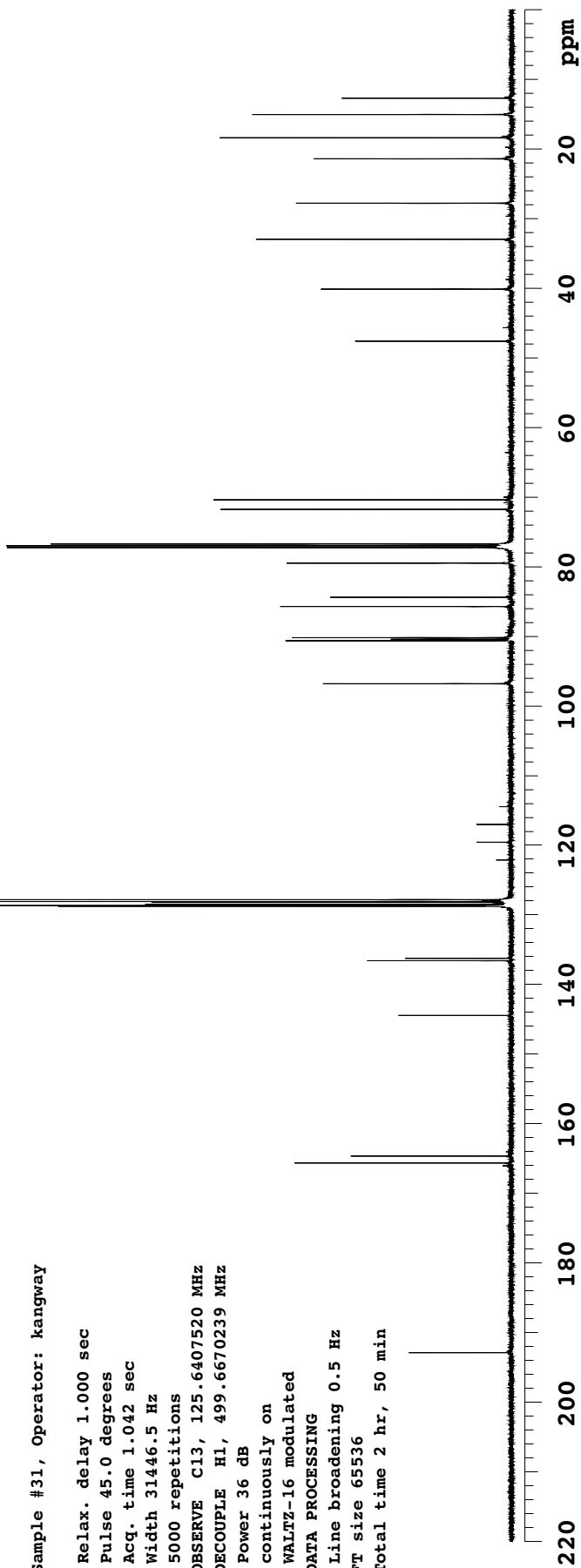
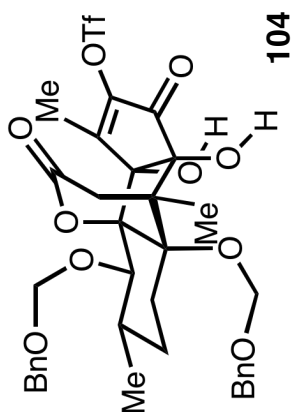
KVC25-255

Sample Name:
KVC25-255
Data Collected on:
indy.caltech.edu-inova500
Archive directory:
/home/kangway/vnmrsys/data
Sample directory:
KVC25-255
FidFile: CARBON01

Pulse Sequence: CARBON (s2pul)
Solvent: cdcl3
Data collected on: Mar 10 2016

Sample #31, Operator: kangway

Relax. delay 1.000 sec
Pulse 45.0 degrees
Acq. time 1.042 sec
Width 31446.5 Hz
5000 repetitions
OBSERVE C13, 125.6407520 MHz
DECOUPLE H1, 499.6670239 MHz
Power 36 dB
continuously on
WALTZ-16 modulated
DATA PROCESSING
Line broadening 0.5 Hz
FT size 65536
Total time 2 hr, 50 min

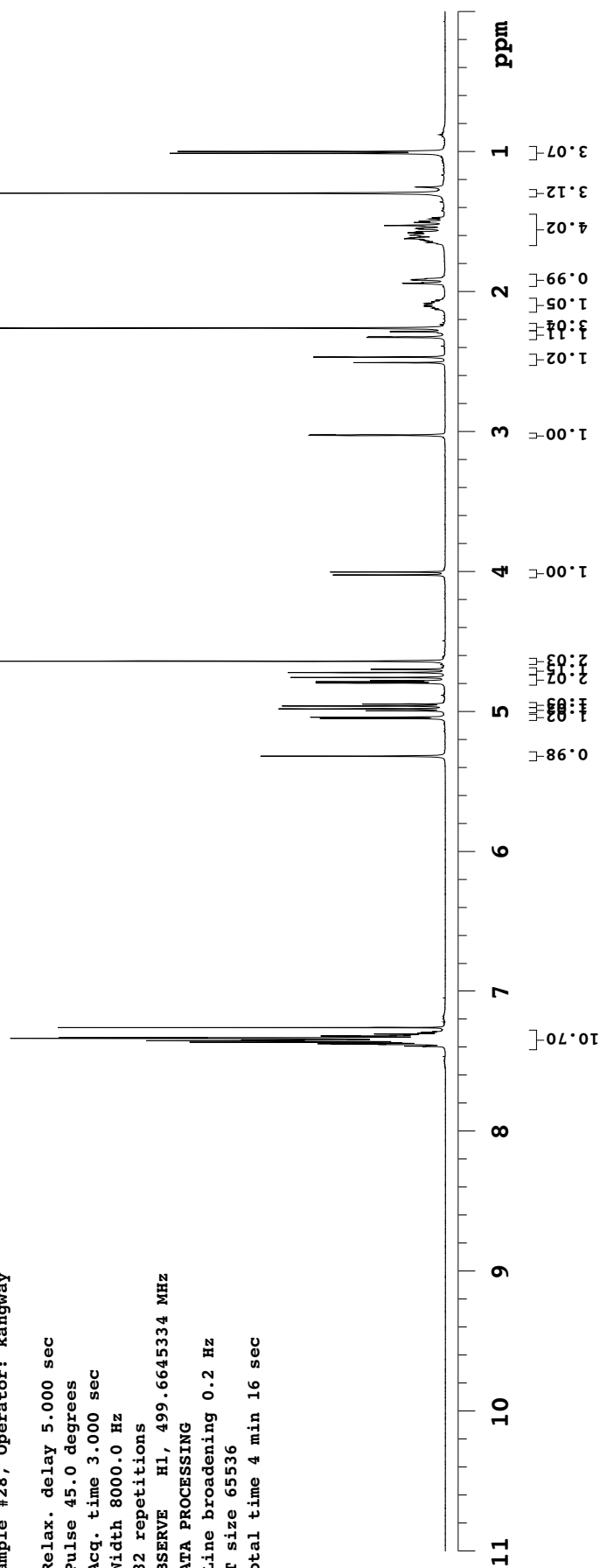
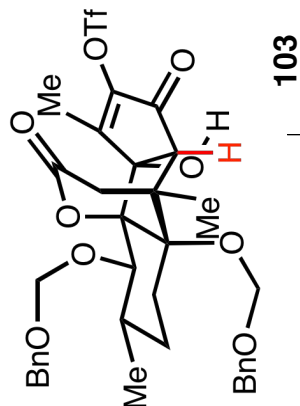


```

Sample #28, Operator: kangway

Relax. delay 5.000 sec
Pulse 45.0 degrees
Acq. time 3.000 sec
Width 8000.0 Hz
32 repetitions
OBSERVE H1, 499.6645334 MHz
DATA PROCESSING
Line broadening 0.2 Hz
FFT size 65536
Total time 4 min 16 sec

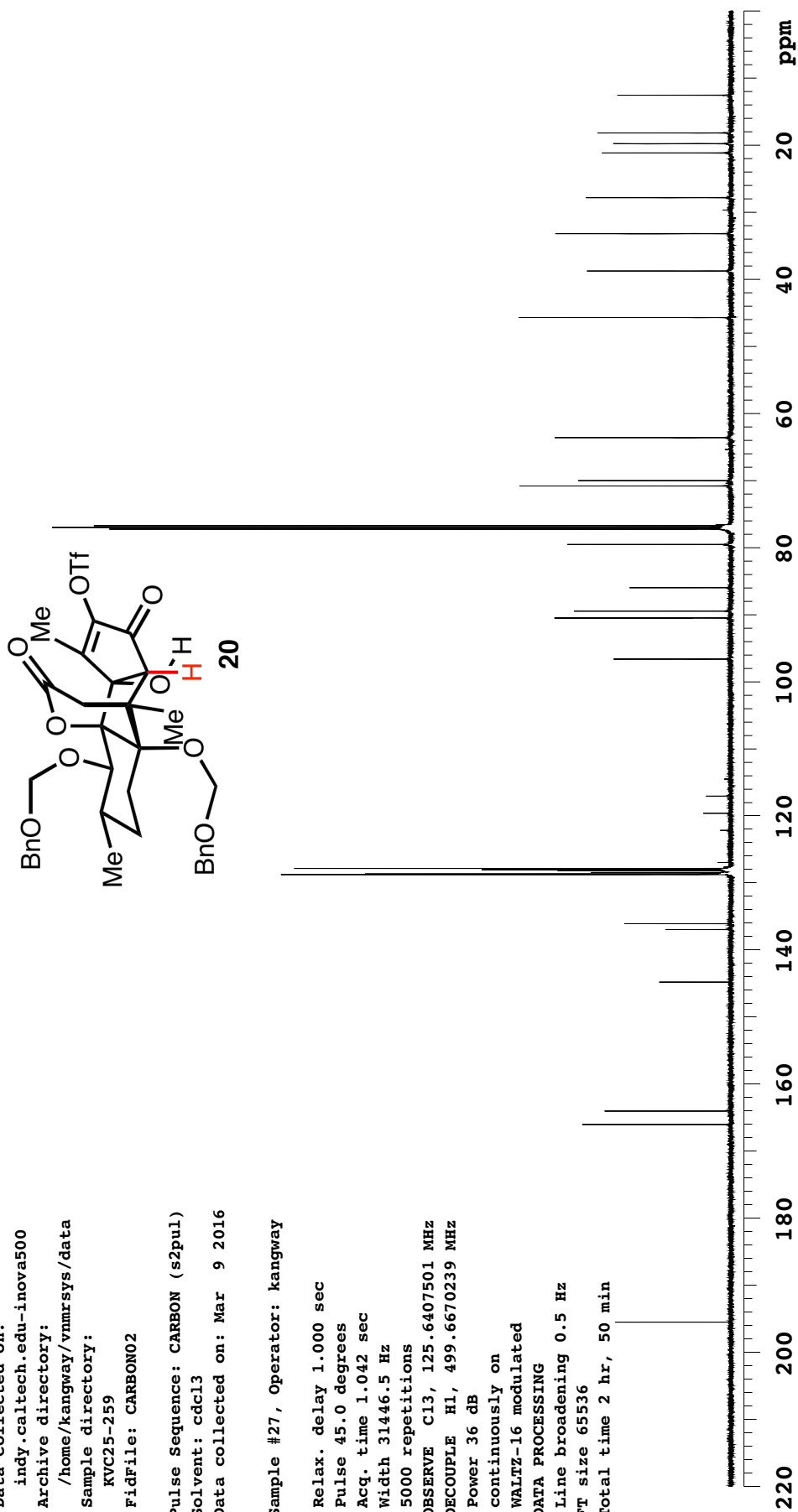
```



KVC25-259

Sample Name:
KVC25-259
Data Collected on:
indy.caltech.edu-inova500
Archive directory:
/home/kangway/vnmrsys/data
Sample directory:
KVC25-259
FidFile: CARBON02
Pulse Sequence: CARBON (s2pul)
Solvent: cdcl3
Data collected on: Mar 9 2016

Sample #27, Operator: kangway
Relax. delay 1.000 sec
Pulse 45.0 degrees
Acq. time 1.042 sec
Width 31446.5 Hz
5000 repetitions
OBSERVE C13, 125.6407501 MHz
DECOUPLE H1, 499.6670239 MHz
Power 36 dB
continuously on
WALTZ-16 modulated
DATA PROCESSING
Line broadening 0.5 Hz
FT size 65536
Total time 2 hr, 50 min



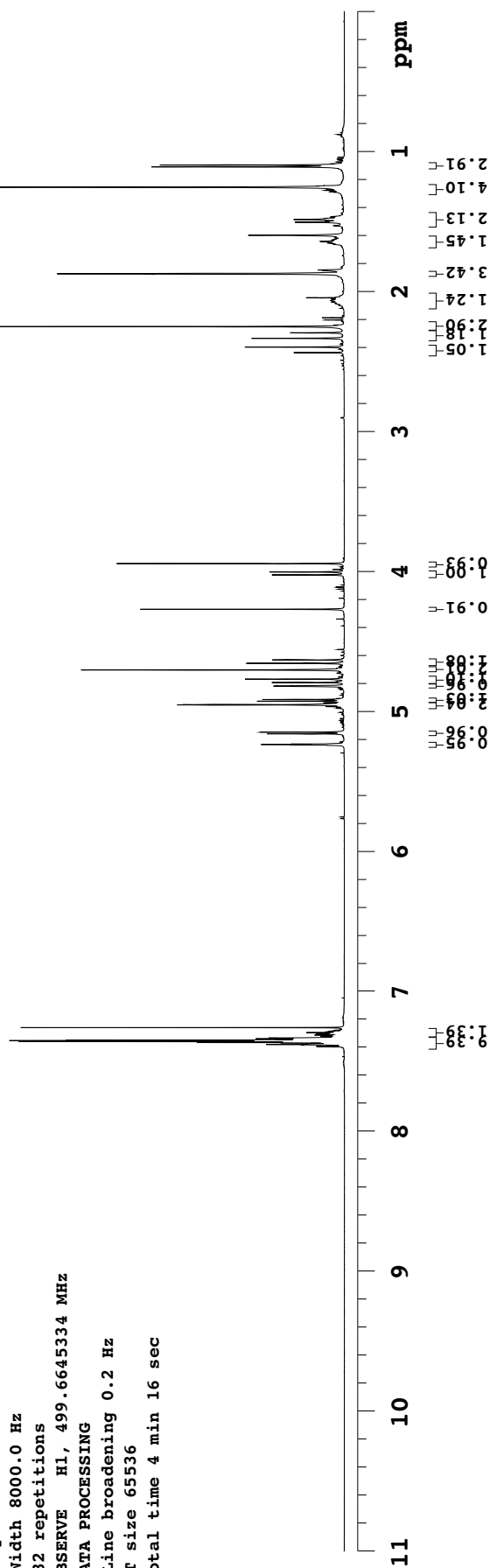
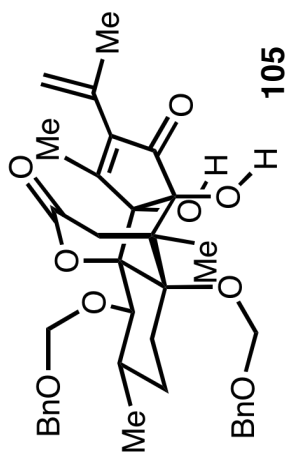
KVC25-269

Sample Name:
KVC25-269
Data Collected on:
indy.caltech.edu-inova500
Archive directory:
/home/kangway/vnmrsys/data
Sample directory:
KVC25-269
FidFile: PROTON01

Pulse Sequence: PROTON (s2pul)
Solvent: cdcl3
Data collected on: Mar 10 2016

Sample #32, Operator: kangway

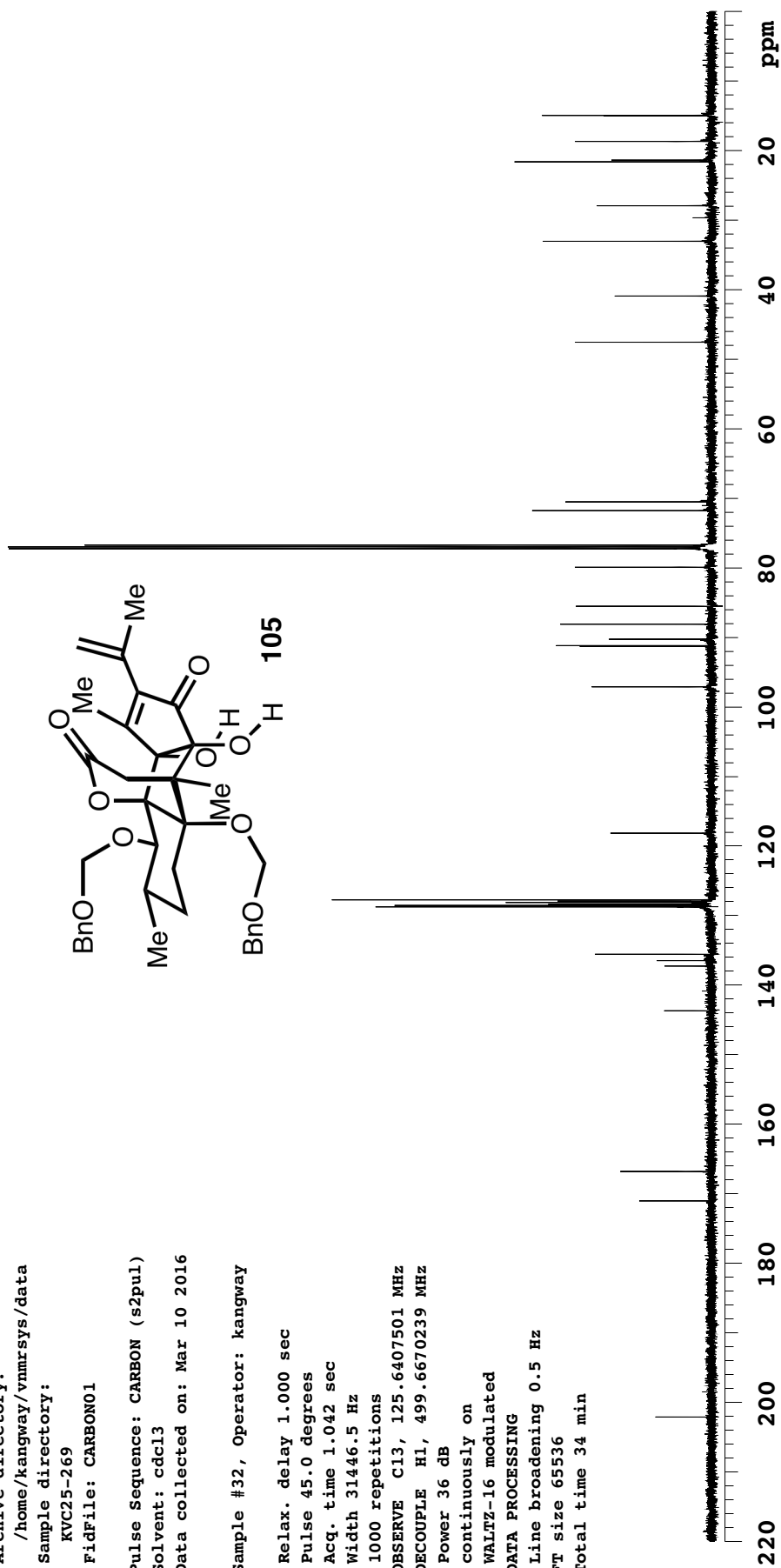
Relax. delay 5.000 sec
Pulse 45.0 degrees
Acq. time 3.000 sec
Width 8000.0 Hz
32 repetitions
OBSERVE H1, 499.6645334 MHz
DATA PROCESSING
Line broadening 0.2 Hz
FT size 65536
Total time 4 min 16 sec



KVC25-269

Sample Name:
KVC25-269
Data Collected on:
indy.caltech.edu-inova500
Archive directory:
/home/kangway/vnmrsys/data
Sample directory:
KVC25-269
FidFile: CARBON01
Pulse Sequence: CARBON (s2pul)
Solvent: cdcl3
Data collected on: Mar 10 2016

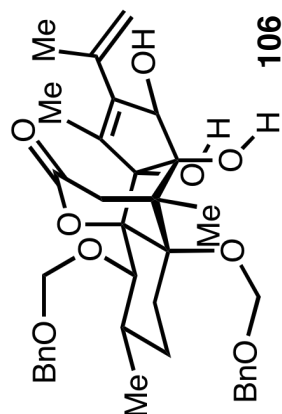
Sample #32, Operator: kangway
Relax. delay 1.000 sec
Pulse 45.0 degrees
Acq. time 1.042 sec
Width 3146.5 Hz
1000 repetitions
OBSERVE C13, 125.6407501 MHz
DECOUPLE H1, 499.6670239 MHz
Power 36 dB
continuously on
WALTZ-16 modulated
DATA PROCESSING
Line broadening 0.5 Hz
FT size 65536
Total time 34 min



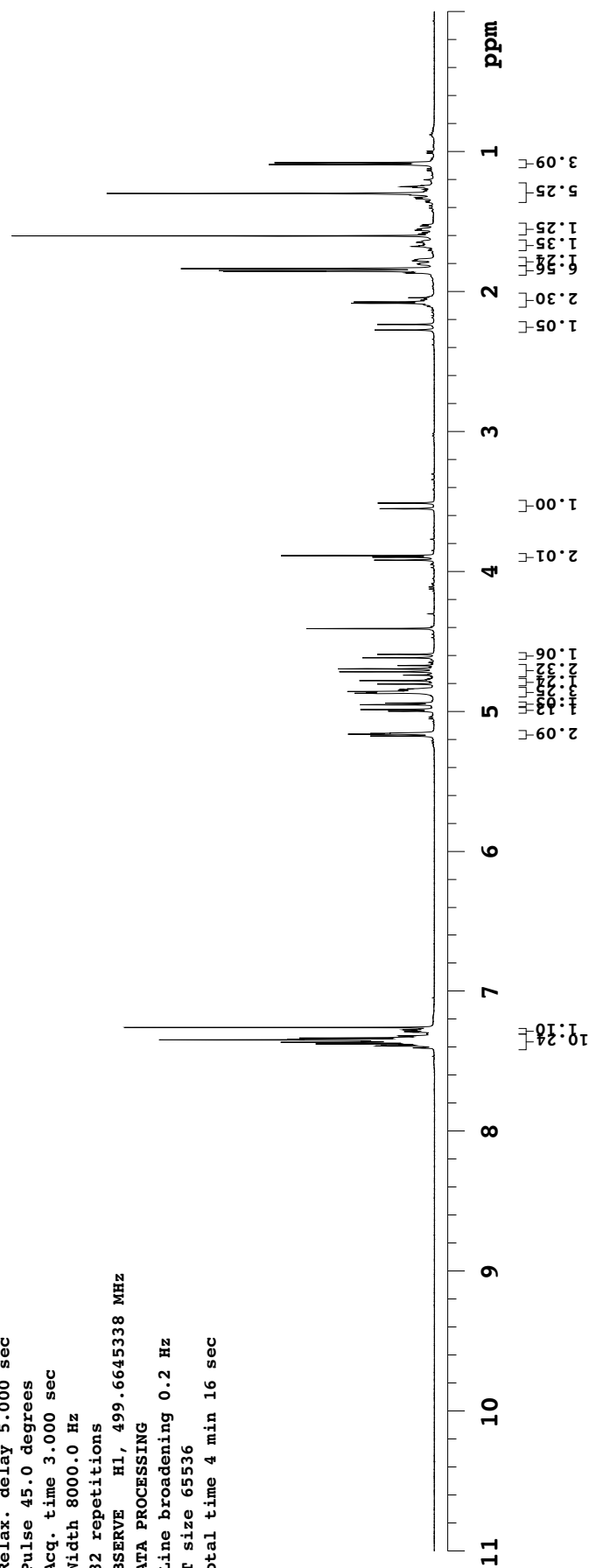
KVC25-261

Sample Name:
KVC25-261
Data Collected on:
indy.caltech.edu-inova500
Archive directory:
/home/kangway/vnmrsys/data
Sample directory:
KVC25-261
FidFile: PROTON01
Pulse Sequence: PROTON (s2pul)
Solvent: cdcl3
Data collected on: Mar 11 2016

Sample #34, Operator: kangway
Relax. delay 5.000 sec
Pulse 45.0 degrees
Acq. time 3.000 sec
Width 8000.0 Hz
32 repetitions
OBSERVE H1, 499.6645338 MHz
DATA PROCESSING
Line broadening 0.2 Hz
FT size 65536
Total time 4 min 16 sec



106



KVC25-261

Sample Name:

KVC25-261

Data Collected on:

indy.caltech.edu-inova500

Archive directory:

/home/kangway/vnmrsys/data

Sample directory:

KVC25-261

FidFile: CARBON01

Pulse Sequence: CARBON (s2pul)

Solvent: cdcl3

Data collected on: Mar 11 2016

Sample #34, Operator: kangway

Relax. delay 1.000 sec

Pulse 45.0 degrees

Acq. time 1.042 sec

Width 31446.5 Hz

2000 repetitions

OBSERVE C13, 125.6407491 MHz

DECOUPLE H1, 499.6670239 MHz

Power 36 dB

continuously on

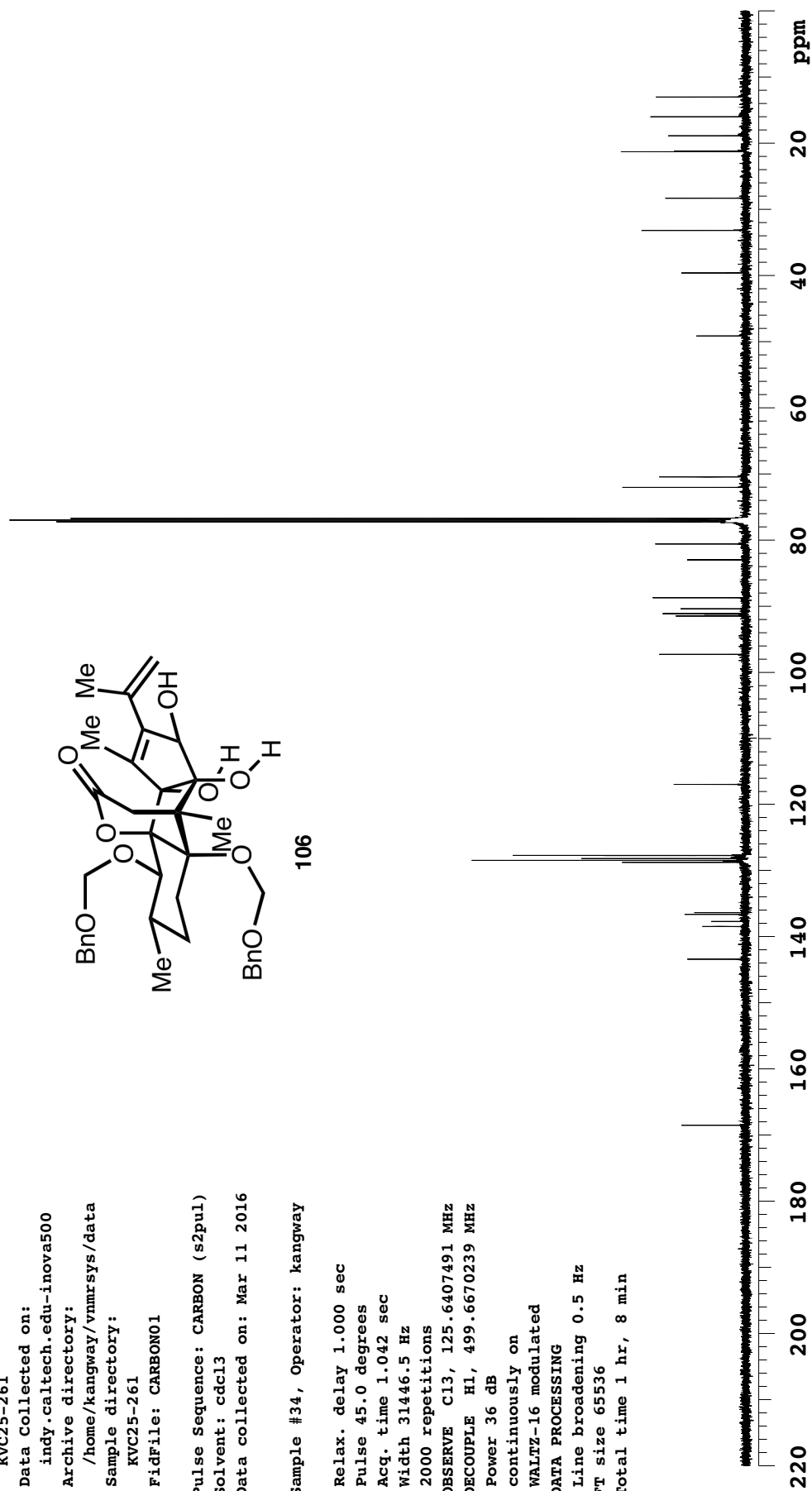
WALTZ-16 modulated

DATA PROCESSING

Line broadening 0.5 Hz

FT size 65536

Total time 1 hr, 8 min



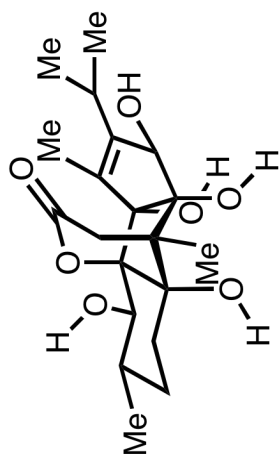
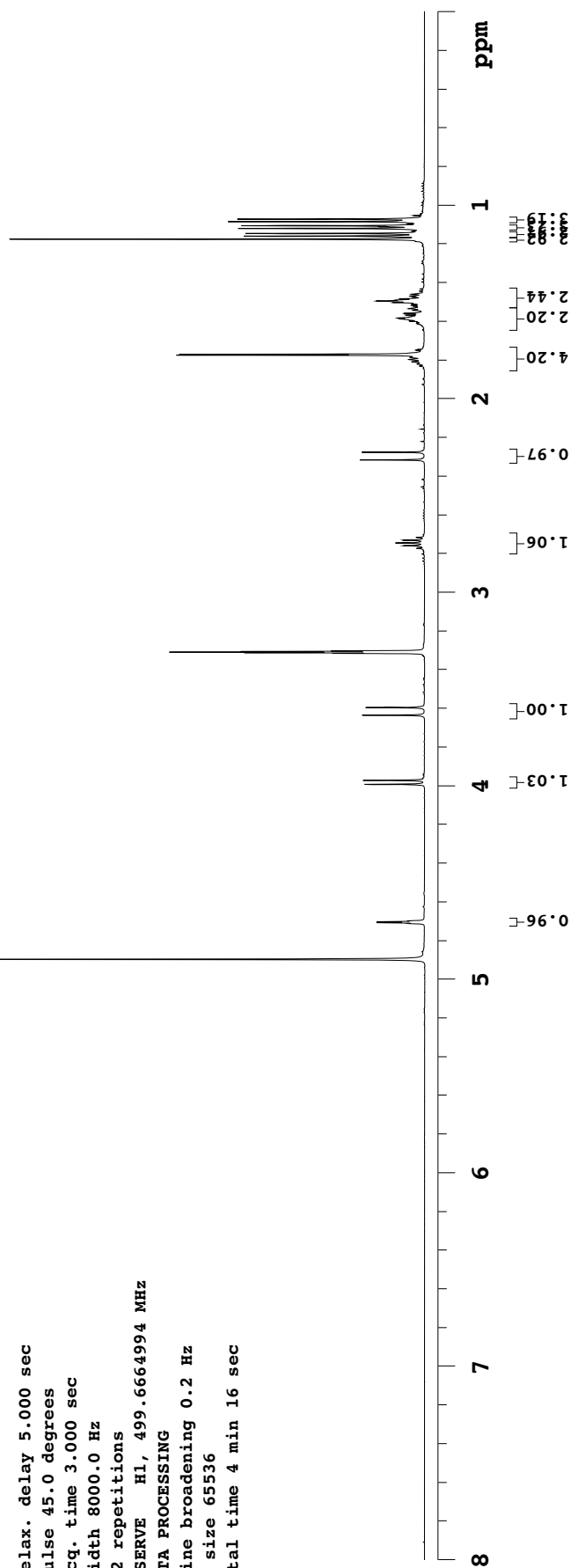
KVC25-263

Sample Name:
KVC25-263
Data Collected on:
indy.caltech.edu-inova500
Archive directory:
/home/kangway/vnmrsys/data
Sample directory:
KVC25-263
FidFile: PROTON01

Pulse Sequence: PROTON (s2pul)
Solvent: cd3od
Data collected on: Mar 12 2016

Sample #11, Operator: kangway

Relax. delay 5.000 sec
Pulse 45.0 degrees
Acq. time 3.000 sec
Width 8000.0 Hz
32 repetitions
OBSERVE H1, 499.6664994 MHz
DATA PROCESSING
Line broadening 0.2 Hz
FT size 65536
Total time 4 min 16 sec

*(+)-anhydroyanodol (3)*

KVC25-263

Sample Name:

KVC25-263

Data Collected on:

indy.caltech.edu-inova500

Archive directory:

/home/kangway/vnmrsys/data

Sample directory:

KVC25-263

FidFile: CARBON01

Pulse Sequence: CARBON (s2pul)

Solvent: cd3od

Data collected on: Mar 12 2016

Sample #11, Operator: kangway

Relax. delay 1.000 sec

Pulse 45.0 degrees

Acq. time 1.042 sec

Width 31446.5 Hz

1000 repetitions

OBSERVE C13, 125.6410635 MHz

DECOUPLE H1, 499.6689926 MHz

Power 36 dB

continuously on

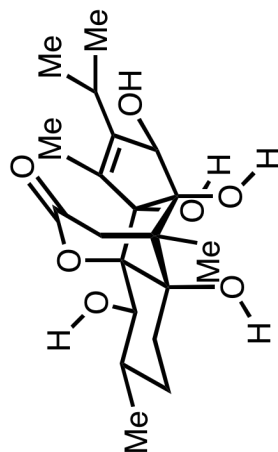
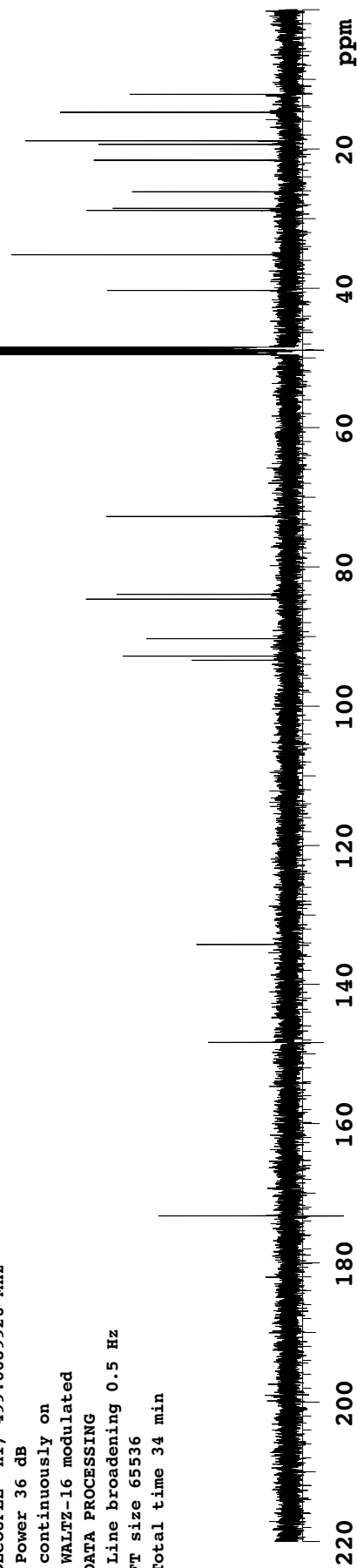
WALTZ-16 modulated

DATA PROCESSING

Line broadening 0.5 Hz

FT size 65536

Total time 34 min

*(+)-anhydroryanodol (3)*

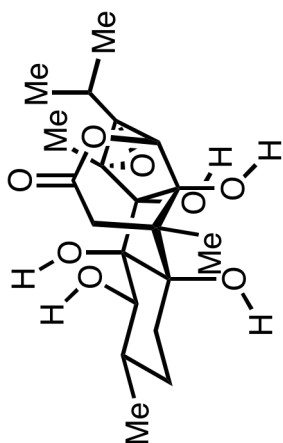
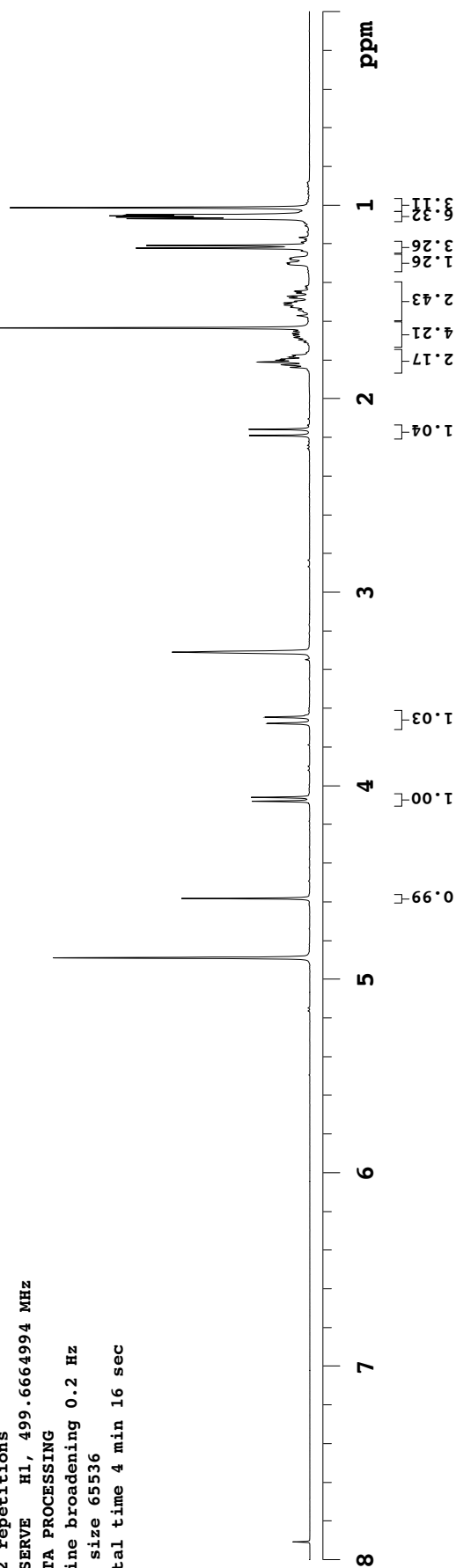
KVC25-265

Sample Name:
KVC25-265
Data Collected on:
indy.caltech.edu-inova500
Archive directory:
/home/kangway/vnmrsys/data
Sample directory:
KVC25-265
FidFile: PROTON01

Pulse Sequence: PROTON (s2pul)
Solvent: cd3od
Data collected on: Mar 13 2016

Sample #20, Operator: kangway

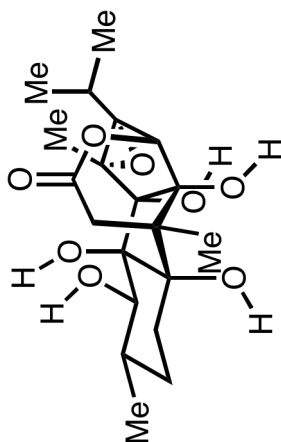
Relax. delay 5.000 sec
Pulse 45.0 degrees
Acq. time 3.000 sec
Width 8000.0 Hz
32 repetitions
OBSERVE H1, 499.6664994 MHz
DATA PROCESSING
Line broadening 0.2 Hz
FT size 65536
Total time 4 min 16 sec

(-)-epianhydroryanodol epoxide (**21**)

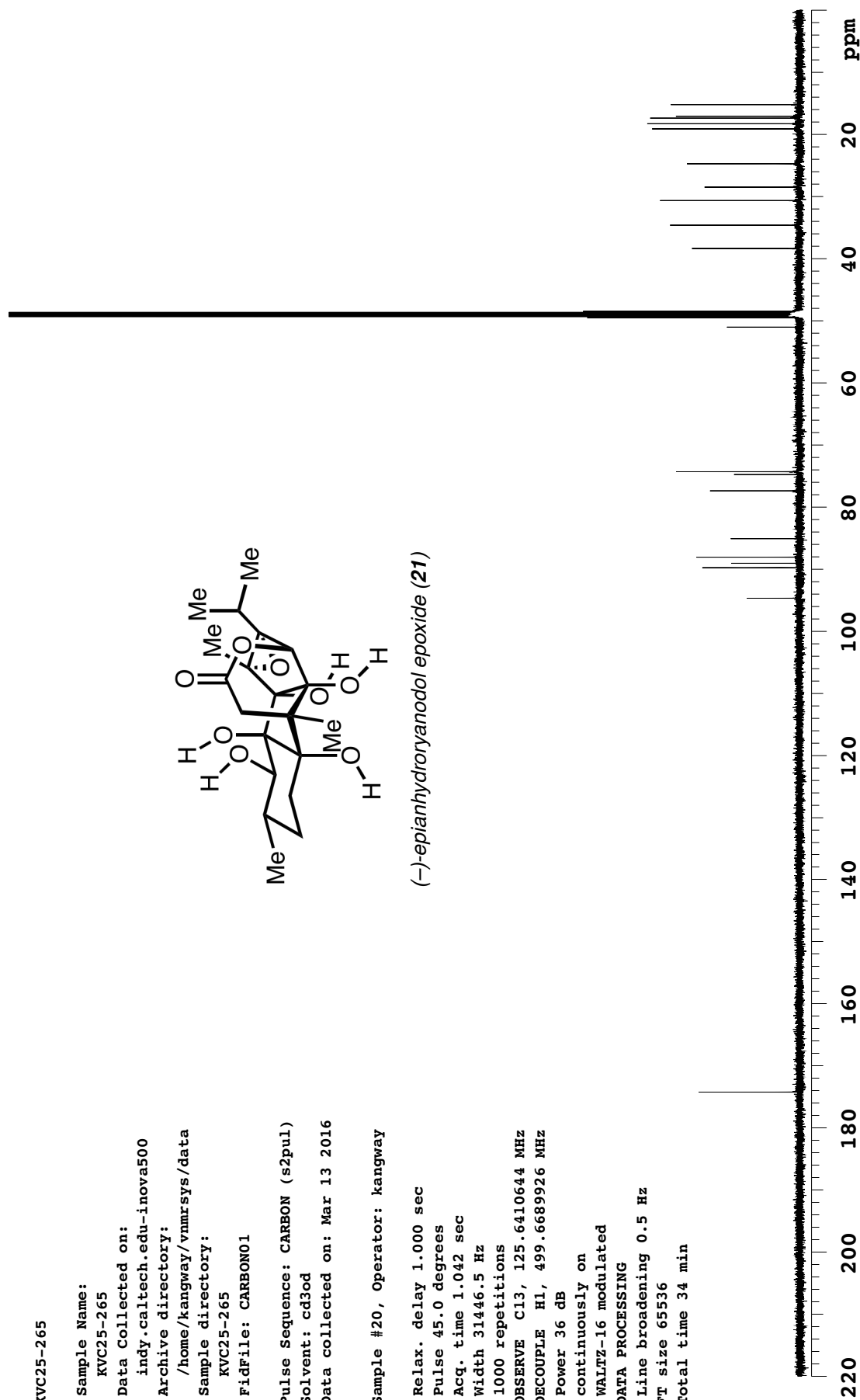
KVC25-265

Sample Name:
KVC25-265
Data Collected on:
indy.caltech.edu-inova500
Archive directory:
/home/kangway/vnmrsys/data
Sample directory:
KVC25-265
FidFile: CARBON01
Pulse Sequence: CARBON (s2pul)
Solvent: cd3od
Data collected on: Mar 13 2016

Sample #20, Operator: kangway
Relax. delay 1.000 sec
Pulse 45.0 degrees
Acq. time 1.042 sec
Width 3146.5 Hz
1000 repetitions
OBSERVE C13, 125.6410644 MHz
DECOUPLE H1, 499.6689926 MHz
Power 36 dB
continuously on
WALTZ-16 modulated
DATA PROCESSING
Line broadening 0.5 Hz
FT size 65536
Total time 34 min



(-)-epianhydroryanodol epoxide (21)

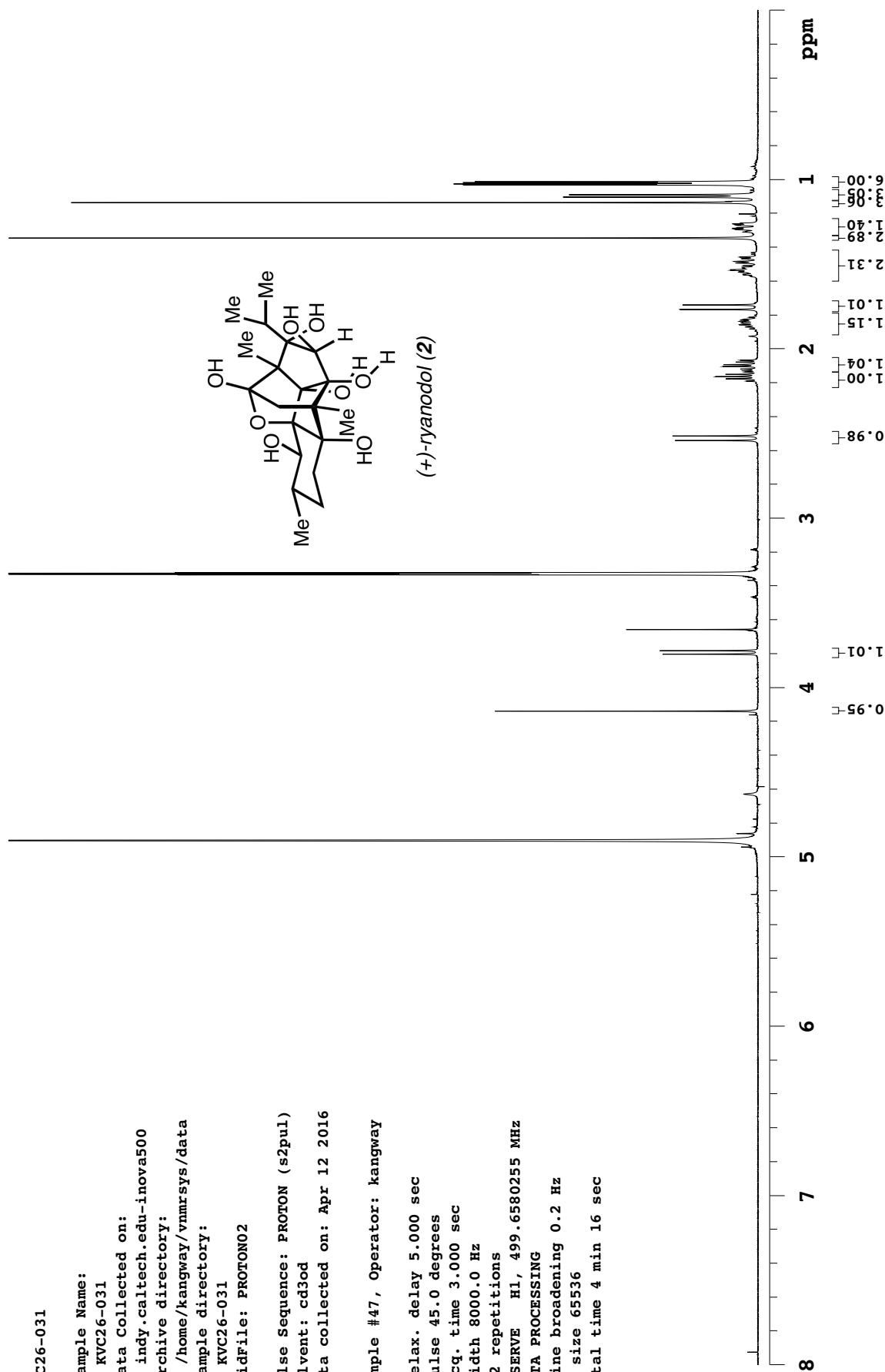
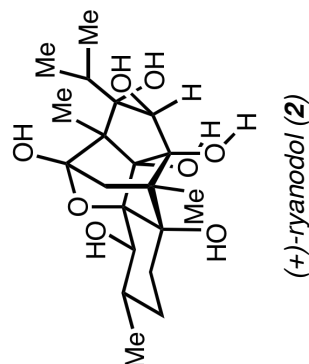


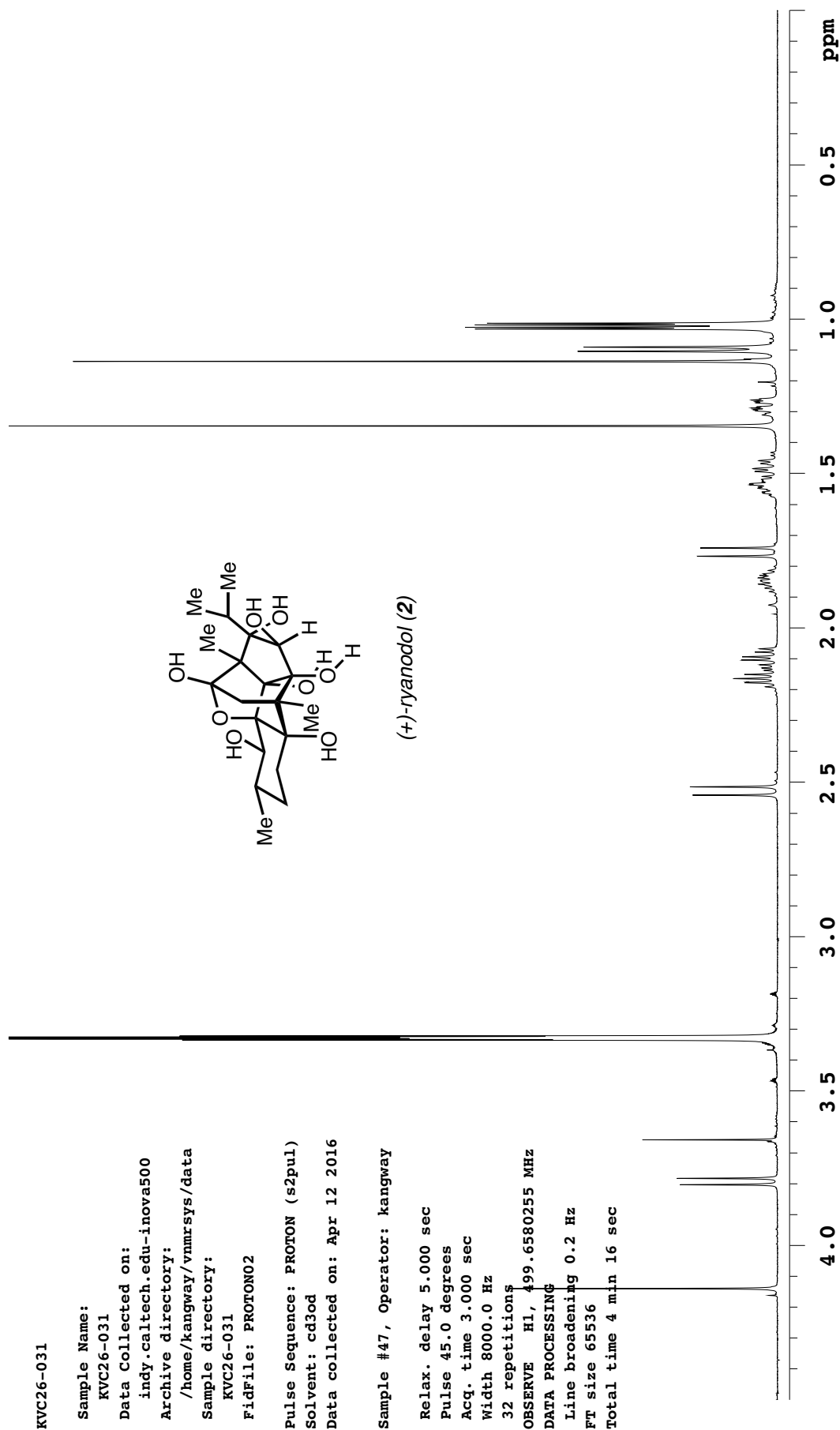
```

Sample #47, Operator: kangway

Relax. delay 5.000 sec
Pulse 45.0 degrees
Acq. time 3.000 sec
Width 8000.0 Hz
32 repetitions
OBSERVE H1, 499.6580255 MHz
DATA PROCESSING
Line broadening 0.2 Hz
FFT size 65536
Total time 4 min 16 sec

```

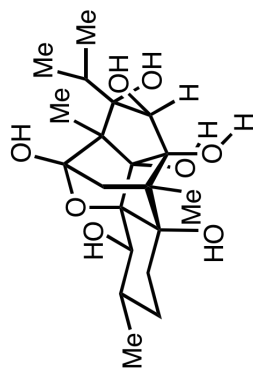




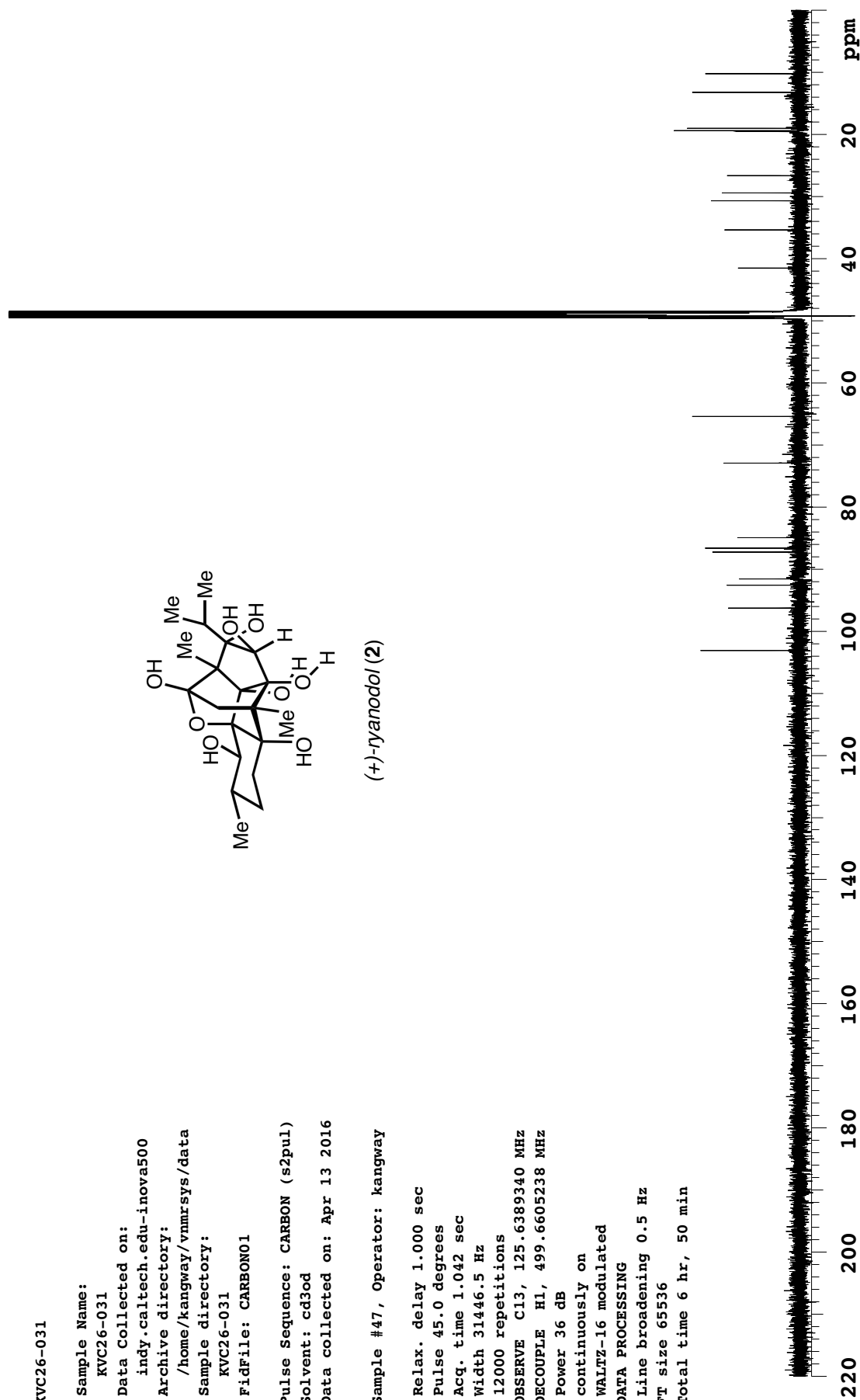
KVC26-031

Sample Name:
KVC26-031
Data Collected on:
indy.caltech.edu-inova500
Archive directory:
/home/kangway/vnmrsys/data
Sample directory:
KVC26-031
FidFile: CARBON01
Pulse Sequence: CARBON (s2pul)
Solvent: cd3od
Data collected on: Apr 13 2016

Sample #47, Operator: kangway
Relax. delay 1.000 sec
Pulse 45.0 degrees
Acq. time 1.042 sec
Width 31446.5 Hz
12000 repetitions
OBSERVE C13, 125.6389340 MHz
DECOUPLE H1, 499.6605238 MHz
Power 36 dB
continuously on
WALTZ-16 modulated
DATA PROCESSING
Line broadening 0.5 Hz
FT size 65536
Total time 6 hr, 50 min



(+)-ryanodol (2)



KVC26-031

Sample Name:

KVC26-031

Data Collected on:

indy.caltech.edu-inova500

Archive directory:

/home/kangway/vnmrsys/data

Sample directory:

KVC26-031

FidFile: CARBON01

Pulse Sequence: CARBON (s2pul)

Solvent: cd3od

Data collected on: Apr 13 2016

Sample #47, Operator: kangway

Relax. delay 1.000 sec

Pulse 45.0 degrees

Acq. time 1.042 sec

Width 31446.5 Hz

12000 repetitions

OBSERVE C13, 125.6389340 MHz

DECOUPLE H1, 499.6605238 MHz

Power 36 dB

continuously on

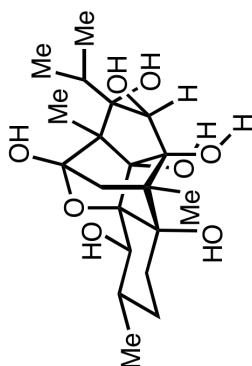
WALTZ-16 modulated

DATA PROCESSING

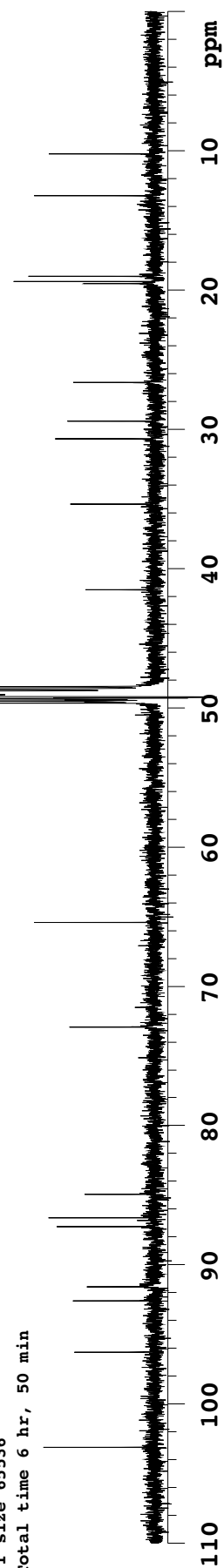
Line broadening 0.5 Hz

FT size 65536

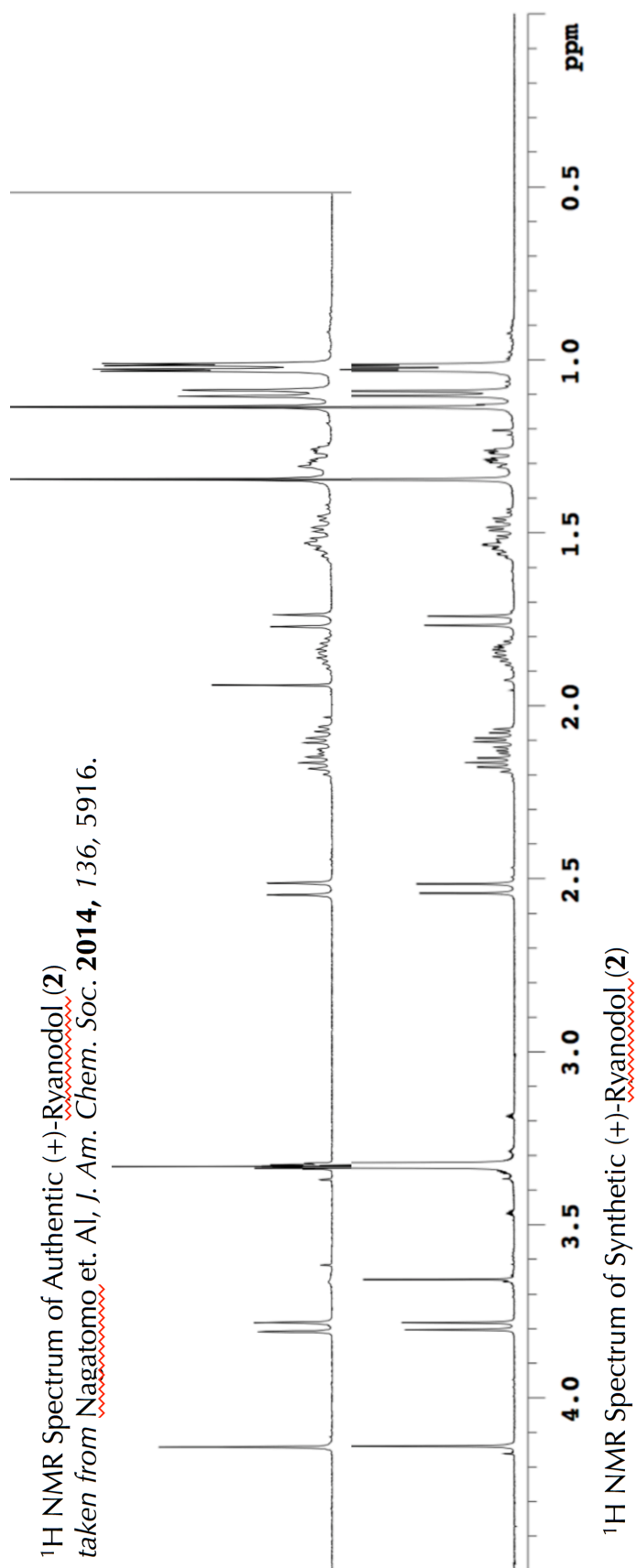
Total time 6 hr, 50 min



(+)-ryanodol (2)



¹H NMR Spectral Overlay Comparison of Authentic vs. Synthetic (+)-Ryanodol

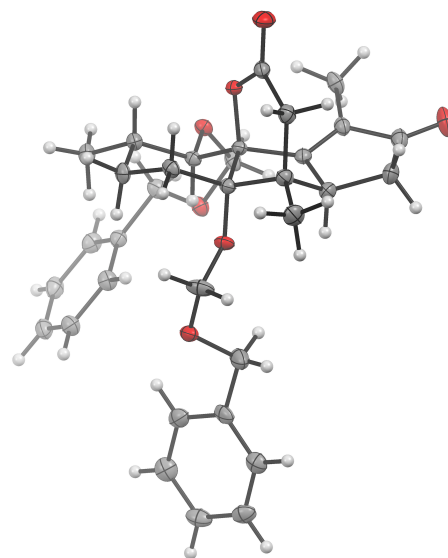


Appendix 2

X-Ray Crystallography Report Relevant to Chapter 2

A2.1 X-RAY STRUCTURE OF TETRACYCLE **99a**

Crystals of **99a** were grown from slow, repeated crystallization from Et₂O and found to be suitable for X-ray diffraction. Low-temperature diffraction data (ϕ - and ω -scans) were collected on a Bruker AXS D8 VENTURE KAPPA diffractometer coupled to a PHOTON 100 CMOS detector with Cu-K α radiation ($\lambda = 1.54178$ Å) from an I μ S micro-source. All diffractometer manipulations, including data collection integration, and



scaling were carried out using the Bruker APEXII software. Absorption corrections were applied using SADABS.² The structure was solved by intrinsic phasing using SHELXT and refined against F^2 on all data by full-matrix least squares with SHELXL-2014 using established refinement techniques and with an extinction correction of 0.00106(15). All non-hydrogen atoms were refined using anisotropic displacement parameters. All hydrogen atoms were included into the model at geometrically calculated positions and refined using a riding model. Compound **99a** crystallizes in the orthorhombic space group $P2_12_12_1$ and absolute configuration was determined by anomalous dispersion (Flack = -0.02(8)). CCDC deposition number 1478621 contains the supplementary crystallographic data for **99a**. This data can be obtained free of charge from The Cambridge Crystallographic Data Centre via

www.ccdc.cam.ac.uk/data_request/cif.

Table A.2.1. Crystal data and structure refinement for p16083_O_a.

Identification code	p16083_o_a	
Empirical formula	C33 H38 O7	
Formula weight	546.63	
Temperature	100 K	
Wavelength	1.54178 Å	
Crystal system	Orthorhombic	
Space group	P2 ₁ 2 ₁ 2 ₁	
Unit cell dimensions	a = 7.5193(3) Å	$\alpha = 90^\circ$.
	b = 9.9691(4) Å	$\beta = 90^\circ$.
	c = 37.1447(17) Å	$\gamma = 90^\circ$.
Volume	2784.4(2) Å ³	
Z	4	
Density (calculated)	1.304 Mg/m ³	
Absorption coefficient	0.735 mm ⁻¹	
F(000)	1168	
Crystal size	0.22 x 0.15 x 0.12 mm ³	
Theta range for data collection	2.379 to 78.722°.	
Index ranges	-9 ≤ h ≤ 8, -11 ≤ k ≤ 12, -44 ≤ l ≤ 46	
Reflections collected	25520	
Independent reflections	5891 [R(int) = 0.0654]	
Completeness to theta = 67.679°	100.0 %	
Absorption correction	Semi-empirical from equivalents	
Max. and min. transmission	0.7542 and 0.6748	
Refinement method	Full-matrix least-squares on F ²	
Data / restraints / parameters	5891 / 0 / 369	
Goodness-of-fit on F ²	1.054	
Final R indices [I > 2σ(I)]	R1 = 0.0332, wR2 = 0.0756	
R indices (all data)	R1 = 0.0395, wR2 = 0.0783	
Absolute structure parameter	-0.02(8)	
Extinction coefficient	0.00106(15)	
Largest diff. peak and hole	0.388 and -0.305 e.Å ⁻³	

Table 2. Atomic coordinates ($\times 10^4$) and equivalent isotropic displacement parameters ($\text{\AA}^2 \times 10^3$) for p16083_O_a. $U(\text{eq})$ is defined as one third of the trace of the orthogonalized U_{ij} tensor.

	x	y	z	U(eq)
O(4)	2446(2)	7582(1)	3543(1)	18(1)
O(3)	4(2)	4472(1)	3389(1)	16(1)
O(5)	3759(2)	9341(2)	3828(1)	21(1)
O(6)	2900(2)	3729(1)	3863(1)	17(1)
O(7)	5698(2)	4343(2)	4094(1)	20(1)
O(2)	-2174(2)	3906(2)	3026(1)	27(1)
O(1)	4183(3)	3802(2)	2313(1)	34(1)
C(10)	2201(3)	5059(2)	3829(1)	15(1)
C(29)	6237(3)	5835(2)	4718(1)	20(1)
C(15)	-1057(3)	4716(2)	3102(1)	18(1)
C(28)	6510(3)	4451(2)	4716(1)	18(1)
C(9)	664(3)	5251(2)	4097(1)	17(1)
C(16)	4771(3)	3678(2)	3818(1)	20(1)
C(6)	919(3)	6838(2)	3422(1)	16(1)
C(12)	2662(3)	5171(2)	3110(1)	16(1)
C(5)	684(3)	6979(2)	3008(1)	19(1)
C(33)	7460(3)	3870(2)	4998(1)	22(1)
C(1)	3222(3)	4090(2)	2927(1)	19(1)
C(22)	6786(3)	10036(2)	3812(1)	24(1)
C(4)	2507(3)	6424(2)	2883(1)	20(1)
C(14)	-850(3)	6035(2)	2901(1)	20(1)
C(31)	7840(3)	6022(2)	5278(1)	24(1)
C(19)	5755(3)	3586(2)	4421(1)	21(1)
C(11)	1544(3)	5350(2)	3447(1)	14(1)
C(7)	-659(3)	7050(2)	3672(1)	18(1)
C(30)	6905(3)	6619(2)	4997(1)	23(1)
C(27)	7190(3)	9695(2)	4167(1)	26(1)
C(21)	1297(3)	5035(2)	4483(1)	22(1)
C(32)	8119(3)	4649(2)	5278(1)	24(1)
C(2)	3570(3)	4510(2)	2549(1)	23(1)
C(8)	-140(3)	6662(2)	4058(1)	20(1)
C(3)	2884(3)	5936(2)	2500(1)	25(1)
C(25)	9588(3)	11287(2)	4169(1)	28(1)
C(23)	7809(3)	10996(2)	3640(1)	24(1)
C(20)	311(3)	8385(2)	2862(1)	26(1)
C(17)	3378(3)	2659(2)	3039(1)	23(1)
C(24)	9198(3)	11617(2)	3817(1)	26(1)
C(26)	8583(3)	10318(2)	4347(1)	27(1)
C(13)	2247(3)	8959(2)	3642(1)	28(1)

C(18)	5294(3)	9365(3)	3607(1)	33(1)
-------	---------	---------	---------	-------

Table 3. Bond lengths [\AA] and angles [$^\circ$] for *p16083_O_a*.

O(4)-C(6)	1.439(2)
O(4)-C(13)	1.429(2)
O(3)-C(15)	1.354(2)
O(3)-C(11)	1.467(2)
O(5)-C(13)	1.384(3)
O(5)-C(18)	1.416(3)
O(6)-C(10)	1.432(2)
O(6)-C(16)	1.418(3)
O(7)-C(16)	1.406(2)
O(7)-C(19)	1.430(2)
O(2)-C(15)	1.199(3)
O(1)-C(2)	1.217(3)
C(10)-H(10)	1.0000
C(10)-C(9)	1.536(3)
C(10)-C(11)	1.532(3)
C(29)-H(29)	0.9500
C(29)-C(28)	1.395(3)
C(29)-C(30)	1.391(3)
C(15)-C(14)	1.521(3)
C(28)-C(33)	1.393(3)
C(28)-C(19)	1.507(3)
C(9)-C(21)	1.528(3)
C(9)-C(8)	1.537(3)
C(9)-H(9)	0.94(3)
C(16)-H(16A)	0.9900
C(16)-H(16B)	0.9900
C(6)-C(5)	1.556(3)
C(6)-C(11)	1.559(3)
C(6)-C(7)	1.521(3)
C(12)-C(1)	1.340(3)
C(12)-C(4)	1.511(3)
C(12)-C(11)	1.518(3)
C(5)-C(4)	1.549(3)
C(5)-C(14)	1.541(3)
C(5)-C(20)	1.528(3)
C(33)-H(33)	0.9500
C(33)-C(32)	1.387(3)
C(1)-C(2)	1.490(3)
C(1)-C(17)	1.491(3)
C(22)-C(27)	1.397(3)
C(22)-C(23)	1.384(3)

C(22)-C(18)	1.510(3)
C(4)-H(4)	1.0000
C(4)-C(3)	1.529(3)
C(14)-H(14A)	0.9900
C(14)-H(14B)	0.9900
C(31)-H(31)	0.9500
C(31)-C(30)	1.390(3)
C(31)-C(32)	1.385(3)
C(19)-H(19A)	0.9900
C(19)-H(19B)	0.9900
C(7)-H(7A)	0.9900
C(7)-H(7B)	0.9900
C(7)-C(8)	1.537(3)
C(30)-H(30)	0.9500
C(27)-H(27)	0.9500
C(27)-C(26)	1.389(3)
C(21)-H(21A)	0.9800
C(21)-H(21B)	0.9800
C(21)-H(21C)	0.9800
C(32)-H(32)	0.9500
C(2)-C(3)	1.523(3)
C(8)-H(8A)	0.9900
C(8)-H(8B)	0.9900
C(3)-H(3A)	0.9900
C(3)-H(3B)	0.9900
C(25)-H(25)	0.9500
C(25)-C(24)	1.379(3)
C(25)-C(26)	1.392(3)
C(23)-H(23)	0.9500
C(23)-C(24)	1.381(3)
C(20)-H(20A)	0.9800
C(20)-H(20B)	0.9800
C(20)-H(20C)	0.9800
C(17)-H(17A)	0.9800
C(17)-H(17B)	0.9800
C(17)-H(17C)	0.9800
C(24)-H(24)	0.9500
C(26)-H(26)	0.9500
C(13)-H(13A)	0.9900
C(13)-H(13B)	0.9900
C(18)-H(18A)	0.9900
C(18)-H(18B)	0.9900
C(13)-O(4)-C(6)	119.45(16)
C(15)-O(3)-C(11)	118.19(15)
C(13)-O(5)-C(18)	112.66(18)
C(16)-O(6)-C(10)	112.76(15)

C(16)-O(7)-C(19)	112.65(16)
O(6)-C(10)-H(10)	108.6
O(6)-C(10)-C(9)	109.59(15)
O(6)-C(10)-C(11)	111.99(15)
C(9)-C(10)-H(10)	108.6
C(11)-C(10)-H(10)	108.6
C(11)-C(10)-C(9)	109.48(16)
C(28)-C(29)-H(29)	119.8
C(30)-C(29)-H(29)	119.8
C(30)-C(29)-C(28)	120.5(2)
O(3)-C(15)-C(14)	118.85(18)
O(2)-C(15)-O(3)	118.52(19)
O(2)-C(15)-C(14)	122.55(19)
C(29)-C(28)-C(19)	120.96(19)
C(33)-C(28)-C(29)	118.8(2)
C(33)-C(28)-C(19)	120.19(19)
C(10)-C(9)-C(8)	110.51(16)
C(10)-C(9)-H(9)	108.2(15)
C(21)-C(9)-C(10)	110.86(17)
C(21)-C(9)-C(8)	109.77(16)
C(21)-C(9)-H(9)	108.1(15)
C(8)-C(9)-H(9)	109.4(15)
O(6)-C(16)-H(16A)	109.0
O(6)-C(16)-H(16B)	109.0
O(7)-C(16)-O(6)	112.95(17)
O(7)-C(16)-H(16A)	109.0
O(7)-C(16)-H(16B)	109.0
H(16A)-C(16)-H(16B)	107.8
O(4)-C(6)-C(5)	110.72(16)
O(4)-C(6)-C(11)	103.40(15)
O(4)-C(6)-C(7)	111.10(16)
C(5)-C(6)-C(11)	100.27(15)
C(7)-C(6)-C(5)	120.16(17)
C(7)-C(6)-C(11)	109.33(16)
C(1)-C(12)-C(4)	114.03(17)
C(1)-C(12)-C(11)	133.24(19)
C(4)-C(12)-C(11)	108.62(17)
C(4)-C(5)-C(6)	99.35(16)
C(14)-C(5)-C(6)	106.56(16)
C(14)-C(5)-C(4)	111.53(17)
C(20)-C(5)-C(6)	116.95(17)
C(20)-C(5)-C(4)	112.65(18)
C(20)-C(5)-C(14)	109.38(18)
C(28)-C(33)-H(33)	119.6
C(32)-C(33)-C(28)	120.8(2)
C(32)-C(33)-H(33)	119.6

C(12)-C(1)-C(2)	107.81(19)
C(12)-C(1)-C(17)	130.82(19)
C(2)-C(1)-C(17)	121.18(18)
C(27)-C(22)-C(18)	121.9(2)
C(23)-C(22)-C(27)	118.9(2)
C(23)-C(22)-C(18)	119.2(2)
C(12)-C(4)-C(5)	101.40(16)
C(12)-C(4)-H(4)	108.9
C(12)-C(4)-C(3)	103.95(17)
C(5)-C(4)-H(4)	108.9
C(3)-C(4)-C(5)	123.74(19)
C(3)-C(4)-H(4)	108.9
C(15)-C(14)-C(5)	118.56(17)
C(15)-C(14)-H(14A)	107.7
C(15)-C(14)-H(14B)	107.7
C(5)-C(14)-H(14A)	107.7
C(5)-C(14)-H(14B)	107.7
H(14A)-C(14)-H(14B)	107.1
C(30)-C(31)-H(31)	120.0
C(32)-C(31)-H(31)	120.0
C(32)-C(31)-C(30)	120.0(2)
O(7)-C(19)-C(28)	109.14(17)
O(7)-C(19)-H(19A)	109.9
O(7)-C(19)-H(19B)	109.9
C(28)-C(19)-H(19A)	109.9
C(28)-C(19)-H(19B)	109.9
H(19A)-C(19)-H(19B)	108.3
O(3)-C(11)-C(10)	106.06(15)
O(3)-C(11)-C(6)	108.76(15)
O(3)-C(11)-C(12)	104.30(15)
C(10)-C(11)-C(6)	109.37(15)
C(12)-C(11)-C(10)	124.31(17)
C(12)-C(11)-C(6)	103.31(16)
C(6)-C(7)-H(7A)	109.7
C(6)-C(7)-H(7B)	109.7
C(6)-C(7)-C(8)	109.69(17)
H(7A)-C(7)-H(7B)	108.2
C(8)-C(7)-H(7A)	109.7
C(8)-C(7)-H(7B)	109.7
C(29)-C(30)-H(30)	120.0
C(31)-C(30)-C(29)	120.0(2)
C(31)-C(30)-H(30)	120.0
C(22)-C(27)-H(27)	119.7
C(26)-C(27)-C(22)	120.6(2)
C(26)-C(27)-H(27)	119.7
C(9)-C(21)-H(21A)	109.5

C(9)-C(21)-H(21B)	109.5
C(9)-C(21)-H(21C)	109.5
H(21A)-C(21)-H(21B)	109.5
H(21A)-C(21)-H(21C)	109.5
H(21B)-C(21)-H(21C)	109.5
C(33)-C(32)-H(32)	120.0
C(31)-C(32)-C(33)	120.0(2)
C(31)-C(32)-H(32)	120.0
O(1)-C(2)-C(1)	125.7(2)
O(1)-C(2)-C(3)	125.8(2)
C(1)-C(2)-C(3)	108.36(17)
C(9)-C(8)-H(8A)	108.6
C(9)-C(8)-H(8B)	108.6
C(7)-C(8)-C(9)	114.61(16)
C(7)-C(8)-H(8A)	108.6
C(7)-C(8)-H(8B)	108.6
H(8A)-C(8)-H(8B)	107.6
C(4)-C(3)-H(3A)	110.9
C(4)-C(3)-H(3B)	110.9
C(2)-C(3)-C(4)	104.41(17)
C(2)-C(3)-H(3A)	110.9
C(2)-C(3)-H(3B)	110.9
H(3A)-C(3)-H(3B)	108.9
C(24)-C(25)-H(25)	120.0
C(24)-C(25)-C(26)	120.0(2)
C(26)-C(25)-H(25)	120.0
C(22)-C(23)-H(23)	119.7
C(24)-C(23)-C(22)	120.6(2)
C(24)-C(23)-H(23)	119.7
C(5)-C(20)-H(20A)	109.5
C(5)-C(20)-H(20B)	109.5
C(5)-C(20)-H(20C)	109.5
H(20A)-C(20)-H(20B)	109.5
H(20A)-C(20)-H(20C)	109.5
H(20B)-C(20)-H(20C)	109.5
C(1)-C(17)-H(17A)	109.5
C(1)-C(17)-H(17B)	109.5
C(1)-C(17)-H(17C)	109.5
H(17A)-C(17)-H(17B)	109.5
H(17A)-C(17)-H(17C)	109.5
H(17B)-C(17)-H(17C)	109.5
C(25)-C(24)-C(23)	120.4(2)
C(25)-C(24)-H(24)	119.8
C(23)-C(24)-H(24)	119.8
C(27)-C(26)-C(25)	119.4(2)
C(27)-C(26)-H(26)	120.3

C(25)-C(26)-H(26)	120.3
O(4)-C(13)-H(13A)	110.1
O(4)-C(13)-H(13B)	110.1
O(5)-C(13)-O(4)	107.86(18)
O(5)-C(13)-H(13A)	110.1
O(5)-C(13)-H(13B)	110.1
H(13A)-C(13)-H(13B)	108.4
O(5)-C(18)-C(22)	108.78(18)
O(5)-C(18)-H(18A)	109.9
O(5)-C(18)-H(18B)	109.9
C(22)-C(18)-H(18A)	109.9
C(22)-C(18)-H(18B)	109.9
H(18A)-C(18)-H(18B)	108.3

Table A.2.4. Anisotropic displacement parameters ($\text{\AA}^2 \times 10^3$) for p16083_O_a. The anisotropic displacement factor exponent takes the form: $-2p^2 [h^2 a^{*2} U^{11} + \dots + 2h k a^* b^* U^{12}]$

	U11	U22	U33	U23	U13	U12
O(4)	17(1)	11(1)	24(1)	-3(1)	-1(1)	-1(1)
O(3)	15(1)	16(1)	16(1)	0(1)	-1(1)	-3(1)
O(5)	18(1)	19(1)	24(1)	-6(1)	2(1)	-3(1)
O(6)	18(1)	14(1)	19(1)	-1(1)	-1(1)	2(1)
O(7)	21(1)	23(1)	16(1)	-1(1)	-4(1)	2(1)
O(2)	27(1)	30(1)	25(1)	0(1)	-6(1)	-12(1)
O(1)	36(1)	46(1)	19(1)	-9(1)	4(1)	11(1)
C(10)	15(1)	14(1)	16(1)	-2(1)	0(1)	1(1)
C(29)	19(1)	21(1)	20(1)	1(1)	-2(1)	3(1)
C(15)	17(1)	22(1)	15(1)	-2(1)	1(1)	-1(1)
C(28)	17(1)	20(1)	17(1)	1(1)	0(1)	-1(1)
C(9)	18(1)	18(1)	15(1)	-2(1)	1(1)	-1(1)
C(16)	18(1)	22(1)	18(1)	-5(1)	-2(1)	6(1)
C(6)	15(1)	15(1)	17(1)	-2(1)	-1(1)	-1(1)
C(12)	14(1)	19(1)	16(1)	-1(1)	0(1)	-2(1)
C(5)	22(1)	16(1)	17(1)	2(1)	-1(1)	-1(1)
C(33)	22(1)	22(1)	22(1)	4(1)	-2(1)	1(1)
C(1)	18(1)	23(1)	17(1)	-4(1)	2(1)	1(1)
C(22)	18(1)	23(1)	30(1)	-13(1)	4(1)	3(1)
C(4)	22(1)	19(1)	17(1)	0(1)	2(1)	-4(1)
C(14)	23(1)	22(1)	16(1)	1(1)	-2(1)	0(1)
C(31)	22(1)	32(1)	17(1)	-5(1)	1(1)	-3(1)
C(19)	24(1)	19(1)	20(1)	1(1)	-5(1)	2(1)
C(11)	14(1)	13(1)	16(1)	-2(1)	1(1)	-2(1)
C(7)	17(1)	18(1)	20(1)	-4(1)	0(1)	3(1)

C(30)	25(1)	22(1)	24(1)	-3(1)	2(1)	1(1)
C(27)	25(1)	18(1)	34(1)	-4(1)	8(1)	1(1)
C(21)	24(1)	27(1)	16(1)	-2(1)	2(1)	1(1)
C(32)	21(1)	34(1)	16(1)	3(1)	-3(1)	-2(1)
C(2)	18(1)	32(1)	18(1)	-4(1)	2(1)	-1(1)
C(8)	19(1)	22(1)	19(1)	-3(1)	5(1)	5(1)
C(3)	30(1)	28(1)	17(1)	1(1)	6(1)	-3(1)
C(25)	21(1)	23(1)	39(1)	-5(1)	-7(1)	0(1)
C(23)	22(1)	21(1)	28(1)	-3(1)	0(1)	6(1)
C(20)	35(1)	20(1)	23(1)	6(1)	-1(1)	0(1)
C(17)	27(1)	22(1)	21(1)	-7(1)	0(1)	7(1)
C(24)	25(1)	16(1)	37(1)	0(1)	2(1)	1(1)
C(26)	26(1)	25(1)	29(1)	1(1)	-2(1)	7(1)
C(13)	24(1)	15(1)	46(1)	-7(1)	-6(1)	0(1)
C(18)	26(1)	42(1)	31(1)	-16(1)	9(1)	-9(1)

Table A.2.5. Hydrogen coordinates ($\times 10^4$) and isotropic displacement parameters ($\text{\AA}^2 \times 10^3$) for *p16083_O_a*.

	x	y	z	U(eq)
H(10)	3165	5713	3890	18
H(29)	5591	6245	4528	24
H(16A)	5153	2728	3811	23
H(16B)	5086	4090	3584	23
H(33)	7660	2929	4999	26
H(4)	3460	7067	2956	24
H(14A)	-1976	6540	2927	24
H(14B)	-715	5823	2642	24
H(31)	8288	6556	5469	29
H(19A)	6507	2780	4388	25
H(19B)	4541	3288	4486	25
H(7A)	-1673	6492	3591	22
H(7B)	-1032	8002	3665	22
H(30)	6721	7562	4996	28
H(27)	6506	9030	4287	31
H(21A)	1624	4092	4517	33
H(21B)	339	5271	4651	33
H(21C)	2334	5605	4530	33
H(32)	8761	4240	5469	28
H(8A)	-1211	6719	4213	24
H(8B)	731	7325	4149	24
H(3A)	1787	5946	2353	30
H(3B)	3791	6507	2383	30

H(25)	10541	11720	4290	33
H(23)	7554	11230	3397	29
H(20A)	-674	8787	2998	39
H(20B)	-10	8328	2607	39
H(20C)	1376	8942	2889	39
H(17A)	4612	2466	3107	35
H(17B)	3028	2077	2838	35
H(17C)	2597	2491	3245	35
H(24)	9888	12275	3696	31
H(26)	8849	10086	4589	32
H(13A)	2100	9520	3424	34
H(13B)	1182	9074	3796	34
H(18A)	5044	9865	3383	40
H(18B)	5641	8438	3542	40
H(9)	-210(30)	4610(20)	4046(6)	17(6)

Table A.2.6. Torsion angles [°] for p16083_O_a.

O(4)-C(6)-C(5)-C(4)	58.24(19)
O(4)-C(6)-C(5)-C(14)	174.15(16)
O(4)-C(6)-C(5)-C(20)	-63.2(2)
O(4)-C(6)-C(11)-O(3)	170.36(14)
O(4)-C(6)-C(11)-C(10)	54.95(19)
O(4)-C(6)-C(11)-C(12)	-79.25(17)
O(4)-C(6)-C(7)-C(8)	-56.4(2)
O(3)-C(15)-C(14)-C(5)	6.1(3)
O(6)-C(10)-C(9)-C(21)	59.6(2)
O(6)-C(10)-C(9)-C(8)	-178.50(15)
O(6)-C(10)-C(11)-O(3)	66.60(19)
O(6)-C(10)-C(11)-C(6)	-176.28(15)
O(6)-C(10)-C(11)-C(12)	-53.9(2)
O(2)-C(15)-C(14)-C(5)	-177.2(2)
O(1)-C(2)-C(3)-C(4)	-172.6(2)
C(10)-O(6)-C(16)-O(7)	66.2(2)
C(10)-C(9)-C(8)-C(7)	51.7(2)
C(29)-C(28)-C(33)-C(32)	0.3(3)
C(29)-C(28)-C(19)-O(7)	31.6(3)
C(15)-O(3)-C(11)-C(10)	166.62(15)
C(15)-O(3)-C(11)-C(6)	49.1(2)
C(15)-O(3)-C(11)-C(12)	-60.6(2)
C(28)-C(29)-C(30)-C(31)	-0.5(3)
C(28)-C(33)-C(32)-C(31)	-0.3(3)
C(9)-C(10)-C(11)-O(3)	-55.16(19)
C(9)-C(10)-C(11)-C(6)	61.96(19)

C(9)-C(10)-C(11)-C(12)	-175.67(17)
C(16)-O(6)-C(10)-C(9)	-143.36(17)
C(16)-O(6)-C(10)-C(11)	94.94(19)
C(16)-O(7)-C(19)-C(28)	-171.20(17)
C(6)-O(4)-C(13)-O(5)	165.61(17)
C(6)-C(5)-C(4)-C(12)	46.43(18)
C(6)-C(5)-C(4)-C(3)	161.92(18)
C(6)-C(5)-C(14)-C(15)	-35.0(2)
C(6)-C(7)-C(8)-C(9)	-52.8(2)
C(12)-C(1)-C(2)-O(1)	175.9(2)
C(12)-C(1)-C(2)-C(3)	-8.8(2)
C(12)-C(4)-C(3)-C(2)	-10.5(2)
C(5)-C(6)-C(11)-O(3)	-75.25(17)
C(5)-C(6)-C(11)-C(10)	169.34(16)
C(5)-C(6)-C(11)-C(12)	35.13(18)
C(5)-C(6)-C(7)-C(8)	172.11(17)
C(5)-C(4)-C(3)-C(2)	-124.8(2)
C(33)-C(28)-C(19)-O(7)	-150.05(19)
C(1)-C(12)-C(4)-C(5)	135.25(18)
C(1)-C(12)-C(4)-C(3)	5.9(2)
C(1)-C(12)-C(11)-O(3)	-47.8(3)
C(1)-C(12)-C(11)-C(10)	73.5(3)
C(1)-C(12)-C(11)-C(6)	-161.5(2)
C(1)-C(2)-C(3)-C(4)	12.0(2)
C(22)-C(27)-C(26)-C(25)	-0.3(3)
C(22)-C(23)-C(24)-C(25)	0.1(3)
C(4)-C(12)-C(1)-C(2)	1.7(2)
C(4)-C(12)-C(1)-C(17)	-173.2(2)
C(4)-C(12)-C(11)-O(3)	107.26(18)
C(4)-C(12)-C(11)-C(10)	-131.43(19)
C(4)-C(12)-C(11)-C(6)	-6.4(2)
C(4)-C(5)-C(14)-C(15)	72.4(2)
C(14)-C(5)-C(4)-C(12)	-65.6(2)
C(14)-C(5)-C(4)-C(3)	49.9(3)
C(19)-O(7)-C(16)-O(6)	76.3(2)
C(19)-C(28)-C(33)-C(32)	-178.1(2)
C(11)-O(3)-C(15)-O(2)	170.39(18)
C(11)-O(3)-C(15)-C(14)	-12.7(2)
C(11)-C(10)-C(9)-C(21)	-177.25(16)
C(11)-C(10)-C(9)-C(8)	-55.3(2)
C(11)-C(6)-C(5)-C(4)	-50.44(17)
C(11)-C(6)-C(5)-C(14)	65.47(19)
C(11)-C(6)-C(5)-C(20)	-171.89(19)
C(11)-C(6)-C(7)-C(8)	57.1(2)
C(11)-C(12)-C(1)-C(2)	155.8(2)
C(11)-C(12)-C(1)-C(17)	-19.2(4)

C(11)-C(12)-C(4)-C(5)	-25.1(2)
C(11)-C(12)-C(4)-C(3)	-154.45(17)
C(7)-C(6)-C(5)-C(4)	-170.07(17)
C(7)-C(6)-C(5)-C(14)	-54.2(2)
C(7)-C(6)-C(5)-C(20)	68.5(3)
C(7)-C(6)-C(11)-O(3)	52.0(2)
C(7)-C(6)-C(11)-C(10)	-63.5(2)
C(7)-C(6)-C(11)-C(12)	162.34(16)
C(30)-C(29)-C(28)-C(33)	0.0(3)
C(30)-C(29)-C(28)-C(19)	178.5(2)
C(30)-C(31)-C(32)-C(33)	-0.2(4)
C(27)-C(22)-C(23)-C(24)	-0.6(3)
C(27)-C(22)-C(18)-O(5)	47.4(3)
C(21)-C(9)-C(8)-C(7)	174.31(18)
C(32)-C(31)-C(30)-C(29)	0.5(4)
C(23)-C(22)-C(27)-C(26)	0.7(3)
C(23)-C(22)-C(18)-O(5)	-134.1(2)
C(20)-C(5)-C(4)-C(12)	170.93(17)
C(20)-C(5)-C(4)-C(3)	-73.6(3)
C(20)-C(5)-C(14)-C(15)	-162.34(18)
C(17)-C(1)-C(2)-O(1)	-8.6(4)
C(17)-C(1)-C(2)-C(3)	166.7(2)
C(24)-C(25)-C(26)-C(27)	-0.2(3)
C(26)-C(25)-C(24)-C(23)	0.3(3)
C(13)-O(4)-C(6)-C(5)	88.7(2)
C(13)-O(4)-C(6)-C(11)	-164.68(18)
C(13)-O(4)-C(6)-C(7)	-47.5(2)
C(13)-O(5)-C(18)-C(22)	169.40(19)
C(18)-O(5)-C(13)-O(4)	67.5(2)
C(18)-C(22)-C(27)-C(26)	179.2(2)
C(18)-C(22)-C(23)-C(24)	-179.2(2)

ABOUT THE AUTHOR

Kangway V. Chuang was born in Urbana, IL on October 11th, 1988. He attended the University of Illinois Laboratory High School, graduating in 2006. That fall, he commenced studies at the California Institute of Technology in Pasadena, CA. As an undergraduate, he first performed research in the laboratory of Professor Bil Clemons during the summer of 2008. The following year, he began research in the laboratory of Professor Sarah Reisman, where he carried out his senior thesis research on the addition of organometallic nucleophiles into quinone-derived imines and their application in alkaloid synthesis. After graduating with a B.S. in Chemistry in 2010, he remained at the same Institute of Technology to pursue a Ph. D. in the Reisman laboratory, where his research has focused on the total synthesis of complex natural products.